UNIVERSITÀ
DI TORINO

Università degli Studi di Torino

Dipartimento di Psicologia
Dottorato di Ricerca in Neuroscienze
Ciclo XXXIV

Movement kinematics as a window into social decision-making

Tesi presentata da: **Giacomo Turri**

Tutor: **Prof. Cristina Becchio**
Co-tutor: **Prof. Massimiliano Pontil**

Coordinatore del Dottorato: **Prof. Andrea Calvo**

Anni Accademici 2018-2022
Settore scientifico-disciplinare di afferenza: M-PSI/01

Abstract

Many decisions in our daily lives are made within a social context and are often accompanied by uncertain outcomes. Crucially, these decisions are often expressed through actions. A convergence of modeling, behavioral, and neural data shows that the way people move can provide valuable insights into cognitive states and ongoing decision processes. While recent studies have begun to shed light on the underlying brain processes of social decision-making, knowledge about the kinematics of social decisions and whether movements can reveal any aspects of them is still limited.

This thesis aims to investigate whether and to what extent social decisions are expressed in movement kinematics. To this end, we developed a motor version of the Ultimatum Game in which participants acted as responders, and we tracked their movement kinematics using a motion capture system. We analyzed the kinematic data following two different approaches: (i) a multivariate linear decoding model at the single-subject, single-trial level and (ii) linear mixed-effects modeling at the group-level.

With the first approach, we were able to map the parameters of social decisions onto the single-trial kinematics of individual responders. This analysis revealed that movement kinematics contained predictive information about both the responders' choice (accept versus reject) and the fairness (fair versus unfair) of a proposed offer. Upon further analyses of the responder-specific models, we observed that this information is expressed in personalized kinematic patterns consistent within a given responder but vary among them.

With the second approach, we explored whether, at the group-level, kinematic features related to the vigor of reaching were influenced by the social decision variables. We found that, for accepted offers, the vigor of reaching increased as a function of the offer level; i.e., as the amount of the offer increased, responders' reaction time became shorter and peak velocity higher. Concerning rejections, we documented the opposite pattern: vigor of reaching increased as the offer level decreased, meaning that vigor increased the more unfair the offer was.

Taken together, these findings contribute to the existing literature on the link between decision-making and sensorimotor control by showing that hand kinematics can provide information not only about individual decisions but also about more intricate social decisions.

Contents

List of Figures

List of Tables

1. Introduction

1.1 Motivation

Imagine that you are on your classic Sunday bike ride when you come to a fork in the road: you know that either road could take you back home, but while you are familiar with the road on your left, you have never taken the road on the right, which, while known for its scenic views, is also more physically demanding. As you stand at the fork in the road, you must decide whether to take the familiar left road or to try the unknown right road. So, what are you going to do? Your decision depends on many factors, such as your risk-taking tendencies and your level of fatigue. This scenario well exemplifies decision-making under uncertainty, as not all potential outcomes are known. Also, in this situation, any decision will only affect yourself, making it an example of *individual decision-making*.

Now, consider the same scenario, but this time you are not alone: you are with an old friend who is unfamiliar with the roads. This time, you have to choose between two familiar roads: the first is flatter but longer, and the second is faster but has a steep slope. As you are in a hurry, you would prefer to take the second road, but your friend is new to cycling and would be struggling on that steep slope. Again, your decision depends on various factors, such as how much of a hurry you are in and how much you care about your friend; his/her well-being, preferences, and opinions become crucial to you characterizing your decision-making as social (*social decision-making*).

Despite the differences between individual and social decision-making, the process of choosing one option among several involves the complex integration of various cognitive, emotional, and environmental factors. This complexity has led researchers to examine the issue from different perspectives and levels of analysis.

A commonly adopted paradigm for studying social decision-making is that of socio-economic games. These games (e.g., Ultimatum Game, Prisoner's Dilemma, Trust Game, etc.) usually involve two or more players and are aimed at understanding people's social preferences (i.e., people's tendency to care not only about themselves but also about the well-being of others). For example, the *Ultimatum Game* is an experiment that tests social norms of fairness by having one participant (i.e., the *proposer*) receive a sum of money and then propose to split it with another participant (i.e., the *responder*). The responder can either agree to the proposal, resulting in the transfer of money, or decline it, resulting in neither participant receiving anything.

In almost all experiments that exploit these paradigms, participants are taught to interact with other partners through key presses or verbally. However, in everyday life, most of our decisions require physical action. Today, a large body of evidence demonstrates that internal cognitive states leak into motor outputs (Dotan et al., 2019; Gallivan et al., 2018; Gordon et al., 2021; Shadmehr et al., 2019; Song & Nakayama, 2009; Wispinski et al., 2020). Therefore, by leveraging movement kinematics, we should be able to unravel the flow of social decision processes. Only a few studies have tried to understand whether the movement of individuals reflects and externalizes aspects of social decision-making. For example, Kieslich and Hilbig (2014) discovered that in a two-person social dilemma game, the average trajectories were more curved when individuals defected than when they cooperated, suggesting that defection entailed more conflict. However, it is yet to be determined whether social decisions may be predicted from the movement parameters of individual reaching movements.

To bridge this gap, with this dissertation we propose a motor version of the Ultimatum Game and conduct rigorous computational analyses, paving the way for a better understanding of this matter. The aims of the present research are:

(i) to investigate whether and how movement kinematics contains predictive information of social decisions;

(ii) to examine the individuals' kinematic pattern related to social decisions;

(iii) to explore whether social decision variables influence the vigor of movements.

1.2 Thesis outline

The thesis is composed of 5 Chapters and is structured as follows.

In the current chapter (**Chapter 1**), I introduced the rationale and objectives of this work.

In **Chapter 2**, I provide a general background for the whole research, divided into the following sections.

- The first section (2.1) begins with an overview of the classical theories of decision-making and then describes new perspectives that have emerged through the recent interdisciplinary approach of neuroeconomics.
- The second section (2.2) introduces the Ultimatum Game, the behavioral economics game at the heart of the works presented in this dissertation, showing the main behavioral and neural findings.
- The third section (2.3) gives a general overview of decision-making models and illustrates the crucial role of movement kinematics in elucidating the flow of hidden cognitive states.

In **Chapter 3**, I present the experimental study based on a motor version of the Ultimatum Game used to test the hypothesis that social decisions may be predicted from movement kinematics. The acquired data, analyzed at the single-subject, single-trial level, proved that reaching kinematics encodes social decision variables in an individualized pattern.

In **Chapter 4**, I present additional analyses of the data acquired from the experimental study shown in Chapter 3. In particular, a group-level analysis showed that social decision variables modulated vigor of reaching.

Finally, in **Chapter 5**, I conclude the thesis with a summary of the obtained results and provide future research directions built upon the evidence of this work.

2. Background

2.1 1. The rise of neuroeconomics: integrating multiple approaches and perspectives

From the moment we wake up to the moment we fall asleep, we are constantly challenged to make decisions. These can be as trivial as what to eat for breakfast, what to wear before going to work, or whether to have another cup of coffee before lunch. Or, more rarely, they can be life-altering, like accepting or rejecting a new job, a marriage proposal, or moving to another country. Whether trivial or not, the process that leads us to make decisions requires a careful evaluation of alternatives, driven by a complex and constant integration of various environmental, cognitive, social, and emotional factors. The outcomes and dynamics of this process have always fascinated and engaged scholars, particularly economists, psychologists, and neuroscientists, who have approached the subject from different perspectives and using different techniques because of their diverse backgrounds. Given the interdisciplinary nature of this field, in the following sections, I briefly review the classical economic theories developed mainly by mathematicians and economists to more recent theories that have emerged from the efforts of psychologists and neuroscientists.

2.1.1 Expected utility theory

Expected utility theory is a formal economic framework, developed by John von Neumann and Oskar Morgenstern, for modeling how individuals make decisions under uncertainty (von Neumann & Morgenstern, 1944). It is based on the assumption that individuals are rational decision-makers seeking to maximize their expected utility from a given choice (Savage, 1954). Expected utility is formally defined as the sum of the

probabilities of all possible outcomes multiplied by the utility of each outcome, where the utility of an outcome represents the subjective value or preference that an individual assigns to it. In other words, if an individual is faced with the choice between two options, A and B, with the respective probabilities, $p(\mathrm{A})$ and $p(\mathrm{B})$, and the respective utilities, $u(\mathrm{A})$ and $u(\mathrm{B})$, the expected utility of each option is calculated as follows: $U(\mathrm{A}) = p(\mathrm{A}) * u(\mathrm{A}); U(\mathrm{B}) = p(\mathrm{B}) * u(\mathrm{B})$. The individual will choose the option with the higher expected utility.

For example, in the decision to take or not take an umbrella (U) when leaving the house, with a 50% chance of rain (R) inferred from the weather forecast (i.e., $p(\mathrm{R}) = 0.5$), we can assign a subjective value (0: worst outcome; 100: best outcome) to the four possible outcomes (resulting from the combinations of 'umbrella'/'no umbrella' and 'rain'/'no rain'). Thus, the expected utility theory would support the following: the decision to take the umbrella could be associated with a value of 60 in case of rain, $u(\mathrm{U} + \mathrm{R}) = 60$, and 30 in case of no rain, $u(\mathrm{U} + \text{no R}) = 60$; the decision to leave it at home it would be associated with a value of 0 in case of rain, $u(\text{no U} + \mathrm{R}) = 0$, and 100 in case of no rain, $u(\text{no U} + \text{no R}) = 100$. According to the calculations predicted by the theory, the preferred choice should be not to take the umbrella since its utility would be greater than the decision to take it:

$$U(\text{no U}) = p(\mathrm{R}) * u(\text{no U} + \mathrm{R}) + p(\mathrm{R}) * u(\text{no U} + \text{no R}) = 0.5 * 0 + 0.5 * 100 = 50$$
$$U(\mathrm{U}) = p(\mathrm{R}) * u(\mathrm{U} + \mathrm{R}) + p(\mathrm{R}) * u(\mathrm{U} + \text{no R}) = 0.5 * 60 + 0.5 * 30 = 45$$

This would be the reasoning of a rational decision-maker seeking optimality (Sanfey et al., 2006). However, empirical research has demonstrated how the predictions of the expected utility theorem do not always match the individuals' observed choices. Maurice Allais conducted a famous experiment in which participants were presented with two choices: a certain outcome or a gamble with a higher expected value but with uncertainty (Allais, 1953). The results showed that participants preferred a certain outcome, which is contrary to the predictions of the expected utility theory. This finding, known as the Allais paradox, was later explained by introducing the concept of risk aversion, which states that individuals are willing to give up some expected value to reduce uncertainty (Kahneman & Tversky, 1979).

Expected utility theory has been criticized for its assumptions. One of the main criticisms is that the theory assumes that individuals are rational and have stable preferences, which may not always be the case in real-world decision-making (Kahneman & Tversky, 1979). Additionally, the theory does not account for other factors that may influence decision-making, such as emotions, cognitive biases, and social norms (Rabin, 2000). However, despite its limits and drawbacks, the theory, as shown below, has proven helpful in studying and identifying the neural representation of subjective utility computation (Sanfey, 2007).

2.1.2 Game theory

Game theory is a mathematical tool used to analyze decision-making in situations where the outcomes depend on the choices of individuals or groups (von Neumann & Morgenstern, 1944). The theory originated in the early 20th century and has been widely applied in various fields, including economics, political science, psychology, and biology (Camerer, 2003).

At the core of game theory is the concept of *game*, which can be thought of as a set of rules that dictate the interactions between two or more individuals (i.e., the *players*) and affect the outcomes (i.e., the *payoffs*) of all involved parties. These rules can be formalized through a mathematical model, including the players, their strategies, and the payoffs associated with each combination of strategies. To understand the decision-making process in these situations, game theorists often rely on the concept of *homo oeconomicus*, which is the assumption that individuals act rationally and self-interestedly in order to maximize their utility or profit. Therefore, if all players behave rationally, they will adopt that set of strategies defined by the Nash equilibrium (Nash, 1950), from which no player can unilaterally increase his/her gain anymore.

Hence, Nash equilibrium is a set of strategies, one for each player, such that no player has the incentive to change their strategy given the other players' strategies. In other words, each player is playing his/her best possible strategy given the strategies of the others, and there is no benefit in changing one's strategy. This concept is essential in understanding how players will behave in a given game and can be used to predict the game's outcome.

One example of a game that can exhibit a Nash equilibrium is the *prisoner's dilemma*

(Rapoport & Chammah, 1965). In this game, two prisoners (A and B) are each given the option to confess (defect) or remain silent (cooperate). The set of all possible combinations of defection and cooperation is {(C,C), (C,D), (D,C), (D,D)} as expressed in the payoff matrix (Table 2.1). If both defect, they both receive a sentence of five years in prison. If both cooperate, they both receive a sentence of two years. If one defects and the other cooperates, the defector will be set free while the silent prisoner receives a sentence of ten years. Deriving the utility for each possible combination, for player A it follows that: (D,C)>(C,C)>(D,D)>(C,D).

At Nash equilibrium, both players choose to defect since this is their best strategy given the other player's strategy. Indeed, by cooperating, they maximize their payoff; however, neither player is motivated to cooperate since unilateral cooperation would move the player from the third worst payoff (D,D) to the worst of all (C,D). This shows how Nash equilibrium can result in sub-optimal outcomes for all players.

As with expected utility theory, game theory is based on strong assumptions, and some of these are not met in real-world situations. For example, contrary to the prediction of game theory, research has shown that subjects playing the prisoners' dilemma chose to cooperate rather than defect about half of the time (Sally, 1995). More generally, it is quite unusual for individuals to behave according to the predictions of game theory and adopt the strategies suggested by Nash equilibrium (Camerer, 2003). Actually, people tend to approximate optimal decision-making strategies through a set of heuristic routines, which may be driven by emotional processes or experience (Lee, 2006). Individuals who must make decisions in interactive environments usually favor less selfish solutions, valuing factors such as equity and reciprocity (Sanfey, 2007).

Another economic game that has challenged the assumptions of expected utility theory is the Ultimatum Game, in which players' actual behavior diverges significantly from the

	B cooperate	B defect
A cooperate	Both serves 2 years	A serves 10 years B is set free
A defect	A is set free B serves 10 years	Both serves 5 years

Table 2.1: Payoff matrix for prisoners' dilemma.

equilibrium situation that the theory predicts. This will be explored in more detail ahead in the chapter.

2.1.3 Prospect theory

Prospect theory, developed by Daniel Kahneman and Amos Tversky, aims to improve the representativeness of expected utility theory in describing human decision-making (Kahneman & Tversky, 1979). Despite being generally accepted as a 'normative' model of rational choice and widely applied as a 'descriptive' model of economic behavior, expected utility theory often fails to accurately depict human decision-making in real-world scenarios. As pointed out by Kahneman and Tversky, one of the phenomena that challenge the theory is the so-called *certainty effect*. This effect is manifested on the occasion of the Allais paradox (Allais, 1953); despite the higher expected utility, people overweight outcomes considered certain over those merely probable. Their work also highlighted other significant deviations from the predictions of expected utility theory: the *reflection effect*, the *framing effect*, the *isolation effect*, the overweighting of small probabilities, and magnitude perception. The reflection effect is the tendency for people to be risk-averse when maximizing gains but risk-seeking when minimizing losses. The framing effect shows that risk preferences can change depending on whether a choice is presented in terms of gains or losses, even when the options themselves are held constant. The isolation effect captures the idea that preferences for a choice may change depending on how it is structured sequentially. Finally, people are sensitive to both relative and absolute magnitude leading to an overweighting of small probabilities; people find a difference between 1% and 2% more meaningful than 51% and 52%. Remarkably, a recent study involving about four thousand participants from nineteen different countries replicated almost all of the results published in 1979 by Kahneman and Tversky (Ruggeri et al., 2020).

Therefore, the authors propose the prospect theory, which breaks down the decision-making process into two stages: *editing* and *evaluation*. During the editing stage, preliminary operations yield a more straightforward representation of the prospects. However, these operations can lead to anomalies of preference; the prospects can be edited differently depending on the context in which it appears, resulting in different outcomes. Then, in the evaluation stage, the decision-maker evaluates the edited prospects and is supposed to choose the highest-value prospect. Nevertheless, the evaluation process can be biased, leading to the overvaluation of high-probability prospects and the underval-

uation of low-probability ones. This can lead to irrational decision-making, as people may make choices that are not in their best interests due to their biases and cognitive constraints, i.e., *bounded rationality* (Simon, 1957).

Overall, this model, supported by empirical data, provides a more reliable understanding of human decision-making than the previous model of expected utility theory. Unsurprisingly, the 1979 article has become one of the most influential and cited in the economic and psychological sciences.

2.1.4 The heuristics approach

The concept of *heuristic* in decision-making refers to using mental shortcuts or rules of thumb to solve everyday life problems (Kahneman, 2011). These mental shortcuts allow individuals to make decisions quickly and efficiently, often without requiring extensive analysis or consideration of all available options (Gigerenzer & Gaissmaier, 2011). They are a crucial aspect of human cognition and are used to reduce the cognitive load in certain situations, for example, when dealing with many options.

There are several types of heuristics that individuals may use in decision-making. One commonly studied heuristic is the *availability heuristic*, which is the tendency to base judgments on information readily available in memory. For example, suppose an individual is asked to estimate the likelihood of an event occurring. In that case, the individual may base his/her decision on the number of times he/she has personally experienced that event or seen it reported in the media. This heuristic can lead to distorted judgments and decisions, as individuals may only consider some relevant information or may rely too heavily on incomplete or biased data.

Another heuristic is the *representativeness heuristic*, which is the tendency to judge the probability of an event based on how closely it resembles a prototypical example. This heuristic can lead to overgeneralization and stereotypes. One example of the representativeness heuristic is when a person is trying to guess the occupation of a person they just met. They may make assumptions based on the person's appearance, such as assuming that a person with a suit and briefcase is a lawyer, even though many other professions also involve suits and briefcases. They are basing their assumption on how the person appears to them, rather than thinking about the probability of the person being a lawyer

based on actual data.

A third heuristic is the *anchoring and adjustment heuristic*, which is the tendency to rely on initial information (i.e., the *anchor*) as a reference point and make adjustments based on that. For example, suppose an individual is asked to estimate the price of a car. They may anchor their decision on a starting point, such as the price of a similar car they have previously owned, and then adjust their estimate based on additional information about the car. This heuristic can lead to errors in judgment, as the initial anchor may not accurately reflect the true value, and individuals may not make sufficient adjustments based on new information.

These are just a few examples of the many mental shortcuts that people use in decision-making. While heuristics can be helpful in many situations, Tversky and Kahneman (1974) showed that these mental shortcuts can also lead individuals to biases and errors in decision-making, despite encouragement to respond accurately.

2.1.5 The role of emotions

Thanks to the new perspective brought by Tversky and Kahneman, researchers understand that human decision-making is not solely based on rational thinking but can also be influenced by other factors. Economics, psychology, and neuroscience have contributed to this idea, highlighting the importance of these non-rational elements in the decision-making process. The neuroscience approach, characterized by its techniques such as functional magnetic resonance imaging (fMRI), transcranial magnetic stimulation (TMS), and many others, has opened up new opportunities for understanding the brain mechanisms behind human behavior. A recent field called neuroeconomics emerged, aiming to combine insights from economics, psychology, and neuroscience to develop a unified theory of behavior (Glimcher & Rustichini, 2004). This field challenges the long-held belief in economics that behavior is solely guided by rational thinking. Instead, it suggests that other factors, such as emotion and context, also play a role in decision-making (Sanfey et al., 2006).

The two-systems theory was one of the first attempts to define how emotions influence decision processes (Kahneman, 2003; Stanovich & West, 2000). This theory suggests that we have two systems for making decisions: *System 1* and *System 2*. System 1 is

automatic, largely unconscious, and does not require much computational capacity. It involves heuristic processing and is associated with *interactional intelligence* (Levinson, 1995), which allows people to understand and respond to the intentions of others quickly. System 2, on the other hand, involves controlled processing and is associated with analytic intelligence, which refers to the computational processes underlying intelligence. System 2 is typically slower and more effortful than System 1.

Another successful perspective was that of Bechara and Damasio, who proposed the *somatic marker hypothesis* (Bechara & Damasio, 2005). According to this hypothesis, somatic markers, which are physiological responses to emotional stimuli, guide our decision-making by providing a gut feeling or intuition about a particular choice. According to Bechara and Damasio's model, the impact of emotions on decision-making can be either positive or negative, depending on whether they are relevant to the task at hand. If emotions are integrated into the task, they can be beneficial, but if they are unrelated, they can disrupt decision-making. These markers are thought to be stored in the amygdala, insula, ventromedial prefrontal cortex (VMPFC), and brainstem and can be triggered by events or experiences that are emotionally charged. Therefore, these markers affect deliberative reasoning, which is instead found in the anterior and dorsolateral prefrontal cortex (DLPFC) and posterior parietal cortex (PPC).

2.1.6 New perspectives

Although the role of emotional processes in decision-making is widely recognized as crucial, some recent research perspectives have raised criticisms of this view.

For instance, some scholars have questioned the idea that all emotional processes can be grouped into a single system (such as System 1), arguing instead that there are multiple modulatory circuits through which emotions impact decision-making (Phelps et al., 2014). The use of the term limbic system, which suggests the existence of a single emotional center in the brain, has also been criticized. In reality, some regions within the limbic system are more involved in cognitive tasks (such as the hippocampus), while other areas outside the limbic system, such as prefrontal regions, play a significant role in emotional processes (Phelps et al., 2014). This suggests that emotion is not a single entity but a collection of different affective processes that each influence decision-making through their own neural circuits.

Some studies have also shown that the influence of emotional and unconscious processes on behavior may have been overestimated and that, not infrequently, the decision process can be interpreted simply as due to conscious, rational processes (Newell & Shanks, 2014). A reevaluation of human rationality, often considered too corruptible by the activation of affective systems, emerged. For example, as shown in the review by Gigerenzer and Gaissmaier (2011), heuristics, whether rational or irrational, conscious or unconscious, can be as accurate as or more than complex reasoning, debunking the myth that heuristics lead to biases and errors.

Moreover, in an extensive review in 2015, Lerner and colleagues reviewed the past 35 years of literature on emotion and decision-making (Lerner et al., 2015). They highlight the impact that emotions have on our internal decision-making model, which can sometimes be harmful and sometimes helpful, showing the appearance of regularities in how decision-makers' emotions influence their choices. To synthesize all the findings, they proposed the *emotion-imbued choice* model (Figure 2.1), accounting for both traditional (rational) and new emotional inputs. The rational part of this model recalls the concepts of expected utility theory (solid black lines), which require the decision maker to evaluate the options by assessing the utility of each potential outcome for each option. These outcome utilities are combined with options characteristics (such as probabilities and time delays) and decision-maker characteristics (such as risk aversion and discount rate) to create an overall evaluation of each option. The best option is then chosen based on these evaluations. Then, emotions influence this process in two ways: (i) rather than stable preferences, the model allows for constructed preferences so that the expected emotional response to an outcome influences its utility; (ii) emotions felt at the moment of the decision (i.e., current emotions), which are outside the scope of conventional rational models. Sources that can affect current emotions are: characteristics of the decision maker (e.g., anxiety or depression), characteristics of the options (e.g., ambiguous information or uncertain probabilities), the anticipatory effect of predicted emotions on current emotions, contemplation when options are nearly equivalent, incidental emotions due to unrelated factors or events (e.g., weather or mood).

One economic game that has challenged traditional economic theories by fueling the idea that emotional processes influence decision-making is the Ultimatum Game. Since the

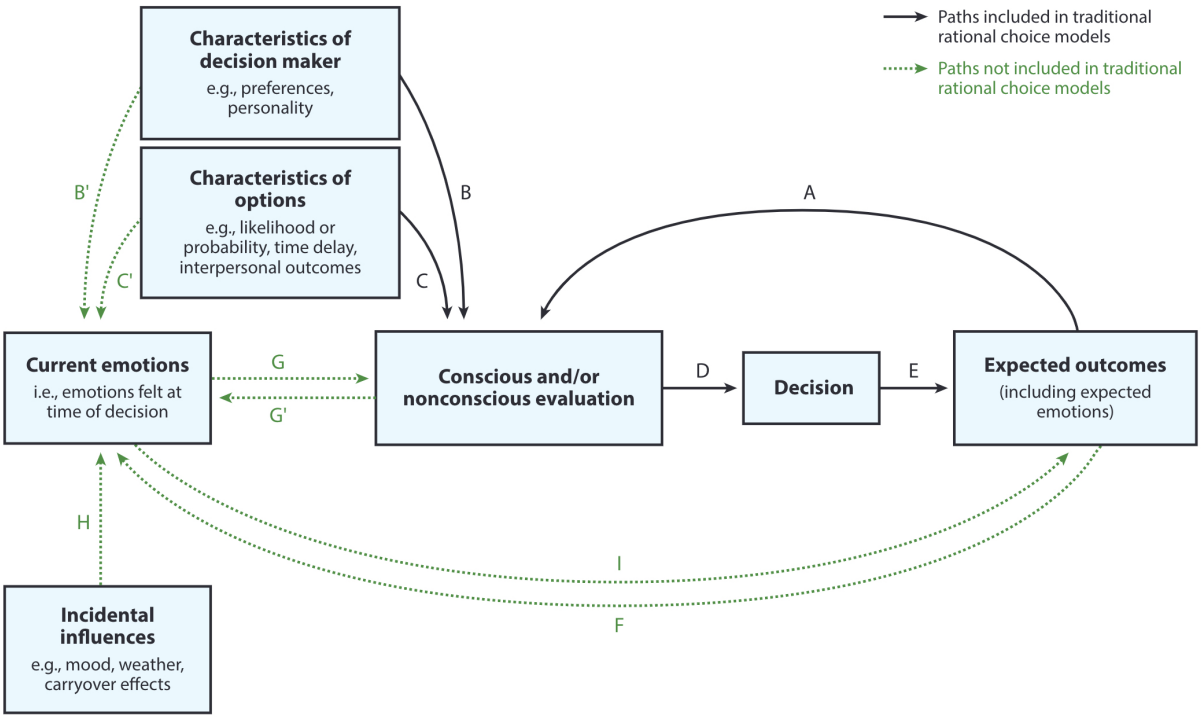

Figure 2.1: Emotion-imbued choice model. Block diagram of the emotion-imbued choice model. Adapted from Lerner et al. (2015).

following work is based on this game, I now provide a more in-depth discussion by briefly reviewing the leading behavioral and neural findings.

2.2 The Ultimatum Game

The *Ultimatum Game* (UG) is a classic experimental paradigm used to study economic decision-making and is often cited as an example of how classical economic theories do not accurately predict human behavior. The game's structure is straightforward in the first version of the game developed by Güth and colleagues forty years ago (Güth et al., 1982). One player (i.e., the *proposer*) is allocated a sum of money that he/she must share with the other player (i.e., the *responder*). The proposer will then make an offer to the responder, who can decide to accept or reject. If the responder accepts, the money will be divided according to the proposer's offer; if the responder rejects, neither of the two players will receive anything.

In accordance with game theory, and particularly Nash equilibrium, proposers, to max-

imize revenue, should always offer the minimum allowable amount, and a fully rational responder should accept any non-zero offer. However, behavioral findings systematically disregard this expectation. On average, proposers usually tend to offer about 40% of the amount (many offer half), and responders often reject unfair offers of about 20% of the total (Camerer & Thaler, 1995).

2.2.1 First behavioral investigations and concerns

One concern that the researchers raised is the amount at stake. The prediction was that as stake increases, the amount that a responder will reject increases but the percentage decreases. In other words, in terms of amount, people are more likely to reject $5 out of $50 than out of $10, whereas, in terms of percentage, people are more likely to accept 10% of a $50 stake than a $10 one. Several studies investigated the effect of stake size (ranging from $10 to $500); surprisingly, only weak effects were reported. A meta-analysis of 31 studies reported an almost zero effect of the stake size on UG offers, indicating that there is no evidence that people offer less money in high-stakes UG (Larney et al., 2019). Concerning rejections, in a study with a $100 stake, Hoffman et al. (1996) reported no change in responders' behavior: they rejected 10, 20, and in some cases, even $30. Overall, it has been concluded that stake size does not influence individuals' behavior.

Another concern raised is the possible influence of cultural and demographical factors, hypothesizing that different behaviors could be found in populations different from the Western one. To investigate this, Henrich et al. (2005) recruited participants from 15 small-scale societies (from 4 different countries) which underwent one-shot UG. They reported high variability among groups' behaviors which reflected the daily habits of these societies. It is worth naming the two opposites. On the one hand, we have populations in Papua New Guinea where proposers often offer more than half of what is at stake, many of which have been rejected. These rejections may result from the fact that in these societies, accepting gifts implies a stringent obligation to reciprocate, and unpaid debts place the recipient in a subordinate position. On the other hand, we have the Machiguenga indigenous population from Peruvian Amazonia, where 75% of proposers' offers were below the 30% of the stake, and almost none of these were rejected. Indeed, this society is almost economically independent at the family level, with little cooperation, sharing, or exchange beyond the family unit. Although Machiguenga's behavior is reminiscent of *homo oeconomicus*, the authors point out that perfect selfish behavior is not present even

among these societies.

It is important to note that when the same participants play multiple UG rounds, their behavior may change, and they may adopt more sophisticated strategies, such as using rejections more frequently, leaning the results toward game theory predictions (Roth & Erev, 1995). Therefore, to avoid strategic thinking, modified versions of the UG have been proposed: the *one-shot* UG, in which the two players interact only once, and the *covered* UG, in which the proposer is not informed of the responder's decision (Civai et al., 2010).

2.2.2 Beyond self-interest

People playing UG behave irrationally, going against their self-interest. Researchers attempting to explain this phenomenon have come up with several theories.

A first attempt posits that proposers are 'sophisticated profit maximizers' (Camerer & Thaler, 1995): they offer more than Nash equilibrium prediction knowing that responders are unlikely to accept unfair offers (Weg & Zwick, 1994). This theory is corroborated by the work of Bolton and Zwick (1995), who tested *the anonymity hypothesis*, which claims that proposers offer fair offers and responders reject unfair offers so as not to appear greedy in the eyes of the experimenters, producing altered UG results. Their experiment confuted this hypothesis by counterposing the *punishment hypothesis*, i.e., responders' willingness to punish proposers who treated them unfairly; proposers knowing this make fair offers to avoid being punished.

Other approaches are based on the social preferences account: people care not only about their self-interest but also the interest of others. Several models have been proposed within this framework (Camerer, 2003).

One is the *inequity aversion* model, in which players care about their payoffs and the differences between their payoffs and those of others (Bolton & Ockenfels, 2000; Fehr & Schmidt, 1999). According to this model, people are motivated by a general dislike for situations in which resources or outcomes are distributed unfairly. They may be willing to sacrifice some of their material payoff to achieve more equitable outcomes.

In contrast to inequity aversion, which focuses on the final distribution of outcomes, theories of *reciprocal fairness* or *negative reciprocity* propose that 'people do not seek uniformly to help other people; rather, they do so according to how generous these other people are being' (Rabin, 1993). According to these theories (Dufwenberg & Kirchsteiger, 2004; Falk & Fischbacher, 2006; Rabin, 1993), people who are motivated to help those who have helped them are the same as punishing those who have harmed them. This means that if one person takes actions that reduce the payoff of another person in order to benefit themselves, the other person may respond by punishing the first person for their unfair behavior. However, if the distribution of outcomes is randomly determined, the second person is less likely to punish the first person for receiving a higher payoff (Blount, 1995; Falk & Fischbacher, 2006). These results corroborate the idea that people punish unfairness rather than reject inequity (Camerer & Thaler, 1995). Following these theories, rejections in the UG paradigm can be seen as a means to punish misbehaving proposers.

Although punishing someone who has acted unfairly, incurring a self-loss, may seem irrational, researchers pointed out that this behavior has an evolutionary role (Boyd et al., 2003). This phenomenon took the name of *altruistic punishment*: they argue that punishing defectors, even if it comes at a cost to the individual, is a natural part of human behavior and is an effective way to maintain cooperation in a group over the long term.

2.2.3 Neural correlates of Ultimatum Game

The advent of neuroscience and its methodologies in the study of social decision-making paved the way for more in-depth investigations into the mechanisms underlying responder behavior in the UG. The focus of these studies has been on identifying the most involved brain areas, clarifying the role of specific networks and how they interact during the course of the game.

The first fMRI study to investigate which brain areas were activated in subjects playing UG in the role of responders was conducted by Sanfey et al. (2003). Their prediction was to find activations of neural structures usually involved in both emotional and cognitive processing and that the magnitude of activation in these structures might predict the subsequent decision. To verify this hypothesis, participants played rounds of UG against human agents or a computer while lying inside the scanner. The offers, in both condi-

tions, followed a predetermined algorithm (half fair, half unfair) ensuring that the same set of offers was administered to all subjects. The only difference between conditions was the participants' belief that they were actually playing with another person or a computer.

Their behavioral results were in line with the previous UG experiment: fair offers were all accepted with a decreasing acceptance rate as the offer's value decreased, and the acceptance rate of unfair offers was significantly higher for the computer condition than for the human partner condition. Regarding neural structures, in the human partner condition, they found a greater activation for unfair compared to fair offers of bilateral anterior insula, dorsolateral prefrontal cortex (DLPFC), and anterior cingulate cortex (ACC) (Figure 2.2).

- Activation of the bilateral anterior insula to unfair offers is particularly interesting, as noted by the authors, since it is usually associated with negative emotions such as anger and disgust (Calder et al., 2001). It shows its greater activation for rejections (Figure 2.2B), and the authors hypothesized that its activation reflects the negative emotions felt at an unfair offer, thus triggering rejection.

- Activation of the DLPFC is usually linked to cognitive processes such as goal maintenance (Miller & Cohen, 2001) and executive control (Wagner et al., 2001). According to the authors, its activation was associated with the rational aspects of the task, representing an attempt to maintain the goal of reward maximization by inhibiting the emotional response.

- Activation of the ACC is associated with cognitive conflicts (Botvinick et al., 1999; MacDonald et al., 2000) and the authors speculated that it might reflect the cognitive and emotional conflict present in the UG.

However, more recent studies have disagreed with some of the above interpretations. In particular, negative emotions should not always be considered as a trigger for rejection of the offer. For example, Civai et al. (2010) submitted the participants, in the role of responders, to two different conditions of the UG: in one condition, participants played the traditional UG deciding for themselves (*myself* condition); in the other condition, participants played UG on behalf of a third-party (*third-party* condition). Their behavioral results showed no differences between the two conditions; the participants rejected unfair offers even when playing on behalf of third parties. Following the reasoning of Sanfey et al. (2003), this should elicit the same negative emotions that subjects experience

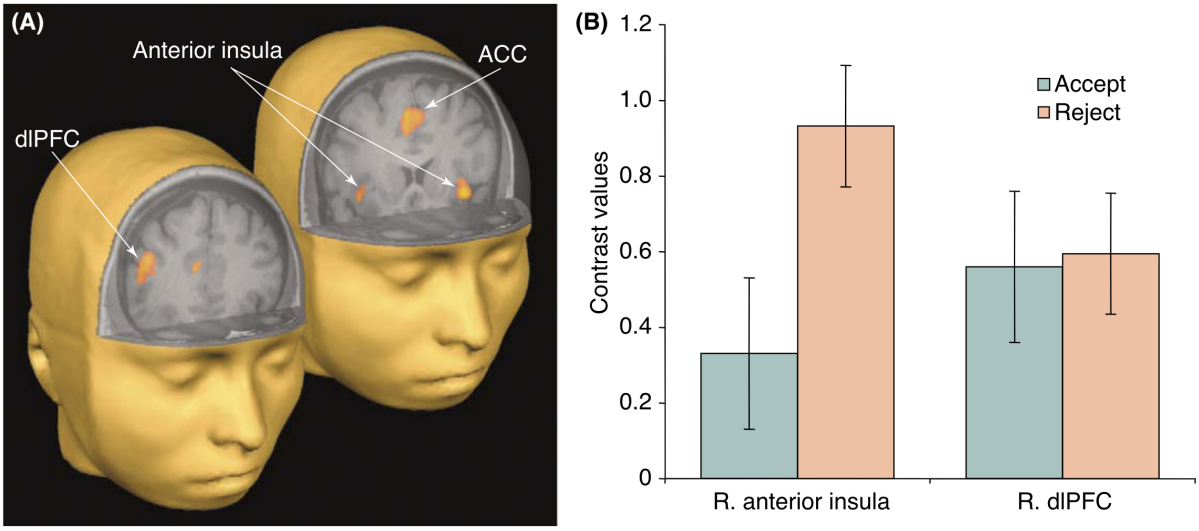

Figure 2.2: Active brain areas in response to unfair offers. (**A**) Localization of the activated areas related to the presentation of an unfair offer, showing activation of bilateral anterior insula, dorsolateral prefrontal cortex (DLPFC), and anterior cingulate cortex (ACC). (**B**) Involvement of right anterior insula and right DLPFC in the decision to accept or reject the offer. Adapted from Sanfey et al. (2006).

when they play for themselves. In contrast, Civai et al. (2010) measured participants' skin conductance response (SCR), which is known to reflect the arousal component of experienced emotions, and found emotional activation only in the myself condition. Their results suggested that rejections can be interpreted primarily as a reaction to perceived unfairness and that negative emotions play a role only in cases where unfair offers are aimed directly at the individual.

A follow-up study by Corradi-Dell'Acqua et al. (2013) used the same paradigm proposed by Civai et al. (2010). It aimed to investigate the neural correlates associated with direct personal involvement in an unfair situation (myself condition) and those associated with fairness considerations when indirectly involved in an unfair situation (third-party condition). Their results showed an activation of the anterior insula in both myself and third-party conditions, and it was more active for rejections. This suggests that this area plays a role in reacting to unfairness rather than to negative emotion. Regarding the emotional processes elicited by the myself condition, the authors found increased activation of the ventral medial prefrontal cortex (VMPFC) and right DLPFC, which were also more active when the unfair offer was rejected. According to the researchers, these areas may be part of a neural circuitry implicated in monitoring emotional reactions. Other studies

go in this direction (Baumgartner et al., 2011; Knoch et al., 2008, 2006). Knoch et al. (2006) applied repetitive transcranial magnetic stimulation (rTMS) to the right DLPFC of responders, disrupting its functionality. Although participants continued to perceive offers as unfair, they found an increase in the acceptance rate: the authors suggested that right DLPFC plays a crucial role in fairness perception, overriding self-interest to maintain and enforce fairness goals. In a further study, Knoch et al. (2008) replicated this result by applying transcranial direct current stimulation (tDCS). In summary, following receipt of an unfair offer, while right DLPFC seems to promote normative behavior (Spitzer et al., 2007) (contrary to what Sanfey et al. (2003) hypothesized), VMPFC activation overcomes the motivation to sanction norm violations favoring self-interest (Civai et al., 2012; Corradi-Dell'Acqua et al., 2013). Hence, the connectivity between DLPFC and VMPFC may implement the costly, normative decision to reject unfair offers (Gabay et al., 2014).

Additionally, it has been hypothesized that other brain regions besides the insula may contribute to the emotional reaction observed in first-person play. In particular, some studies show activation of the cerebellum in response to unfair offers, regardless of the decision made (Gabay et al., 2014).

While the studies above focused on unfairness and rejections, Tabibnia et al. (2008) investigated the neural circuitry related to fairness perception and discovered that regions commonly associated with the reward system, such as the ventral striatum, amygdala, and VMPFC, were also linked to a preference for fair outcomes. Still regarding the reward system, in a study using positron emission tomography (PET), de Quervain et al. (2004) showed that when participants actively punished defectors, activated the dorsal striatum, which has been implicated in the processing of rewards deriving from goal-directed actions (Fehr & Camerer, 2007). Notably, the magnitude of activation correlated with the willingness of the participants to incur a greater loss to achieve a greater punishment. These findings suggest the idea that punishing social norm violators is satisfactory.

In summary, these neuroscientific studies have helped shed light on the neural underpinnings of responder's behavior in the UG. Both rational and emotional processes influence decision-making, and the brain structures responsible for mediating these processes have been identified. Moreover, rejections would occur independently of the influence of negative emotions but because of rational goal-oriented behavior: punishing social norm

defectors.

2.3 Decision-making models and movement kinematics

Imagine you are on a hot summer day when a terrible thirst assails you. You head to the refrigerator, open it, and you are faced with a dilemma: take the pitcher of iced tea on the left or the bottle of sparkling water with lemon on the right. How do you decide between these two options, and how do you translate the decision into the movement necessary to implement it? As with most decisions, it involves reducing many alternatives to a single goal, and, as is often the case, this requires the effort of physical action.

In this section, I briefly review the central perspective and theories developed in the study of decisions requiring physical action. I start from good-based models, which assume that decision-making and action planning are two distinct serial events, to action-based models, which assume a close link between decision-making and action processing.

2.3.1 Good-based models: a serial perspective

According to good-based models in decision-making, the brain evaluates the potential outcomes of different options at a level of abstract value representations and makes decisions based on the relative value of those outcomes (Padoa-Schioppa, 2011). Concerning the relationship between a decision and its associated action, in a good-based model, the decision-making process is treated as a separate module of a serial process. After the representation of the available options has been made available by the perceptual processes and decision-making processes have used this to choose which action to take, the corresponding movement is then planned (Wispinski et al., 2020). To better understand how this selection among options occurs, a series of decision-making models based on accumulating evidence up to a threshold has been proposed (Bogacz, 2007; Gold & Shadlen, 2007).

Most decision-making models have been formalized by studying perceptual decisions, i.e., very simple decisions that rely only on one's sensory perceptions. In this way, variables are minimized so that only the essential features of the decision-making process can be identified. Among the most commonly used paradigms is the random-dot motion (RDM) task (Britten et al., 1992). It consists of a cloud of moving dots presented on a computer screen: a portion of the dots move in a single direction, while the remainder moves ran-

domly. The task is to indicate the predominant direction of the dots' movement.

Intracranial recordings of brain activation in monkeys subjected to RDM task, which had been taught to indicate the dots' movement direction through saccadic eye movements, have made it possible to identify circuits fundamental to understanding how decision-making processes work. The most interesting activations concern the sensory and association cortices. These are the medial temporal area, which contains sensory neurons sensitive to the direction of movement (Britten et al., 1993), and the lateral intraparietal area, an associative area of the posterior parietal cortex positioned midway in the sensorimotor chain, which receives information from the medial temporal area and projects it to the frontal eye fields and superior colliculus, responsible for eye movements (Shadlen & Newsome, 2001). The specific activation patterns observed in these regions led to hypothesizing the essential mechanisms of perceptual decision-making. Specifically, sensory areas would represent the different alternatives in terms of sensory evidence, while parietal neurons would be responsible for the accumulation of this evidence, and their activity would reflect the formation of the final decision (Gold & Shadlen, 2007). Lately, Donner et al. (2009), using magnetoencephalography, supported this thesis in a study with humans.

Inspired by these results, computational models that attempt to mimic this behavior and exhibit similar characteristics have been devised. A common feature of these models is that the decision is based on a sequence of observations. With each observation, more and more evidence is accumulated until a certain level of confidence is reached that allows a decision to be made. This is represented by crossing the decision boundary (Gold & Shadlen, 2007). Two of the most widely used models are the race (Smith & Vickers, 1988) and drift-diffusion (Ratcliff & Rouder, 1998) models. Race model is defined by several independent accumulators and the decision is made the first time one of these accumulators crosses a fixed decision threshold. In contrast, with drift-diffusion model, decisions are based on relative evidence. The difference in evidence between options is accumulated until an upper or lower bound is reached corresponding to the two options under consideration.

A further development of the aforementioned models is the Leaky Competing Accumulator (LCA) model (Usher & McClelland, 2001). In this model, accumulators integrate the

sensory information by increasing their activation during the presentation of the stimulus. However, the more the activation of one accumulator increases, the more it will exert inhibition on the other, thus decreasing its activation. As with the other models, the decision is assumed to be final once either accumulator reaches a certain activation threshold.

Despite these models' success and widespread use, recent research shows that decision-making is more complex than simple evidence accumulation models can describe (Wispinski et al., 2020). One major limitation of these models, and, more in general, of good-based models, is that they assume that processes related to decision-making are completed before movement is initiated, suggesting serial processing of perception, decision-making and, lastly, movement planning.

2.3.2 Action-based models: the interplay between cognition and action

So far, one might intuitively assume that the decision-making process follows a linear path of this kind: first, all available information is accumulated; this information is then processed and integrated with more detail; finally, the integration process leads to a final choice that is translated into actual behavior. This reasoning is consistent with traditional cognitive theories, which tend to view perceptual, cognitive, and motor systems separately: perceptual systems would be devoted to constructing a representation of the world through sensory information; cognitive systems would use these representations, along with information accumulated in memory, to construct knowledge, make judgments, and make choices; finally, motor systems would implement decisions in behavior through planning and execution of movements (Cisek, 2007).

This subdivision of neural systems is undoubtedly useful for descriptive purposes, as it provides a straightforward overview of behavior and makes the functional role of specific brain regions easier to interpret. However, numerous scientists are increasingly promoting a unified view of internal processes. They argue that perception, cognition, and motor control actually operate in an integrated manner and are part of a single system (Dotan et al., 2019; Gallivan et al., 2018; Song & Nakayama, 2009; Wispinski et al., 2020).

Under this view, action-based models of decision-making state that available options are represented and selected in sensorimotor maps of the environment, where options

preserve their relative spatial relation to the deciding agent. So, the representation of every option is sensorimotor, reflecting details of the movement associated with acting on each alternative. The sensorimotor maps would contain information about the movements associated with successfully interacting with the object, i.e., *object affordance* (Cisek, 2007). These affordance competition maps give rise to what has been called attentional landscapes or desirability density functions, which originate in a unified system involving the parietal and frontal cortex. According to this theory, this competition is influenced by inputs from cortical regions (e.g., prefrontal cortex) and subcortical (e.g., basal ganglia), and it is a continuous process that sometimes occurs even during the execution of the movement itself. It is argued that the specification of the fundamental parameters of movement occurs prior to the final selection of motor action, or at least that they are processes that occur simultaneously and continuously, allowing for the rapid adaptations necessary for living in a dynamic world (Cisek & Pastor-Bernier, 2014). Essentially, the nervous system may address the questions of specification (how to do it) before performing selection (what to do) (Cisek, 2007). Hence, in the action-based models, when one option is chosen, the focus is on selecting some aspect of an action to perform rather than selecting an abstract representation and then planning an action, as is the case in goal-based models. Thus, decision-making within the action-based framework is about evaluating the value of different possible actions, intending to move the body through the physical world in a way that navigates a landscape of behavioral relevance represented by a neural map (Pezzulo & Cisek, 2016).

2.3.3 The key role of movement kinematics

Given what has been discussed in the previous sections, even the simplest decision would involve a mechanism of competition among possible alternatives or among potential actions. Moreover, this competition need not necessarily be resolved before the final decision is made but could also occur during the execution of the selected action. If this reasoning is correct, the decision-making process would not be viewed as serial and discrete but as a continuous process.

Experiments in the field of decision-making, and more generally in the psychological domain, usually use instruments that we might call discrete. In most cases, participants are asked to respond through key presses, saccadic eye movements, or verbally. These methods are useful for limiting the variables involved and for targeting the phenomena of

interest; however, they are ballistic and enforce that decision-making occurs exclusively during the response time and therefore do not allow the dynamics of internal processes to be shown (Song & Nakayama, 2009; Wispinski et al., 2020).

Attempts to unravel the continuous nature of internal processes were made using continuous dependent measures. This was achieved by developing tasks in which participants, to provide the answer, had to perform an action (e.g., hand or eye movement). Today, there is a long list of studies that brings evidence of how in-flight movements during multiple target choice tasks are affected by the evolution of the decision process and how this enables us to have continuous access to it (for reviews, see (Dotan et al., 2019; Gallivan et al., 2018; Gordon et al., 2021; Shadmehr et al., 2019; Song & Nakayama, 2009; Wispinski et al., 2020)).

A notable example of how cognitive and perceptual processes are fluid and continuous are changes of mind, i.e., the rare but reliable observation that individuals, who have begun an action toward one option, switch to another option mid-flight before the action is completed, suggesting that the decision process is continuous throughout the movement (Resulaj et al., 2009).

Most experiments that fall under this perspective have been primarily concerned with perceptual phenomena or low-level cognition. A seminal work exploiting this strategy is the one by Spivey et al. (2005), which aimed to investigate the temporal dynamics of recognizing spoken words. The task required participants to move a computer mouse to click on a target picture while a distractor picture was presented on the opposite side of the screen. The results, shown in Figure 2.3, revealed that mouse-moving trajectories were more attracted to a distractor when the names of the target and distractor were phonologically similar, e.g., picture and pickle, than dissimilar, e.g., picture and jacket. The direction and magnitude of the curved trajectories reveal the activated word and the level of competition between words over time, indicating a dynamic online competition between simultaneously activated lexical representations.

Another study used finger tracking to demonstrate that the categorization of numerical stimuli is not discrete, but that their mental representation places them on a spectrum from smallest to largest (Song & Nakayama, 2008). This representation influences their

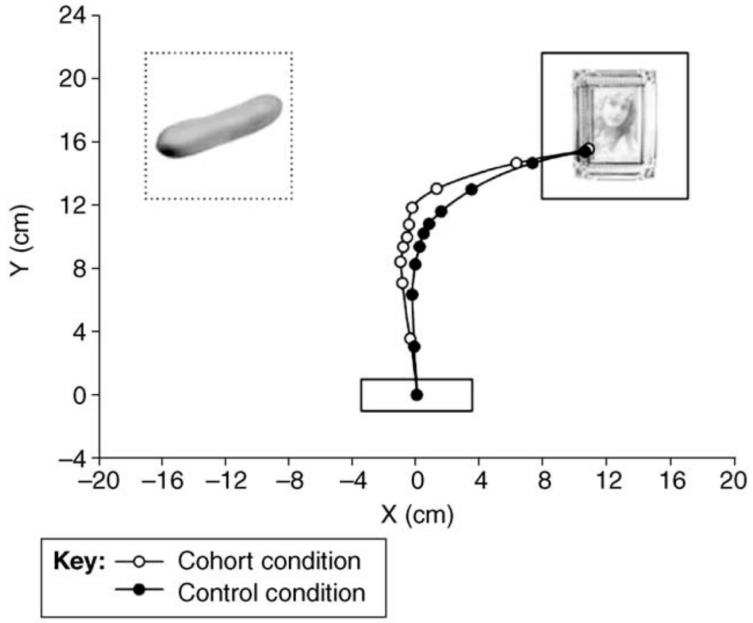

Figure 2.3: Mouse-moving trajectories reveal the dynamics of spoken word recognition. After hearing a word (e.g., picture), participants clicked on the corresponding target image. In the control condition, participants heard phonologically dissimilar words (e.g., picture and jacket); in the cohort condition, the words were phonologically similar (e.g., picture and pickle). The trajectory revealed a greater curvature towards the distractor in the cohort condition. Adapted from Spivey et al. (2005).

recognition and it was evident in the movement. In their experiment, participants were asked to indicate whether the presented number was smaller or larger than five by pointing to the left or right of the central point. The numerically close the target number was to five, the more the trajectory was curved and deflected toward the center; the further the number was from five, the more direct the trajectory was (Figure 2.4).

Continuous choice-reaching tasks are useful not only for investigating perception, attention, and language but also for studying higher-level cognitive decisions as they closely mimic real-world scenarios. In a study, McKinstry et al. (2008) showed the unfolding of the decision-making process in an experiment where participants had to make decisions based solely on internal criteria. Their task was to answer questions categorically ('yes' or 'no') and use the computer mouse to reach the box corresponding to the chosen answer. The questions were intentionally designed to have different truth values. In fact, they had previously been presented to a sample of other participants and were ranked according to how many people on average answered 'yes' to them, e.g., 'Is a thousand more than

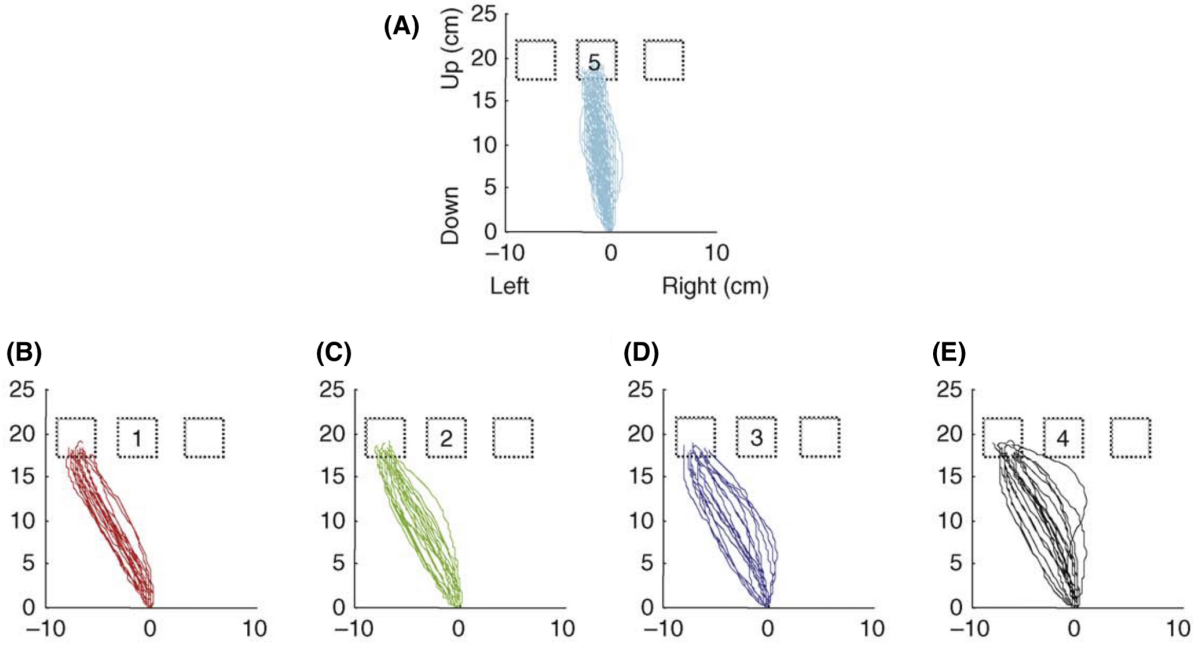

Figure 2.4: Reach trajectories reveal spatial number representation. Participants were asked to indicate whether the number shown in the central square was equal to, greater, or less than 5. (**A**) reports the trajectories for 'equal to' and (**B-E**) reports 'less than' 5. Lower panels show how the trajectories are more curved and less straight towards the left square as the target number in the central square approaches 5. Adapted from Song and Nakayama (2008).

a billion?' 0% 'yes', or 'Is murder sometimes justifiable?' 60% 'yes'. The results showed a difference between the two types of answers ('yes' versus 'no'): their trajectories had different temporal and spatial characteristics. Moreover, a difference was also found depending on the type of question: low-truth questions had more curvature and lower peak velocity than high-truth questions.

In summary, the above results highlight how movement analysis can provide numerous insights into decision-making processes. This is confirmed by a growing body of evidence examining the dynamics of high-level cognitive processes through continuous variables, which has been successfully used to advance knowledge in a variety of fields and contexts (e.g., linguistics (Spivey et al., 2005), number representation (Song & Nakayama, 2008), degree of confidence (Dotan et al., 2018), changes of mind (Barca & Pezzulo, 2015; Resulaj et al., 2009), and even intention prediction (Cavallo et al., 2016; Patri et al., 2020) and decision-making (Kieslich & Hilbig, 2014; Turri et al., 2022)).

2.3.4 The reach-to-grasp movement

Movements that are best suited to capture the continuity of internal processes are those of the upper limbs. Unlike the gaze, the hand moves in physical space, allowing for easier detection of its movements, and its movement has various features that can be observed and measured (Freeman et al., 2011). Indeed, the experiments discussed so far have focused on the trajectory of hand motion, studying pointing movements either directly, through a sensor placed on the hand (Song & Nakayama, 2008), or indirectly, through mouse-tracking (McKinstry et al., 2008; Spivey et al., 2005). However, pointing movements are not the only ones that have been used in the study of cognitive processes.

In everyday life, one of the actions we perform most frequently is to grasp an object in our surroundings. It is a movement we perform so often that we do not even realize how complex it is; it requires the perception of the object characteristics, action selection, movement planning, multi-joint coordination, and force regulation. This movement is referred to in the literature as *reach-to-grasp* and is one of the first goal-directed behaviors to develop during infancy.

For experimental purposes, one might think that reach-to-grasp movement is uninteresting since it consistently exhibits the same characteristics in every situation. Instead, experimental research has revealed numerous characteristics that vary according to different factors (Castiello, 2005). Grasping an object is an action that is largely influenced by the characteristics of the object itself. For example, depending on the object's size, two types of grasping can be distinguished: precision and power grips. However, size is not the only feature that has been shown to exert an influence on movement: it also varies according to the shape, material, fragility, and weight of the object (Jeannerod, 1981).

Moreover, the surprising thing about reach-to-grasp movement is that its kinematics are influenced not only by external features but also by the agent's mental state. Even if the object to be grasped is exactly the same, the movement differs depending on the underlying intention. Grasping a bottle, for example, has very different characteristics depending on whether the agent wants to pour the contents into a glass, place it elsewhere, throw it, or pass it to someone else (Ansuini et al., 2008). This is coherent with the *concepts of orders of planning* proposed by Rosenbaum et al. (2012): *first-order planning* for object manipulation involves adapting one's behavior to the current task, such as

adjusting the orientation of one's hand to grasp an object or adjusting grip aperture based on the object's size; *second-order planning*, instead, not only considers the current task but also anticipates and prepares for the next task to be performed. This is confirmed by further research showing that the synergy of advanced movement tracking techniques (i.e., motion capture systems) and machine learning techniques (e.g., multivariate decoding methods) enabled the unraveling and quantitative measurement of internal mental states information hidden in movement kinematics (Ansuini et al., 2015; Becchio et al., 2018; Cavallo et al., 2016; Montobbio et al., 2022; Patri et al., 2020; Turri et al., 2022). This research proves how the reach-to-grasp movement is particularly valuable for investigating the temporal evolution of decision-making. Indeed, unlike the pointing movement, it is an action that frequently occurs in people's lives, and most importantly, it is a movement that is highly affected by internal processes in several of its kinematic variables.

2.3.5 The vigor of a movement

Why do we run toward the people we love, but only walk toward others? Why, in general, do we move faster toward things we value more? These questions fascinated neuroscientists, who, over the past decade, showed that vigor of eye and hand movement reflects not only the choice made but also the subjective value associated with that choice (see Shadmehr et al. (2019) for a review). That is, if we want to know the extent to which an individual prefers a particular option among several, we can ask the individual to pick each one at a time. The option with the greatest velocity and shortest reaction time will be the preferred one. Then, calculating the difference in velocity and reaction time between options will allow us to quantify the extent to which that option is preferred over the others.

One of the first attempts to investigate whether the reward modulates saccades is by Xu-Wilson et al. (2009). In this study, participants maintained their gaze at a fixation point while a small image appeared at a distance of 15° for a brief period. The image could be a face, an inverted face, an object, or noise. Participants were instructed to keep their gaze on the fixation point until the image disappeared and then to move their eyes to a new fixation point. Upon completing the eye movement, they were rewarded with the image for 1 second. This experiment found that when participants would see a face, they made faster saccades than when they were shown an unrewarding noise image. This suggests that the anticipation of a reward can affect saccade velocity. A similar result

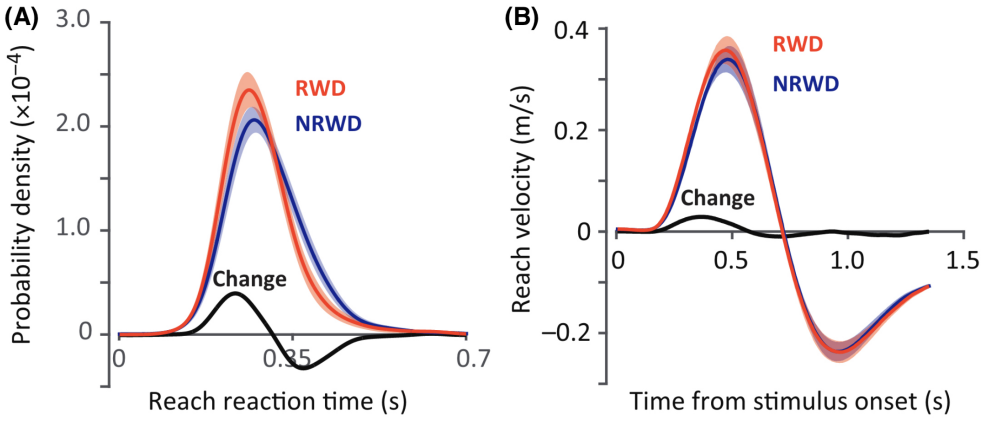

Figure 2.5: Effect of reward on reaction time and reach velocity. (**A**) Probability density of reaction time associated with rewarded (RWD) and non-rewarded (NRWD) targets. Reaction times were shorter in the rewarded condition. (**B**) Hand reach velocity as a function of time in rewarded (RWD) and non-rewarded (NRWD) conditions. Reach velocity was faster in the rewarded condition. Adapted from Summerside et al. (2018).

was previously observed in a study on monkeys (Kawagoe et al., 1998).

More recently, it has been investigated whether this phenomenon also affects upper limb movements. This was pursued in the study by Summerside et al. (2018), which found that increased reward affected the vigor of reaching movements. Participants were asked to perform out-and-back reaching movements to one of four quadrants through a robotic arm. Visual feedback of the hand was blanked out during reaching. Once the hand crossed the outer ring within the quadrant, the outer ring changed color, indicating the end of the trial. Only one quadrant was paired with an abstract reward consisting of a pleasant tone, a visual animation, and points that accumulated but were not associated with money. The study found that when a quadrant was paired with reward, the reaching movement toward that quadrant occurred after a shorter reaction time, with a higher peak velocity and greater amplitude (Figure 2.5). Additionally, movements toward the rewarded quadrant were performed with less variability. A more ecological version of this study, in which reward had subjective value, is the study by Sackaloo et al. (2015). Participants were asked to reach for a candy bar, pick it up, and return it to a starting position. Different candy bars were presented in random order. After the reaching trials, participants filled out a survey describing their preference for the bars. The results showed that reach duration was shortest for the most preferred candy bar and longest for the least preferred bar.

In summary, research demonstrated how vigor can be exploited as a proxy for measuring individuals' degree of preference, providing further evidence of the neural link between decision-making and motor control systems.

3. Study 1: Decoding social decisions from movement kinematics

Published paper: Turri et al. (2022)

3.1 Introduction

A convergence of modeling, behavioral, and neural data indicates that the way individuals move can provide important insights into cognitive states and ongoing decision processes (Becchio et al., 2018; Dotan et al., 2019; Gallivan et al., 2018; Gordon et al., 2021; Shadmehr et al., 2019; Wispinski et al., 2020). For example, in choice paradigms, the trajectory of reaching movements reveals not only the chosen option, reflected by the reaching direction, but also the degree of confidence with which the choice is made, reflected by the hand-speed (Dotan et al., 2018; Seideman et al., 2018). Reaching kinematics can be used to infer intention (Cavallo et al., 2016; Patri et al., 2020), categorization dynamics (Freeman et al., 2016), and reward associations (Chapman et al., 2015). Moreover, specific events within reaching trajectories can be used to detect changes of mind (Barca & Pezzulo, 2015; Resulaj et al., 2009) and changes in confidence (Dotan et al., 2018).

These aforementioned studies examined individual choices, which typically involve clearly defined probabilities and outcomes. However, many of our most important decisions are made in the context of social interactions and are based on the concurrent decisions of others. These social decisions affect not only ourselves but also others, and are therefore shaped by both self- and other-regarding motives (Fehr & Camerer, 2007; Rilling & Sanfey, 2011; Sanfey, 2007). An example of this is when we decide whether or not to help another person – how we balance our aversion to unequal outcomes with economic self-interest.

Only a few studies have considered the possibility that reaching parameters may be useful in interpreting these kinds of social decisions. For example, Kieslich and Hilbig (2014) found that in a two-person-social dilemma game, the trial-averaged trajectories were more curved when individuals defected than when they cooperated, suggesting that defection entailed more conflict. However, whether social decisions may be predicted from the kinematic parameters of individual reaching movements remains an unexplored question.

Here we designed a direct test of this hypothesis by developing a motor version of a widely used behavioral economic game, the Ultimatum Game (Rilling & Sanfey, 2011). In this task, two players – a proposer and a responder – are given the opportunity to split a sum of money in a single interaction. The proposer makes an offer as to how the money should be split. The responder has the option to either accept or reject this offer. If the offer is accepted, the sum is divided as proposed. If it is rejected, neither player receives anything. Game theory predicts that a rational, self-interested, responder will accept any non-zero offer. However, experimental evidence contradicts this prediction. Responders accept fair offers close to the equal split but generally reject low offers, considering them unfair (Camerer, 2003). Of course, punishing the proposer for a low offer is costly for the responder, and therefore the responder faces a conflict between the decision to either accept the low offer, and satisfy economic self-interest, or to reject it, based on inequity aversion (Fehr & Schmidt, 1999), negative reciprocity (Rabin, 1993), or reputational concerns (Yamagishi et al., 2012).

The decision to accept or reject is ultimately communicated through an action. For example, participants accept or reject the offer by pressing one of two buttons (Civai et al., 2012; Corradi-Dell'Acqua et al., 2013). In a classical neuroeconomic setting however, this action is considered merely a means of reporting the choice, and no study has yet examined the relationship between movement kinematics and decision parameters. Do accept and reject preferences influence the way individuals move towards the chosen option? Is the subjective assessment of the received offer reflected in the responders' movements?

One difficulty in addressing these questions is the high variability of movement kinematics across repetitions of the same movement and across individuals - kinematics vary from one trial to another, and from one individual to another (Ting et al., 2015). A common

approach is to average kinematics both over trials and individuals to reduce the effect of movement variability. However, because trial-to-trial and individual-to-individual variations often exceed decision-predictive variations, averaging can obscure how decisions map onto movement parameters. An alternative to averaging is to apply multivariate decoding methods as a tool for investigating information specified in movement kinematics at the single-subject, single-trial level (Becchio et al., 2018; Becchio & Panzeri, 2019; Becchio et al., 2021; Panzeri et al., 2017; Patri et al., 2020). Here, we applied multivariate decoding to explore decision-predictive information encoded in the kinematics of individual responders in the one-shot Ultimatum Game. This approach enabled us to identify highly personalized patterns specifying predictive information about both the fairness of a received offer as well as the choice to either accept or reject that offer.

3.2 Results

We used motion capture to track the arm kinematics of 20 participants while they played a motor version of the one-shot Ultimatum Game. Participants completed two sessions, always in the role of responder. They were told that in each session they would partner with 68 proposers recruited online and play a single iteration of the game with each proposer via a computer interface (Figure 3.1A and Figure A.1). Offers from a pot of €10 were made according to a predetermined algorithm, which ensured that all participants received the same set of fair (€5, €4), mid-range (€3), and unfair (€2, €1) offers. On each trial, participants were instructed to respond by reaching out, grasping, and lifting one of two cylinders labeled 'accept' and 'reject', located to the left/right of the body midline, respectively (Figure 3.1C). We reasoned that if the same object in the same location is grasped differently depending on a responder's choice (accept versus reject), then variations in movement kinematics reflect the choice itself. By the same logic, if the same object, in the same location, is grasped differently depending on the fairness of the offer (fair versus unfair), then variations in movement kinematics reflect a response to the perceived fairness of the offer, independent of the subsequent choice. To ensure that any effects were not due to the direction of movement, we reversed the positions (left and right) of 'accept' and 'reject' cylinders across sessions.

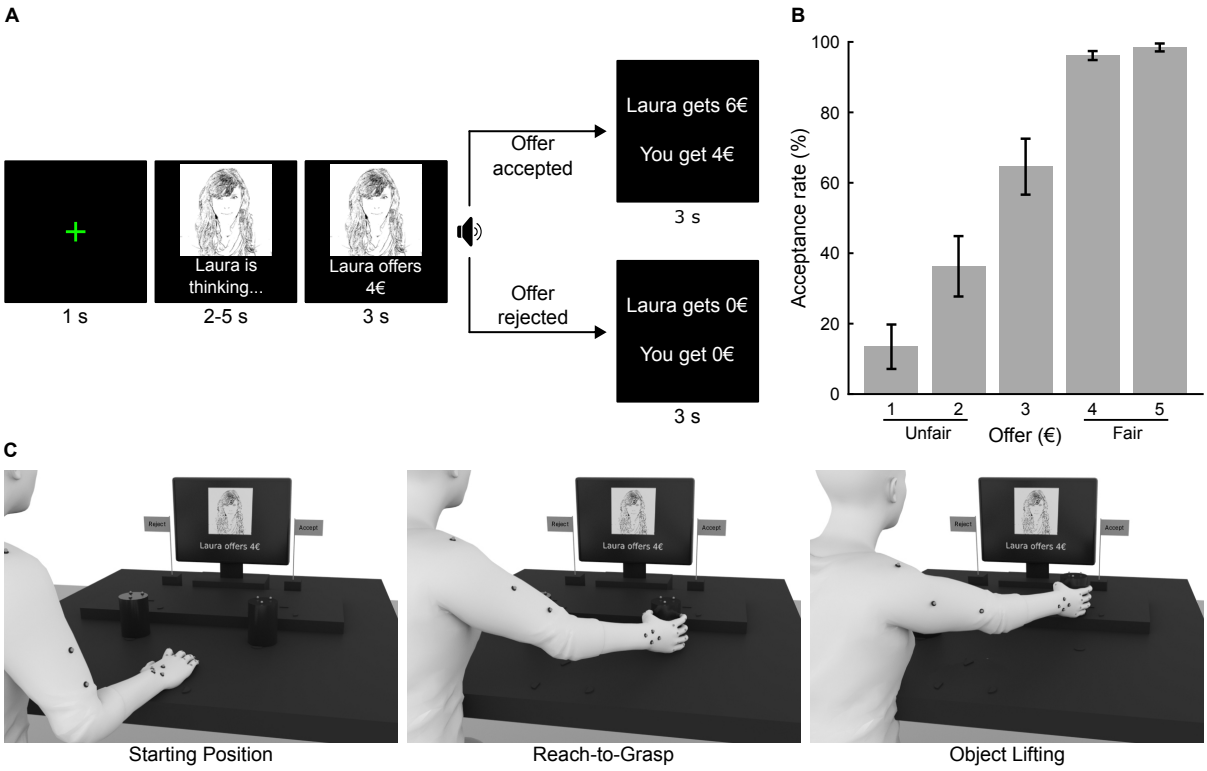

Figure 3.1: Trial design, experimental design, and behavioral results. (**A**) Trial design of the Ultimatum Game task. (**B**) Average acceptance rates (±SEM) of the 20 responders. (**C**) Schematic of experimental design.

3.2.1 Acceptance rates

Acceptance rates, computed as the number of accepted offers divided by the number of proposed offers across each offer level, were similar to those previously reported in the Ultimatum Game literature (Sanfey, 2007). Participants accepted almost all fair offers (€5: 98.4 ± 1.1%, €4: 96.13 ± 1.3%, mean ± SEM), with decreasing acceptance rates as the offers became less fair (€3: 64.6 ± 7.9%; Figure 3.1B). Unfair offers (€2, €1) were accepted only 36.3 ± 8.6% and 13.4 ± 6.3% of the time, respectively.

3.2.2 Clustered single-responder representations

Kinematic traces revealed large variability across trials and individuals. Figure 3.2A-C shows representative movement traces towards right targets clustered by responder's identity, choice, and fairness. Each line is a reach-to-grasp action. To examine whether there was structure in this behavioral variability, as an exploratory step, we applied a

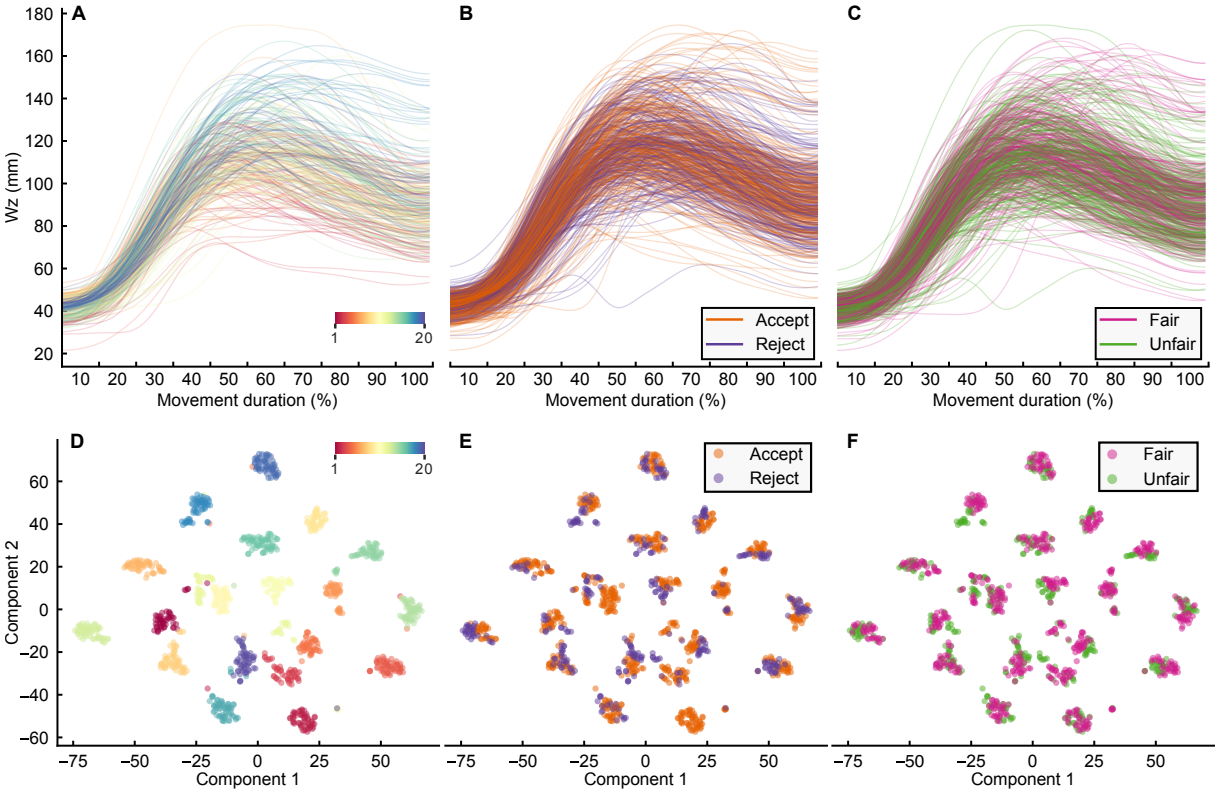

Figure 3.2: Single-trial movement kinematics. (**A**-**C**) Representative kinematic traces of wrist height (W_z) graphed by responder's identity (**A**), choice (**B**), and fairness (**C**). Each line is an individual reach-to-grasp movement. (**D**-**F**) Application of t-SNE to movement traces. Each point represents an individual reach-to-grasp movement embedded into a two-dimensional space using t-SNE. Points are color-coded based on the responder's identity (**D**), choice (**E**), and fairness (**F**).

non-linear dimensionality reduction technique, namely the t-distributed stochastic neighbor embedding (t-SNE) (van der Maaten & Hinton, 2008) (Figure 3.2D-F), to reduce the dimensionality of kinematic data to two dimensions. The proximity of traces in this reduced space reflects the similarity of traces in the high-dimensional kinematic space. t-SNE revealed a reliable segmentation of the 1000 traces into 20 isolated clusters. Color coding traces based on responders' identities revealed that each cluster almost perfectly identified an individual responder (Figure 3.2D). Within each cluster, traces showed further separation between accepted and rejected offers (Figure 3.2E), as well as between fair and unfair offers (Figure 3.2F). This suggests that social decision parameters are expressed in individualized motor patterns.

3.2.3 Decoding choice and fairness from movement kinematics of individual responders

To determine the relationship between social decision parameters and trial-to-trial variations in each responder's kinematics, we trained, separately for each responder, a logistic regression classifier to predict the responder's upcoming choice (accept versus reject) based on the unfolding of movement parameters during individual trials. By the same logic, we trained a logistic regression classifier to predict, for each responder, the fairness of the proposed offer (fair versus unfair). The training set comprised, for each responder, fair (€4, €5) and unfair (€1, €2) offers. Logistic regression classifiers find a set of linear weights on kinematic features that maximize the cross-validated probability of correctly decoding the decision parameter for the individual responder. To ensure that these weights reflected true kinematic profiles (and not mixtures of movements towards left and right targets), we trained separate logistic regression classifiers for the left and right targets. We compared responder-specific logistic regression models with a set of alternative responder-specific classifiers of varying form and complexity. We verified that logistic regression classifiers performed better than or comparable to the alternative classifiers (see Figure A.2; Table A.2).

Figure 3.3A shows the balanced prediction accuracies of individual responder classifiers trained on rightward movements. For both choice and fairness classifications, prediction accuracies were significantly higher than those expected for trial-shuffled data (in which the association between kinematic data and choice/fairness labels had been removed by shuffling) or random guesses (Figure 3.3A and Table A.1). The balanced prediction accuracies of individual responder classifiers trained on leftward movements were qualitatively similar (Figure A.3 and Table A.1).

The above results were obtained by training and testing separate logistic regression classifiers for each responder. In a control analysis, to test the individuality of motor patterns, we trained a logistic regression classifier using data from all but one responder and then tested them on the left-out responder. If patterns are idiosyncratic, we would not expect classifiers to generalize to the unseen responder. In line with this prediction, classifiers trained with this leave-one-subject-out cross-validation scheme showed chance performance (Figure A.4 and Table A.1), indicating that the relationship between kinematics and social decision parameters learned in one responder was not generalizable to

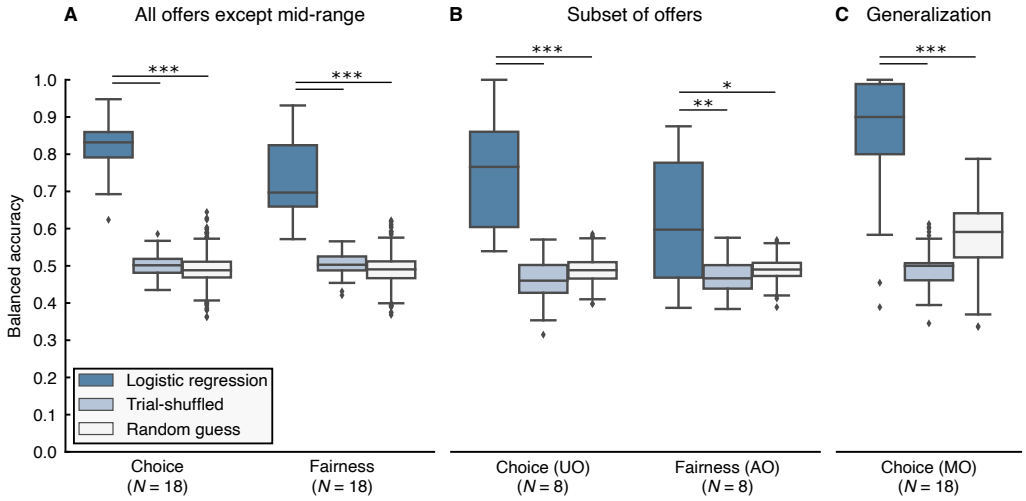

Figure 3.3: Performance of logistic regression classifiers trained with rightward movements. (**A**) Boxplots of balanced prediction accuracies of responder-specific logistic regression classifiers trained on rightward movements to predict choice and fairness. Prediction accuracies were significantly higher for actual data than for trial-shuffled data and random guesses. (**B**) Boxplots of balanced prediction accuracies for choice classification on unfair trials only (UO), and fairness classification on accept trials only (AO). (**C**) Boxplot of balanced prediction accuracies for choice classification on mid-range offers (MO). * indicates $p < 0.05$, ** indicates $p < 0.01$, and *** indicates $p < 0.001$. N indicates the number of responders included in each analysis.

other responders.

3.2.4 Disentangling choice and fairness information

The above results suggest that both the fairness of a proposed offer as well as the decision to accept or reject that offer can be predicted from single-trial kinematics of individual responders. However, given the dependence between fairness and choice – the probability of accepting a fair offer being three times the probability of accepting an unfair offer across trials – the above analysis cannot rule out the possibility that choice-related variations contribute to 'fairness' predictions, and by the same logic, fairness-related variations in movement kinematics contribute to 'choice' predictions.

To decouple the contribution of choice-predictive and fairness-predictive information, we examined the possibility of predicting choice from the kinematics of unfair trials only, and conversely, the possibility of predicting fairness from the kinematics of accepted trials only (because of the few rejected fair trials, predicting choice from fair trials only and

predicting fairness from rejected trials only was not possible). Conditioning the prediction of one class (e.g., choice) on a particular value of the other (e.g., fairness) discounts the effect of the latter on the prediction of the former. As shown in Figure 3.3B, for both classes, the conditional predictions were still consistently superior to those of both trial-shuffled data and random guesses (Table A.1). Taken together, these analyses suggest that movement kinematics contain information about both choice and fairness.

3.2.5 Kinematic choice patterns trained on fair and unfair offers generalize to mid-range offers

The above-described responder-specific choice predictions were trained and tested on fair (€5, €4) and unfair offers (€2, €1), excluding mid-range offers (€3). As a way of assessing the generalizability of kinematic patterns that discriminate between accept and reject choices across offer levels, we tested the ability of responder-specific choice classifiers, trained on fair (€5, €4) and unfair offers (€2, €1) of a given responder, to predict the responder's choice for mid-range offers (€3), not used for training. As shown in Figure 3.3C, the median balanced prediction accuracy across responders was again close to 90% (Table A.1). We, therefore, conclude that, within an individual responder, single-trial kinematics reflect choice information above and beyond the monetary value of the proposed offer.

3.2.6 Kinematic codes for fairness and choice

Having validated the capability of logistic classifiers to predict choice and fairness, we next used them to investigate how information about social decision parameters is specified in the kinematics of individual responders. Figure 3.4 visualizes the contribution (weight) over time of each kinematic feature for both choice predictions (Figure 3.4A) and fairness predictions (Figure 3.4B) for the rightward movements of an individual responder. A positive (negative) logistic regression weight is assigned to a feature that, over trials, is distributed with higher (lower) values for accept compared to reject choices, and for fair compared to unfair offers. For example, at 30% of movement duration, grip aperture (GA) is larger for reject choices and thus is assigned a negative value (Figure 3.4C). This pattern reverses around 70% movement duration when GA is assigned a positive weight. Similarly, GA is larger for fair compared to unfair trials around the time of the maximum hand aperture and is thus assigned a positive weight at 60% and 70% of movement dura-

tion for fairness predictions (Figure 3.4D).

To quantify the degree of (dis-)similarity of kinematic patterns across responders, we computed, separately for choice and fairness, the correlation between the weights of each responder and those of all other responders, separately for rightward movements (Figure 3.5A,B) and leftward movements (Figure A.5A,B). As expected, regression weights correlated weakly across responders, corroborating the idea that the encoding of social decision parameters is idiosyncratic. Nonetheless, it remains possible that across responders some features were used more than others. As an attempt to identify features used more often across responders, we plotted, for each feature, the number of responders for which the feature carried significant choice or fairness information (Figure 3.5C,D). This revealed a widely distributed use of features to encode information. Next, we individuated those features (marked with stars in Figure 3.5C,D) that were used for encoding by a number of responders higher than expected if encoding was distributed randomly across the kinematic space (Table A.3). As shown in Figure 3.5C,D, this analysis produced sparse maps, with few common features expressed, mainly observed at 10% and 100% of movement duration (Table A.3). This is expected because the start position (hand resting on the table) and the final position (hand on the cylinder) are relatively constrained, and inter-individual variability is lower at these time epochs (see Figure A.6). Individualized patterns are thus more likely to overlap at these epochs (Ting et al., 2015). The most used feature (Wx at 10% of movement duration) was employed by 9 out of 18 participants. Similar results were obtained when considering leftward movements (Figure A.5C,D). Viewed collectively, these results suggest that movement traces encode choice and fairness information, and that this information is expressed in highly personalized kinematic patterns, with only a few features common to sub-populations of responders.

3.3 Discussion

Social decisions have been almost exclusively studied in disembodied economic settings, in which the action component is somewhat of an afterthought, reduced to a stereotyped button press (Gordon et al., 2021). In the real world, however, social decisions are embodied into actions that require forward planning (i.e., what am I going to do next) (Becchio et al., 2018), that have associated costs (Kieslich & Hilbig, 2014; Shadmehr et al., 2019), and that can be observed by others (Gordon et al., 2021). This raises the question of

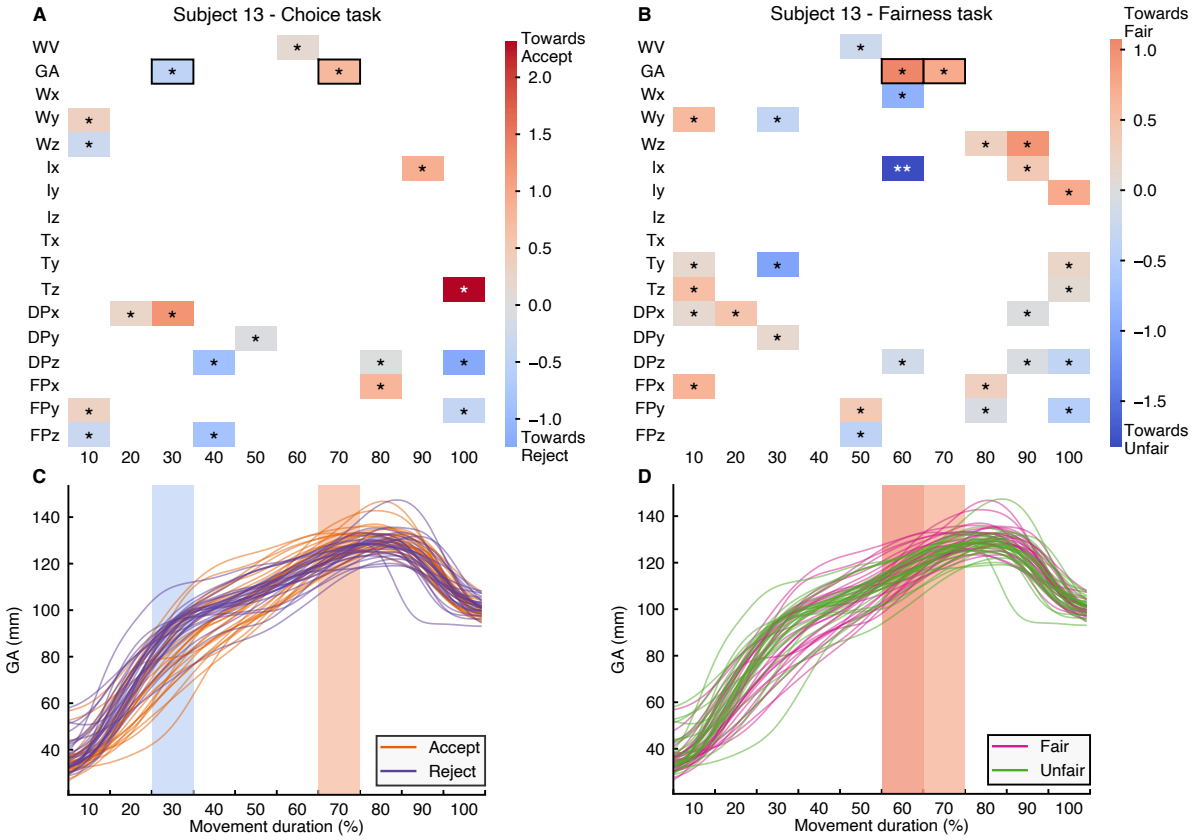

Figure 3.4: Encoding of choice and fairness in the kinematics of an individual responder. (**A** and **B**) Average logistic regression weights for choice (**A**) and fairness (**B**) classifications of rightward movements of an individual responder. (**C** and **D**) Time course of grip aperture (GA) of the same responder graphed by choice (**C**) and fairness (**D**). Each line is an individual reach-to-grasp movement. Time bins corresponding to significant positive and negative weights are highlighted. * indicates $p < 0.05$, ** indicates $p < 0.01$, and *** indicates $p < 0.001$.

whether, and to what extent, social decision parameters might be reflected in action parameters.

To answer this question, we used a multivariate single-subject, single-trial approach to decode key social decision parameters from the kinematics of responders playing a novel motor version of the Ultimatum Game. In this game, the responder faces a conflict between the decision to accept any non-zero offer, and thus maximize self-economic benefit, and the decision to reject non-equitable proposals, and thus punish unfairness (Camerer, 2003). Our approach revealed that movement contains predictive information about both the fairness of a proposed offer and the decision to either accept or reject that offer. These

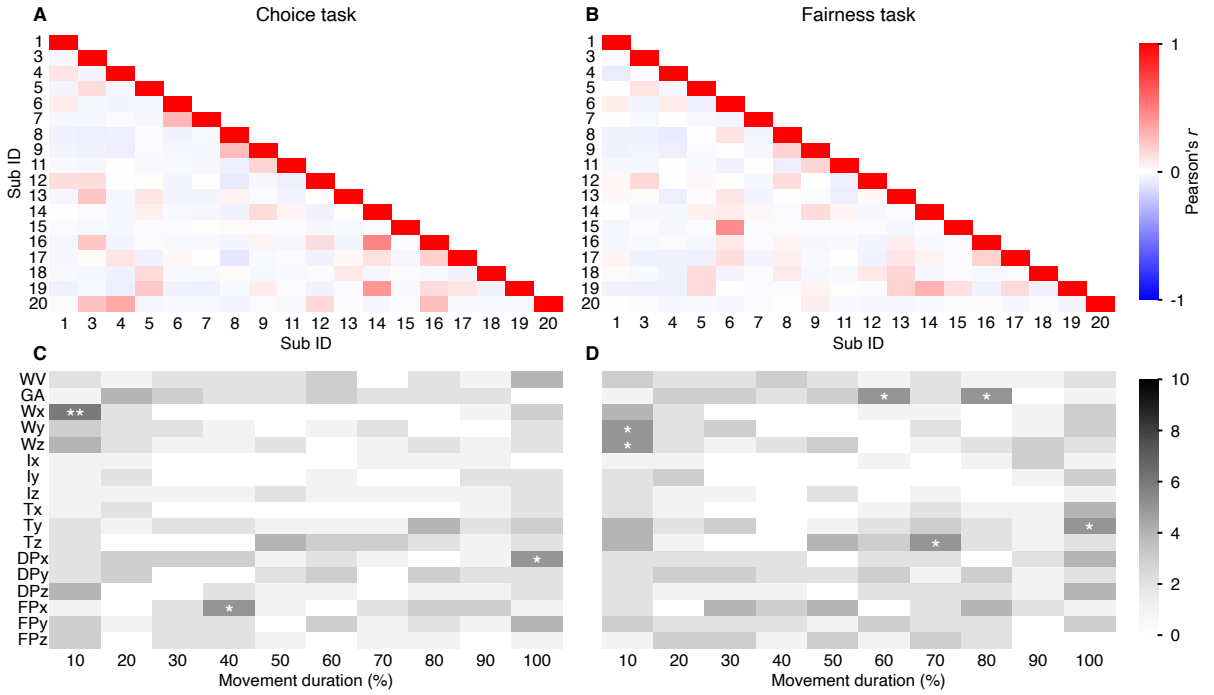

Figure 3.5: Overlap of choice and fairness weights across responders of rightward movements. (**A** and **B**) Pearson correlation of the average logistic regression weights between each pair of responders for rightward movements for choice (**A**) and fairness (**B**) classification. (**C** and **D**) Number of responders, for each feature, for which the feature was statistically significant for choice (**C**) and fairness (**D**) classification. * indicates $p < 0.05$, ** indicates $p < 0.01$, and *** indicates $p < 0.001$.

results suggest that how individuals move toward a choice option reflects social decision parameters and provides an ongoing readout of social decision dynamics.

3.3.1 Individuality in motor coding of social decisions

Each responder embodied a parametrization of choice and fairness information that was both consistent within a given responder and varied from one responder to another. This observation adds to the growing body of evidence documenting the individuality of motor solutions (Ting et al., 2015). Consistent with the suggestions that individual variability is high where the effect of motor output is low (Ting et al., 2015), we found that individual differences were most expressed while the hand was mid-air *en route* to the object.

It is tempting to speculate that above and beyond biomechanics, these differences may reflect differences in how the brain computes social decision parameters. Evidence from

brain imaging studies using the Ultimatum Game (Gabay et al., 2014) indicates that both choice and fairness information are represented in a distributed brain network that prominently includes the anterior insula, anterior cingulate cortex, dorsolateral and dorsomedial prefrontal cortex, supplementary motor area, cerebellum, and putamen. Future studies could examine whether and to what extent variations in fMRI signal within this network covary with movement kinematics.

Leveraging inter-responder differences in activation, covariance analyses between fMRI and kinematic data could then be conducted to identify the motion signatures of different decision strategies. Using fMRI while participants played the Trust Game, a task closely related to the Ultimatum Game, van Baar et al. (2019) found markedly different individual neural substrates for different decision strategies, even under conditions where the two strategies produce the same behavioral output. For example, inequity-averse subjects, motivated by a principled egalitarian rule, shared a distinctive activity pattern in ventromedial prefrontal cortex, dorsal anterior cingulate cortex, supplementary motor area, and bilateral superior occipital cortex. In contrast, guilt-averse subjects, this time motivated by an aversion to harming others, shared a particular activity pattern encompassing bilateral anterior insula, bilateral putamen, dorsomedial prefrontal cortex, and left dorsolateral prefrontal cortex. This demonstrates the utility of considering individual differences in motivations across social choice. Future empirical and modeling studies could usefully examine how kinematics covaries with activity in networks of regions associated with different individual strategies.

Finally, having learned how different strategies are reflected in differences in movement kinematics, future studies could reverse the inference and use kinematics to infer which strategy responders are using and when they are switching to another strategy. Individual decision strategies tend to be consistent across different contexts (Poncela-Casasnovas et al., 2016). However, individuals may apply strategic variability and switch between strategies. Movement kinematics may provide a means to discriminate between strategies and detect changes in strategy.

3.3.2 Readout of decision process during social interactions

In authentic social situations, people interact with others. An implication of our findings is that movement parameters expressing social decisions can be potentially exploited by

other people. In support of this notion, human perceivers can use subtle differences in movement kinematics to predict intention (Cavallo et al., 2016; Patri et al., 2020), discern deception (Sebanz & Shiffrar, 2009), and even infer the value of a poker hand from subtle variations in movement kinematics (Slepian et al., 2013). This suggests that human perceivers are sensitive to information encoded in movement kinematics (Becchio et al., 2018). However, further work is needed to explore the intriguing possibility of whether this sensitivity could extend to understanding motivational strategy and choice information from movement kinematics.

One potential challenge here is related to inter-responder variability of kinematic traces. Under these varying conditions, it might be difficult, if not impossible, for human perceivers to identify common features diagnostic of choice across responders. A strategy to deal with this variability might be to combine different sources of information, for example, kinematics and gaze behavior (Fiedler & Glöckner, 2012; Fiedler et al., 2013; Ghaffari & Fiedler, 2018). In sequential-presentation paradigms, final fixations on alternatives have been shown to be predictive of the subsequent other-regarding choices (Ghaffari & Fiedler, 2018). Future studies could test whether human perceivers are able to integrate information transmitted by gaze and hand behavior to predict social decisions.

3.3.3 Linking social decisions and sensorimotor control

By tracking fairness and choice in reach-to-grasp kinematics, we examined the possibility that parameters of social decisions influence sensorimotor control. Our single-subject, single-trial findings document a specific influence of fairness and choice on the kinematics of reach-to-grasp movements, above and beyond a target motor representation. These results provide a critical addition to the literature linking decision-making and sensorimotor control by suggesting that hand kinematics can reveal hidden parameters not only of individual decisions but also of more complex social decisions.

3.4 Limitations of the study

Here, we emphasize the individuality in motor coding of social decisions. However, our results do not exclude that individual motor signatures cluster into a limited number of motor phenotypes. Much larger sample sizes would be needed to test this hypothesis using unsupervised clustering procedures (Poncela-Casasnovas et al., 2016).

Further investigation is also required to establish the consistency of individual patterns across different strategic settings. Our results show that individual choice patterns for fair/unfair offers generalize to mid-range offers. If individuals exhibit similar kinematic patterns in different experimental settings, this would provide a more robust empirical case for the idea of an individual choice (and fairness) signature.

3.5 Methods

3.5.1 Experimental model and subject details

Based on previous work using logistic regression to decode intention from movement kinematics (e.g., Patri et al. (2020)), we aimed at testing 20 participants. Twenty-one participants completed the task. One participant was excluded from the data analysis because of extremely low acceptance rates of fair offers (acceptance rates were about 3.6 standard deviations below the group mean for both offers of 4 and €5). The remaining 20 participants (10 females; mean age 23; range 20-27) were right-handed with normal or corrected-to-normal vision. None of the participants reported neurological or psychiatric disorders. Written informed consent was obtained from each participant. The research was approved by a local ethical committee (ASL 3 Genovese) and was carried out in accordance with the principles of the revised Helsinki Declaration (World Medical Association General Assembly, 2008). All participants received monetary compensation proportional to the amount of money gained during the experiment (for details, see below). The dataset was collected before any analysis began, and no data was added subsequent to the beginning of analysis.

3.5.2 Method details

Task

Participants played a motor version of the Ultimatum Game as a one-shot game. The Ultimatum Game can also be played with the same two partners interacting repeatedly, see for example Cooper and Dutcher (2011). However, under these circumstances, the game morphs into a reputation game (Kreps et al., 1982), changing both the optimal and actual game strategies. We used the one-shot Ultimatum Game because this version minimizes strategic motives and is thus best suited for studying fairness responses (Rilling & Sanfey, 2011). Participants completed two sessions, always in the role of responder.

They were told that in each session they would play each iteration of the game in real-time with a proposer selected from a pool of 68 different players from the Istituto Italiano di Tecnologia, with whom they would connect via a computer interface. To minimize the use of strategic considerations, they were informed that the same pool of players would participate in both sessions (so that each responder would receive two offers from each proposer) but that proposers would not be informed of responder decisions until the end of the game. The offer could be 1, 2, 3, 4, or 5 out of €10. Participants were informed that if they accepted the offer, the money would be split as proposed; if they rejected the offer, neither player would receive anything. Unbeknownst to participants, the responder was, in fact, computer-simulated, and all participants received the same set of offers.

Apparatus

Each participant sat on a height-adjustable chair, with their right hand and wrist resting on a table. The hand, wrist, and right forearm were oriented on the parasagittal plane passing through the shoulder, and the right hand was in a semi-prone position, with the tips of the thumb and index finger on a tape-marked point, placed on the working space. The workspace (width = 100 cm; length = 110 cm) was covered with black fabric. Two upright cylinders (height = 11 cm; diameter = 7.5 cm; weight = 104 g) were placed in front of the hand position at a comfortable reaching distance (44 cm from the table edge to object), 18 cm to the left and right from body midline. The cylinders were labeled 'accept' and 'reject'. The proposed offer was displayed on each trial on a screen placed on the table together with the silhouette of the randomly selected proposer (see Figure 3.1C for a schematic representation of the experimental setup).

Procedures

Each trial started with a green fixation cross for 1 s presented at the center of the screen, followed by a silhouette of the proposer with the message '[Name of proposer] is thinking...' (e.g., 'Laura is thinking...'). This screen could last 2, 3, 4, or 5 s. The offer then appeared (e.g., 'Laura's offer is €4'), remaining visible for 3 s. Participants were instructed to make their choice within this time window by reaching out, grasping, and moving one of the two cylinders to a target platform (height = 3 cm; length = 27 cm; width = 50 cm). Two marked locations indicated where the cylinder should be placed. After placing the object, participants returned their hands to the starting position. After a tone, the money earned by each participant was displayed for 2 s (e.g., if the participant

accepted the offer: 'Laura gets €6, you get €4', otherwise, if the participant rejected the offer: 'Laura gets €0, you get €0'). Finally, a red fixation cross instructed participants to return, using their left hand, the cylinder to the home position. The trial design is depicted in Figure 3.1A.

As part of the cover story, participants were told that the selection of a proposer required at least 10 players to be connected at the beginning of the trial. If less than 10 players were connected, the computer would automatically generate the instruction to grasp one of the two cylinders (control trials). Each participant completed two sessions, separated by a short break. Each experimental session comprised 80 trials: 68 Ultimatum Game trials and 12 control trials (6 rightward, 6 leftward). In Ultimatum Game trials, each participant saw 12 €1 offers, 12 €2 offers, 12 €3 offers, 16 €4 offers, and 16 €5 offers. The number of offers was chosen based on previous studies (Sanfey et al., 2003) to mimic the offer pattern of a human proposer. Participants were informed that the financial compensation would be proportional to the money gained during the experiment. We debriefed participants at the end of the experiments. Post-experimental interviews confirmed that participants were unaware of the purpose of the study and had believed the cover story. One participant (participant 8) expressed the doubt that proposers were not real players. We verified that excluding the participant did not affect any of the results.

The order of trials was fully randomized across participants. The 'accept' and 'reject' labels assigned to cylinders were counterbalanced across sessions. The silhouette was female (male) in half of the trials (34 Ultimatum Game trials). Using logistic mixed effects models, we verified that neither the gender of the silhouette (proposer) nor that of the responder had any effect on the decision to accept or reject the offer (Table A.6). The E-Prime software (v.2.0.10.242) was used for the randomization of the trials and the synchronization with the kinematic acquisition. The experiment lasted for a total of 70 minutes.

Kinematic data acquisition

We recorded movement kinematics using a near-infrared motion capture system with eight cameras (acquisition frequency = 100 Hz; Motion Capture Vicon system). Cameras were positioned in a semicircle at about 1.5 m from the participant's location. Each participant was outfitted with 30 retro-reflective markers (Ø = 4 mm) placed on the dorsal surface of

the wrist (*wrist*) and hand (*palm*), radial and ulnar region of the wrist (*radio* and *ulna*), trapezoid bone of the thumb (*thu0*), tip, interphalangeal and metacarpophalangeal joints of the thumb (*thu3*, *thu2*, and *thu1* respectively), index (*ind3*, *ind2*, and *ind1*), middle (*mid3*, *mid2*, and *mid1*), ring (*rin3*, *rin2*, and *rin1*) and little finger (*lit3*, *lit2*, and *lit1*), lateral face of the elbow and arm, acromial process of right and left shoulder, sternal fork, xiphoid process of the sternum, and head (two frontal and two posterior, right and left). Three markers were also placed on the top of each cylinder. See Figure A.1A for a layout of marker placement.

Kinematic data preprocessing and computation of kinematic variables

Each trial was individually inspected for correct marker identification and then run through a low-pass Butterworth filter with a 6Hz cutoff. Kinematic variables were chosen to provide a complete description of arm and hand kinematics during reaching and grasping. Specifically, we used custom software (Matlab; MathWorks, Natick, MA) to compute two sets of kinematic variables of interest: F_{Global} variables and F_{Local} variables. F_{Global} variables, expressed with respect to the global frame of reference (the frame of reference of the motion capture system), included the following variables:

- wrist velocity, defined as the module of the three-dimensional velocity vector of the *radio* marker (in mm/s);
- x-, y-, and z-wrist, defined as the x-, y-, and z-component of the *radio* marker (in mm);
- grip aperture, defined as the Euclidean distance between the markers that were placed on the tips of the thumb (*thu3*) and the index finger (*ind3*; in mm); These variables served to characterize the arm kinematics. To characterize hand joint movements, we computed a second set of variables expressed with respect to a local frame of reference centered on the hand (i.e., F_{Local}). Within F_{Local}, we computed the following variables:
- x-, y-, and z-index, defined as the x-, y-, and z-component of the *ind3* marker (in mm);
- x-, y-, and z-thumb, defined as the x-, y-, and z-component of the *thu3* marker (in mm);

- x-, y-, and z-finger plane, defined as the x-, y-, and z-components of the thumb-index plane (defined by the markers *thu3*, *ind3*, and *ind1*). These components provide information about the abduction/adduction movement of the thumb and index finger irrespective of the effects of wrist rotation and of finger flexion/extension (Figure A.1A);

- x-, y-, and z-dorsum plane, defined as the x-, y-, and z-components of the radius-phalanx plane projection (defined by the markers *ind1*, *lit3*, and *wrist*). These components provide information about the abduction, adduction, and rotation of the hand dorsum irrespective of the effects of wrist rotation (Figure A.1A).

We have previously shown that these two sets of variables can be used to capture subtle differences between kinematics associated with different internal states (Cavallo et al., 2016, 2018; Koul et al., 2018; Montobbio et al., 2022; Patri et al., 2020). All variables were calculated only considering the reach-to-grasp phase of the movement, from reach onset (the first time at which the wrist velocity crossed a 20 mm/s threshold) to reach offset (the time at which the wrist velocity dropped below a 20 mm/s threshold). Having verified that movement duration did not vary as a function of choice or fairness ($p > 0.1$ for both parameters and movement directions), kinematic variables were normalized into a percentage of movement duration and analyzed as a continuous series of 10 epochs (0%-10%, 10%-20%, ..., 90%-100%), resulting into 170 kinematic features.

3.5.3 Quantification and Statistical Analysis

Single-trial kinematic vector

We summarized the kinematics of each reach (i.e., trial) as a vector in the 170-dimensional kinematic space spanning the 17 kinematic variables over 10-time epochs.

t-SNE

For visualization, we mapped the 170-dimensional single-trial vector of each trial onto a low-dimensional subspace with t-distributed stochastic neighbor embedding (t-SNE) (Figure 3.2). The perplexity parameter was set to 15 (similar results were obtained with a wide variety of parameters). Traces were then color-coded based on the identity of responders (Figure 3.2D), the choice to accept and reject the proposed offer (Figure 3.2E), and the fairness of the proposed offer (Figure 3.2F). We chose t-SNE because of its ability

to work even in the presence of non-linear relationships between features and outliers (van der Maaten & Hinton, 2008).

Decoding of choice and fairness with responder-specific logistic regression

We used logistic regression, similar to (Patri et al., 2020), to classify choice (accept versus reject) and fairness (fair versus unfair) from the multivariate single-trial kinematic vector, defined as above. The logistic regression choice classifier estimated the probability that a reach expressed the decision to accept the proposed offer as a sigmoid transformation of the kinematic vector in that trial. The equation of the logistic regression model was as follows:

$$P(y = 1|K) = \sigma(\beta_0 + \beta^T K) = \frac{1}{1 + e^{-(\beta_0 + \beta^T K)}} \tag{3.1}$$

$$P(y = 0|K) = 1 - P(y = 1|K) \tag{3.2}$$

where σ is the sigmoid function, K is the kinematic vector, y is the binary response variable ($y = 1$, if the offer is accepted; $y = 0$, if the offer is rejected), β is the vector of the regression coefficients (weights), and β_0 is a bias term.

Similarly, the logistic regression fairness classifier estimated the probability that a reach responded to a fair offer as a sigmoid transformation of the kinematic vector in that trial. The regression model equation was the same as that of the choice regression model, except that the regression was performed using a binary response variable for fairness ($y = 1$, if the proposed offer is fair; $y = 0$, if the proposed offer is unfair). See Figure A.1B for a block diagram of the model.

Both choice and fairness regression classifiers were trained separately for each responder. To be included in the analysis, each responder had to contribute a minimum of four trials in each class in each classification task. The number of trials available for individual responders is reported in Table A.4 and Table A.5.

Training of logistic regression models

To avoid penalizing predictors with larger value ranges, we z-scored the single-trial kinematic vectors within each responder. With the response variable encoded as 0 or 1, a penalized version of the logistic regression classifier was trained by minimizing the nega-

tive binomial log-likelihood LLR with an elastic net regularization (Friedman et al., 2010) defined as:

$$\min_{\beta,\beta_0} L_{LR}(\beta,\beta_0) = \min_{\beta,\beta_0}\Bigg\{ -\left[\frac{1}{n}\sum_{i}^{n} w_i(\beta_0+\beta^T K_i) - log(1+e^{\beta_0+\beta^T K_i})\right] \\ +\lambda\left[\frac{(1-\alpha)||\beta||_2^2}{2}+\alpha||\beta||_1\right]\Bigg\} \tag{3.3}$$

where n is the total number of trials, λ is the regularization parameter, α is a value between 0 and 1 weighing the relative contribution of the L1 and L2 penalty, and w_i is the rescaling weight assigned to the i-th trial that is inversely proportional to class frequencies of training data. The hyperparameter λ was tuned using a nested leave-one-trial-out cross-validation (LOTO-CV) procedure. We used all data available for each responder. An evaluation of how model performance scales with the amount of data is provided in Figure A.7, in which we repeated the responder-specific LR classifications as described here but using only 50% or 75% of the data available for each responder, rather than the full dataset. A grid search procedure was used to find the best λ value within the range `logspace(1, -3, 5)`. To obtain sparser, and thus more interpretable solutions, α was fixed at 0.95. We used $\alpha = 0.95$ because using this value, as shown in Friedman et al. (2010), provides numerical stability. To investigate the robustness and the stability of the solutions as α varied, for each responder, we computed the Pearson correlation between regression weights between each pair of α values in the set [0.5, 0.6, 0.7, 0.8, 0.9, 0.95, 1]. For each classification task, the average across responders of this correlation was always higher than 0.75.

The regression weights β and the bias β_0 were estimated minimizing the loss function $L_{LR}(\beta,\beta_0)$ via coordinate descent (Friedman et al., 2010). The logistic regression models were trained using the Python version (`http://hastie.su.domains/glmnet_python`) of the Glmnet package (Friedman et al., 2010).

Classifying the choice of the responder

For choice classification, the outcome variable was 0 for rejected offers and 1 for accepted offers. We considered only unfair offers (€1, €2) and fair offers (€4, €5) for this analysis. Mid-range offers (€3) were excluded from this analysis. This analysis was conducted over

18 responders for each direction of movement (leftwards and rightwards). The number of trials available for individual responders is reported in Table A.4.

Classifying the fairness of the offer

For fairness classification, the outcome variable was 0 for unfair offers (€1, €2) and 1 for fair offers (€4, €5). The €3 offers were excluded from this analysis. The analysis was conducted over 18 responders for each direction of movement (leftwards and rightwards). The number of trials available for individual responders is reported in Table A.4.

Classifying the choice of the responder using unfair trials only

In this analysis, we classified choice using only the subset of unfair trials. The analysis was conducted over 8 responders for rightward movements and 7 responders for leftward movements. The number of trials available for individual responders is reported in Table A.4.

Classifying the fairness of the offer using accepted trials only

In this analysis, we classified fairness using only the subset of accepted trials. The analysis was conducted over 8 responders for rightward movements and 7 responders for leftward movements. The number of trials available for individual responders is reported in Table A.4.

Generalization of responder's choices to over mid-range offers

In this analysis, the classifiers were trained to classify choice using all but mid-range offers (€3), which were used for testing. This analysis was conducted over 18 responders for each direction of movement (leftwards and rightwards). The number of trials available for individual responders is reported in Table A.5.

Control analysis using leave-one-subject-out cross-validation

In this control analysis, the logistic regression classifiers were trained to classify choice and fairness using data from all but one responder, and then tested it on the left-out responder. This analysis was conducted over 18 responders for each direction of movement (leftwards and rightwards). The hyperparameter λ was tuned using a nested leave-one-subject-out cross-validation procedure. The best λ value was found within the range `logspace(1,`

`-3, 5)` using a grid search procedure, and α was fixed at 0.95. As a test of the robustness of results, we repeated the analysis with values of α ranging from 0.5 to 1 and using k-fold cross-validation instead of leave-one-subject-out cross-validation. In all cases, prediction performance remained at chance for both choice and fairness.

Alternative classification approaches used for comparison

We compared logistic regression (LR in Figure A.2 and Table A.2) models with a set of alternative models in terms of how well they could predict choice and fairness. The results are shown in (Figure A.2 and Table A.2). Below, we briefly describe the alternative models used for comparison.

Multi-Task Logistic Regression classifier. Multi-task learning classifiers leverage useful information contained in related tasks to improve classification performance (Evgeniou et al., 2005). Here, we used multi-task learning (MTLR in Figure A.2 and Table A.2) to simultaneously classify choice (accept versus reject) and fairness (fair versus unfair) from the z-scored multivariate single-trial kinematic vector. The MTLR model was trained by minimizing the negative log-likelihood L_{MTLR} with L2-penalty defined as:

$$\begin{aligned}\min_{\beta,\beta_0} L_{MTLR}(\beta,\beta_0) = \min_{\beta,\beta_0}\Bigg\{\sum_{r=1}^{2}\frac{1}{n}\sum_{i=1}^{n} w_{i,r} log\left(1+e^{-y_{i,r}(\beta_{0,r}+\beta_r^T K_{i,r})}\right) \\ +\lambda_1\left[(1-\alpha)||\beta||_F^2+\alpha||\beta||_{2,1}\right]+\frac{1-\lambda_2}{\lambda_2}\sum_{r=1}^{2}\left\|\beta_r-\frac{1}{2}\sum_{s=1}^{2}\beta_s\right\|^2\Bigg\}\end{aligned} \tag{3.4}$$

where λ_1 is the elastic net regularization parameter, λ_2 is the task-coupling parameter, r and s are indexes that denote the task ($r, s = 1$ choice classification, $r, s = 2$ fairness classification), n is the number of trials, βt is the regression weight, β_0,r is the bias term, $w_{i,r}$ is the rescaling weight, $y_{i,r}$ is the response variable for the given task r in the i-th trial, and $K_{i,r}$ is kinematic vector in the i-th trial. The hyperparameters λ_1 and λ_2 were tuned using a nested LOTO-CV procedure and α was set to 0.95, using a grid search within the range `logspace(-3, 3, 7)` for λ_1, and `linspace(0.1, 1, 19)` for λ_2. The loss function was minimized using the L-BFGS method (Byrd et al., 1995). The MTLR models were implemented using PyTorch (Paszke et al., 2019).

Static Weights Logistic Regression classifier with time-integration. This version of the logistic regression classifier used static (that is, time independent) weights and time integration of evidence, similar to Montobbio et al. (2022). Specifically, the Static Weights Logistic Regression (SWLR in Figure A.2 and Table A.2) model estimated the single-trial cumulative probability $P(y(t)|[K(1),\ldots,K(t)])$ (i.e., the cumulative evidence) in favor of an accepted offer and a fair offer as a function of the time-dependent kinematic vector in that trial up to time t, as follows:

$$P([y(0)=1]) = P([y(0)=0]) = 1/2 \tag{3.5}$$

$$P([y(t)=0]|K(1),\ldots,K(t)) = \sigma(\beta_0 + K(t)\beta + w(y(t-1) - 1/2)) \tag{3.6}$$

$$P([y(t)=1]|K(1),\ldots,K(t)) = 1 - P([y(t)=0]|K(1),\ldots,K(t)) \tag{3.7}$$

where σ is the sigmoid function, β_0 is a bias term, K(t) is the kinematic vector at time epoch t, β is the vector of the regression coefficients (weights), and w is a coefficient weighting the cumulation of evidence over time. In each trial, classification was performed integrating evidence until the end of the movement (100% of movement time). The model was trained by minimizing the negative binomial log-likelihood with L2-penalty via stochastic gradient descent with adaptive moment estimation (Adam) (Kingma & Ba, 2014). The hyperparameter λ, controlling the strength of the L2 regularization, was tuned using a nested 5-fold CV procedure. The best hyperparameter λ was found with a grid search within the range `logspace(1, -3, 5)`.

Encoding-Decoding classifier. This classifier was similar to that used in Runyan et al. (2017). The Encoding-Decoding (ED in Figure A.2 and Table A.2) classifier includes an encoding part, which modeled each kinematic feature as a function of the choice of the responder, the fairness of the proposed offer, and their interaction, and a decoding part, which uses the encoding model to compute (using Bayes' theorem) the posterior probabilities of each responder's outcome given the kinematic parameter. Classification was then made by choosing the response class with the higher posterior probability. The encoding models were linear regression models fitted with the package scikit-learn (Pedregosa et al., 2011). In building response probabilities from the linear regression model, we assumed that noise was Gaussian and, similar to Runyan et al. (2017), that the kinematic features were conditionally independent given the responder's choice and the offer's fairness.

Gaussian Process Regression classifier. We finally classified responses using a Bayesian non-linear regression implemented as a Gaussian process regression (GPR in Figure A.2 and Table A.2) model (Rasmussen & Williams, 2005). The kinematic vectors were considered as noisy observations of a 170-dimensional latent function $f(K)$ defined as a Gaussian process:

$$f(K) \sim GP(m(K), c(K, K')) \tag{3.8}$$

where K, K' are any two vectors in kinematic space. The Gaussian process is specified by the analytical form and hyperparameters of a mean function $m(K)$ (in our case set to zero as kinematic vectors were z-scored for this analysis) and covariance function $c(K, K')$ that specifies the similarity of values between any two vectors in the kinematic space. As a covariance function $c(K, K')$, we chose a squared exponential with automatic relevance determination (SE-ARD) defined as:

$$c_{SE-ARD}(K, K') = \sigma_f^2 \, exp\left(-\frac{1}{2}\sum_{d=1}^{170}\frac{(K_{(d)} - K'_{(d)})^2}{l_d^2}\right) \tag{3.9}$$

where the signal variance σ_f^2 and the length-scales l_d are hyperparameters, and d denotes the feature. Unlike the commonly used squared exponential covariance function, which has a single length-scale for all features, this more complex covariance allows for a different length-scale l_d for each kinematic feature (Rasmussen & Williams, 2005).
We used a Gaussian likelihood function with hyperparameter σ_n^2 to model the level of the response variability, such that any samples of latent function $\boldsymbol{f}$ and observed response $\boldsymbol{y}$ at location $\boldsymbol{K}$ and any new samples (that is, the samples in the test set not used to train the model) of predicted values $\boldsymbol{f}_*$ at the unseen kinematic trials $\boldsymbol{K}_*$, has the following expression:

$$\begin{bmatrix}\boldsymbol{y}\\ \boldsymbol{f}_*\end{bmatrix} \sim N\left(0, \begin{bmatrix}C(\boldsymbol{K}, \boldsymbol{K}) + \sigma_n^2 I & C(\boldsymbol{K}, \boldsymbol{K}_*)\\ C(\boldsymbol{K}_*, \boldsymbol{K}) & C(\boldsymbol{K}_*, \boldsymbol{K}_*)\end{bmatrix}\right) \tag{3.10}$$

By conditioning on a set of observed (training) data points $\boldsymbol{K}$, we obtained a posterior distribution over function values at any unobserved data point, including those in the test set $\boldsymbol{K}_*$. To binarily classify the response in each test set data point, we passed the mean of the predictive function $\bar{f}(\boldsymbol{K}_*)$ through a Heaviside function that returned 0 if $\bar{f}(\boldsymbol{K}_*)$ was less than 0.5, +1 if it was greater than 0.5, and performs a random prediction if it was equal to 0.5.

The model hyperparameters $\boldsymbol{\theta} = [\sigma_f^2, l_d, \sigma_n^2]$ were randomly initialized and optimized during training by minimizing the negative log marginal likelihood (NLML) (Murphy, 2012), defined as:

$$-log\ p(y|\boldsymbol{K}, \boldsymbol{\theta}) = \frac{1}{2} y^T C_y^{-1} y + \frac{1}{2} log|C_y| + \frac{n}{2} log 2\pi \tag{3.11}$$

where $C_y = C(\boldsymbol{K}, \boldsymbol{K}) + \sigma_n^2 I$, and $|C_y|$ is the determinant of the covariance matrix C_y. The NLML was minimized through the Polak-Ribière conjugate gradient (CG) method (Nocedal & Wright, 1999), over a maximum of 1000 iterations. Since the NLML could suffer from local optima (Rasmussen & Williams, 2005), 10 random restarts of the optimizer were performed and the hyperparameters $\boldsymbol{\theta}$ associated with the smaller NLML were selected. The GPR model was fitted using the GPflow (Matthews et al., 2017). Performance was evaluated using LOTO-CV.

Quantification of classification performance

Classification performance was quantified as balanced classification accuracy. The balanced accuracy is the average of true positive and true negative classification rates. The true positive rate is the fraction of positives that are correctly classified as positives, and the true negative rate is the fraction of negatives that are correctly classified as negatives. Balanced accuracy, because it balances accuracies of positive and negative classification groups by their respective sample size, is useful in datasets like ours in which classification outcomes are unbalanced. To avoid overfitting, we computed balanced accuracies on test data using a LOTO-CV for all classifications.

Computation of the statistical significance of classification performance

To test whether classification performance was significantly above chance, we obtained an overall index of task performance by taking the median of the balanced accuracies across all responders. To create a null hypothesis distribution of median balanced accuracies under the assumption that there is no relationship between the kinematic data and the choice or fairness in the same trials, we trained the logistic regression models on trial-shuffled data with the choice/fairness labels randomly shuffled across trials (100 random shuffles without replacement per responder). We then computed an empirical p-value as $p = r/n_c$, where n_c was the number of samples of the null distribution (100 in this case), and r was the number of times where an element of the null distribution was greater than

or equal to that of the logistic regression models. To verify the ability of nonparametric permutation tests to maintain a low False Positive Rate (FPR) that matched the threshold set for significance across all sample sizes used in the analyses of Figure 3.3, following (Ince et al., 2012), we repeated 50 times the analyses in Figure 3.3 using permuted data with null information (rather than from the real data as in Figure 3.3). We found that using a threshold of $p = 0.05$ for significance, the FPR was stable and close to 0.05 in all the analyses (on average, overall all analyses and permutations, FPR was 0.03%). We also obtained an additional, less conservative, random-guess null-hypothesis distribution of 1000 median balanced accuracies using a random classifier with a prior random guess, i.e., a model that generates predictions by respecting the training set's class distribution. Then, an empirical p-value was computed as above.

Computation of the statistical significance of the values of individual logistic regression weights

With LOTO-CV, one set of regression weights is obtained for each left-out trial. For each responder, there are as many sets of regression weights as the number of available trials. To obtain a single set of regression weights from these data, we computed the median of the coefficients across all regression models for a given responder, after removing outliers outside the median * 2.5 times the median absolute deviation. The same procedure (but without removing the outliers) was also applied to regression models trained on trial-shuffled data (100 random shuffles without replacement of the trial labels) to generate a null hypothesis distribution of the values of weights of features under the assumption that there is no relationship between the kinematic data and the choice or fairness in the same trial. The removal of the outliers only in the data distribution but not in the null-hypothesis distribution ensures an ultra-conservative determination of features with significant weights. We then computed from this distribution a two-tailed empirical p-value of the hypothesis that the value of the coefficient (positive or negative) reflected only a random relationship between kinematics and choice or fairness. The p-values of the non-zero coefficients were FDR corrected ($\alpha = 0.05$) for multiple comparisons across all non-zero coefficients.

Computation of cross-correlations of logistic regression coefficients across participants

For each pair of responders, we quantified the similarity of choice or fairness encoding as the Pearson correlation (across kinematic variables and time epochs) between the median across all LOTO-CV models of the absolute value of the encoding weights of the first responder and the same quantity of the second responder.

Computation of the statistical significance of features concentration across participants

For each feature, we quantified x, the number of responders who had a significant weight for that feature. If significant weights were distributed randomly across the kinematic feature space, then x would follow a null-hypothesis binomial distribution with probability $p = M/(170 \cdot n)$, where M is the number of significant weights found over the n responders. To test the hypothesis that the concentration of responders with significant weights of a feature was higher than expected if significant weights were distributed randomly across the kinematic feature space, we thus used a one-tailed binomial test with parameters x, n, and p listed above.

4. Study 2: Social decision-making from a vigor perspective

4.1 Introduction

Every day we face situations that require us to make a decision, from the most trivial (e.g., what to eat for lunch) to the most crucial (e.g., accepting or rejecting a job offer). To better understand how we make decisions, economists introduced the concept of utility (von Neumann & Morgenstern, 1944), i.e., how much one values a particular option. This concept lies at the core of economic decisions and has been used by neuroscientists and psychologists to study the neural basis of decision-making. However, most of these studies merely focus on people's behavior, i.e., their choices, indicating only the order of preference among options (e.g., people chose option A over option B), neglecting the degree of preference that drives people's decisions (e.g., people preferred option A 70% more than option B) (Shadmehr & Ahmed, 2021).

Recent studies have examined how to measure the degree of preference and found that when deliberating among possible options, factors that influence subjective utility (e.g., reward and effort) influence the vigor of movements (Shadmehr et al., 2019). For example, Korbisch et al. (2022); Milstein and Dorris (2007); Xu-Wilson et al. (2009); Yoon et al. (2018, 2020) found that people's eye movements reflect decision variables, showing a higher peak saccade velocity and shorter reaction time when they direct their gaze toward the targets they value most. Utility also modulates reaction time and velocity of reaching acts: Summerside et al. (2018) and Sackaloo et al. (2015) found that the vigor of reaching movements was higher when directed toward rewarded or more valuable targets. Taken together, these findings suggest that vigor can be viewed as a continuous, real-time metric to measure the degree of preference and thus serve as a window into subjective utility,

enabling deeper insights into decision-making processes.

The aforementioned studies adopted paradigms with defined outcomes and probabilities, focusing on studying movement vigor in individual decisions. In contrast, most of our decisions occur during social interactions and are taken by considering the impact they will have on us and others (Fehr & Camerer, 2007; Rilling & Sanfey, 2011; Sanfey, 2007). A better understanding of whether and how vigor movement is expressed in a social context is needed.

Recently in Turri et al. (2022), we found that movement kinematics encodes social decisions using a motor version of an experimental economics game, the Ultimatum Game. There, a proposer receives a sum of money and must propose a split to the responder, who can accept or reject. If the responder accepts, the split is carried out; if the responder rejects, both get nothing. A fully rational responder, guided solely by self-interest, will accept any non-zero offer, as predicted by normative standards in game theory (i.e., Nash equilibrium) (Camerer & Thaler, 1995). Contrary to this prediction, responders behave irrationally and, despite implying a loss of money, reject the low offers perceived as unfair, thus punishing the proposer (Camerer, 2003). Our findings showed that reach-to-grasp movements encode information about both the responders' choice and the fairness of the proposers' offers.

With this in mind, we asked ourselves whether the relationship between the vigor of reaching movements and the subjective expected utility of proposers' offers is still intact in the case of this complex social interaction. If so, we should see a modulation of movement vigor driven by social decision variables, which in this case are the responder's choice and offer level. Therefore, we formulate the hypotheses as follows:

(i) for accepted offers, we hypothesized that vigor of reaching movements would increase with offer level;

(ii) for rejected offers, we contrasted three alternative hypotheses:

  (a) vigor decreases with offer level showing opposite behavior to that of accepted offers;

  (b) vigor increases with offer level and thus is not influenced by responders' choice;

  (c) vigor is unrelated to offer level and remains constant.

Here, we tested these hypotheses by analyzing previously collected data (Turri et al., 2022) focusing on some kinematic features: reaction time, movement time, peak velocity, and time-to-peak velocity.

We observed that responders, when accepting, reacted and moved faster as the offer level increased. Interestingly, the opposite behavior was found for rejected offers, where responders' vigor increased as the offer value decreased. Our findings suggest that movement vigor is influenced by decision variables even in social interactions.

4.2 Results

To test the relationship between vigor and offer level, and how this relationship is modulated by the choice to accept or reject the proposed offer, we analyzed the data collected in Turri et al. (2022).

Briefly, twenty-one participants played a motor version of the Ultimatum Game (UG), acting as responders, and as they played, we tracked their arm kinematics through a motion capture system. Participants underwent two sessions and were told that, in each session, they would be paired with 68 proposers and would play, via a computer interface, a single iteration of the game with each of them (see Figure 4.1A for the trial design). The delivered offers followed a predetermined scheme ensuring that all participants received the same offers. After the offer was presented, to make their choice, participants were instructed to reach, grasp, and lift one of two cylinders labeled 'accept' and 'reject', placed to the left/right of the body midline (Figure 4.1B). To avoid any effect due to the direction of movement, we swapped the cylinders' labels across sessions. Note that the starting and cylinder positions were always the same throughout the experiment, maintaining the effort of the reach-to-grasp acts fixed.

The acceptance rate of UG offers, computed as the number of accepted offers divided by the number of proposals for each offer level, was in line with those reported in previous studies (Gabay et al., 2014). Almost all fair offers were accepted (97.09% and 94.66% for €5 and €4 offers, respectively), while as offers became less fair, the acceptance rate decreased (63.40%, 37.08%, and 15.29% for €3, €2, and €1 offers, respectively).

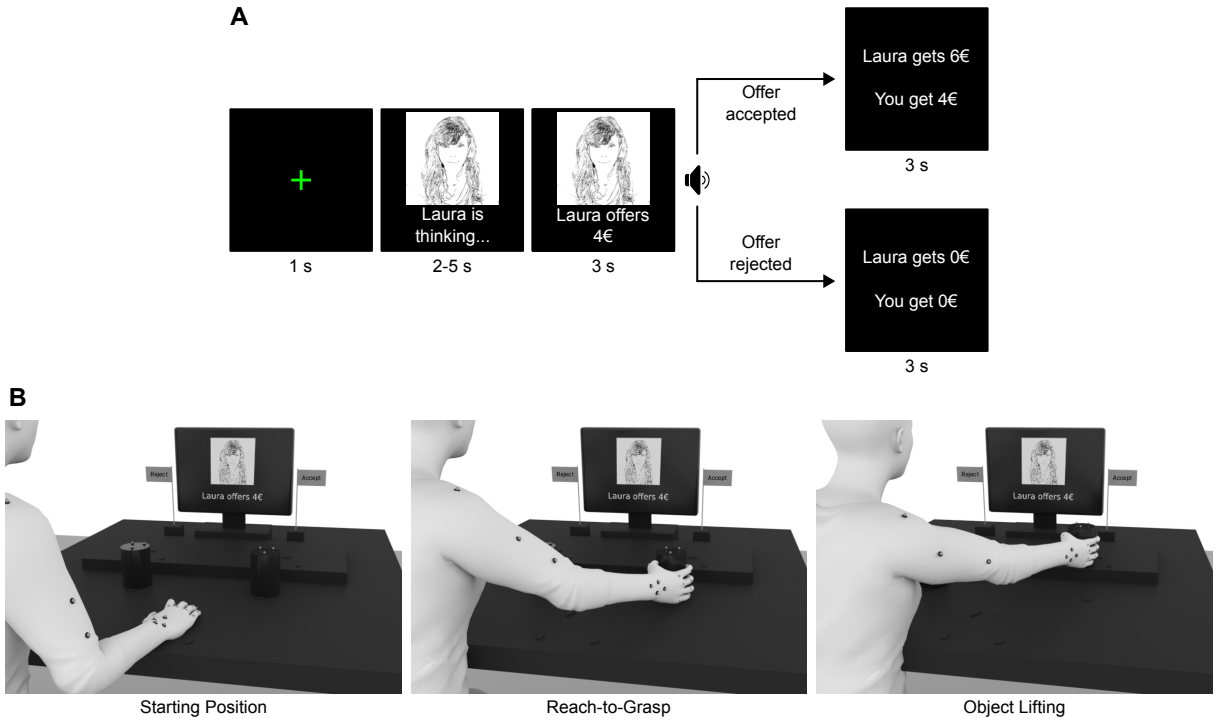

Figure 4.1: Trial and experimental design. (**A**) Trial design of the UG task. (**B**) Outline of experimental design. Adapted from Turri et al. (2022)

4.2.1 Social decision variables affect movement vigor

Based on previous works (Sackaloo et al., 2015; Summerside et al., 2018), we describe vigor of reaching in terms of reaction time (RT), movement time (MT), peak velocity (PV), and time-to-peak velocity (TPV). For example, Summerside et al. (2018) showed that subjects' peak velocities were faster and reaction times were shorter when faced with a rewarded target, indicating a more vigorous act compared to unrewarded targets. Another example is provided by Sackaloo et al. (2015), where the authors showed that subjects' movement time and movement units were significantly smaller when reaching for a candy associated with greater preference. In summary, an increase in vigor is reflected by shorter reaction and movement times, higher peak velocity, and earlier time-to-peak velocity.

We used linear mixed-effects models to statistically test whether responders' vigor, described by the kinematic variables mentioned above, was affected by social decision variables, i.e., offer level and choice. We found a significant effect of interaction between offer

level and responders' choice for RT, MT, PV, and TPV, suggesting that movement vigor is expressed differently between accepted and rejected offers (Figure 4.2, Table B.1, B.2, B.3, B.4, B.6). Specifically, in line with our hypothesis, we observed a positive relationship between vigor and offer level for accepted offers, meaning that participants reacted and moved faster as offer level increased (significant positive slopes for all the dependent variables, Figure 4.2, Table B.6). Concerning rejections, the trend is reversed; participants rejected low-level (unfair) offers more vigorously than higher offers (significant negative slopes for RT, PV, and TPV, Figure 4.2, Table B.6). Furthermore, we computed the difference between the slopes of accepted and rejected offers and observed that the two trends were significantly different for all the dependent variables (Figure 4.2, Table B.6).

As a control analysis, to test that vigor is not expressed by all the kinematic variables, we trained linear mixed-effects models with peak grip aperture (PGA) as the dependent variable, since it should not be modulated by vigor. Indeed, it is well established that grip aperture encodes information about the dimension of the object to be grasped (Ansuini et al., 2015). For example, when grasping a large object, PGA is greater and occurs later than for smaller objects. In our experimental setup (Figure 4.1B), the objects grasped to communicate the decision were identical. Thus, as expected, we did not find a significant main effect of responders' choice or offer level or the interaction between the two (Table B.5, B.6).

4.3 Discussion

Vigor of reaching was primarily investigated by measuring individuals' behavior with paradigms whose goal was to understand whether the degree of preference (Sackaloo et al., 2015) or increased reward (Summerside et al., 2018) was expressed via reaching kinematics. However, the modulation of vigor in the social domain is still under-explored.

In this work, participants played a motor version of UG in the role of responders, and we investigated whether social decision variables influenced the vigor of reach-to-grasp movements. We found that vigor increases according to the offer level for accepted offers, whereas the opposite was found for rejected offers.

Moreover, we noticed that the 'accept' and 'reject' vigor slopes cross at the offer level

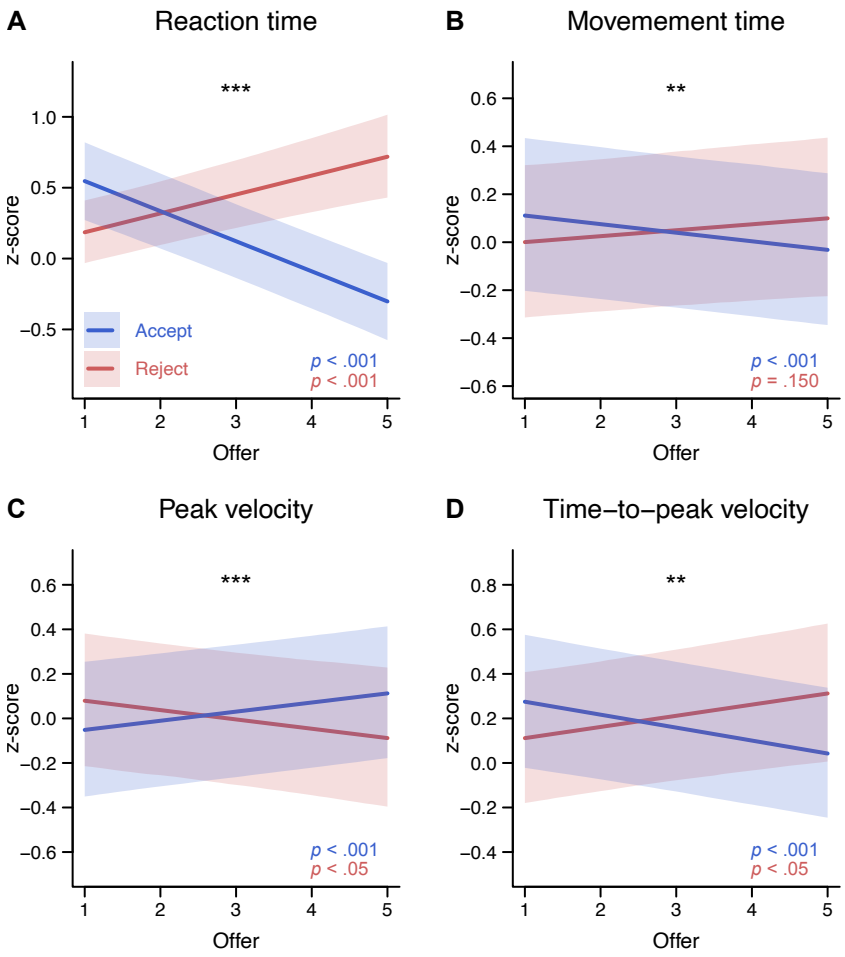

Figure 4.2: Reaction time, movement time, peak, and time-to-peak velocity as a function of decision variables. (**A**-**D**) Slopes of reaction time (**A**), movement time (**B**), peak velocity (**C**), and time-to-peak velocity (**D**) relative to the significant interaction between responders' choice and offer level (offer:choice) obtained with linear mixed effects modeling. Shaded areas represent the 95% bootstrap confidence interval of the slopes and intercepts. The p-values indicate whether the slopes were significantly different from zero. The asterisks indicate the significance level of the comparison between the 'accept slope' and the 'reject slope' (*: $p < .05$, **: $p < .01$, ***: $p < .001$)

of about €2-3. Referring to the behavioral results, we see that at these offer levels the average acceptance rate drops from about 63% for €3 to about 37% for €2 offers, passing through to the indifference point (i.e., 50%). This suggests that the intersection point of vigor slopes could be used to establish the indifference point at which responders switch from accepting to rejecting an offer. This is consistent with the findings of Krajbich et al. (2014), who show that RTs can be used to measure the strength of responders' preferences, with the longest RTs associated with the offer level closest to the indifference point.

4.3.1 Self-loss or other-punishment?

Our research and other studies showed that when presented with two options, individuals' actions tend to be more vigorous toward the most valuable options (Korbisch et al., 2022; Milstein & Dorris, 2007; Sackaloo et al., 2015; Summerside et al., 2018; Xu-Wilson et al., 2009; Yoon et al., 2018, 2020). We encounter this behavior with accepted offers. In fact, responders' representation of offer value in terms of utility is straightforward, and as expected, vigor increases as a function of the offer level.

However, it is intriguing what happens with rejections; as the offer becomes more unfair, the responders' vigor increases. What are the determinants of this behavior? Rejections in the UG are a means to punish the proposer and are exploited by responders who seek to restore balance and promote cooperation (Camerer, 2003; Fehr & Schmidt, 1999; Yamagishi et al., 2012). They can be thought of as characterized by two factors: *self-loss*, which is how much responder is losing, and *other-punishment*, which is the amount of inflicted punishment. Therefore, there are at least three possible explanations for this pattern of behavior.

First, we may assume that responders assign more utility to harsher punishments. This would translate into increased vigor as the offer level decreases, thus, reflecting other-punishment. A PET study by de Quervain et al. (2004) provides evidence for this hypothesis. They discovered that punishing defectors who violate social norms activates the dorsal striatum, which is involved in processing the rewards that result from goal-directed actions (Fehr & Camerer, 2007). Notably, the activation magnitude positively correlated with the severity of the punishment. This behavior falls within the framework of altruistic punishment, where individuals, even in one-shot interactions, are willing to bear a cost to themselves in order to encourage cooperation in human societies (Boyd et al., 2003).

Second, from a utilitarian perspective, we may reason for responders' willingness to punish unfairness as being related to their personal loss. Hence, vigor will decrease as a function of self-loss. In support of this, Civai et al. (2010) found that individuals who rejected unfair offers experienced increased emotional arousal only when the offers were directed against themselves (myself condition), and not against a third-party (third-party condition). This suggests that the increased arousal in the myself condition could be because individuals were incurring a self-loss, whereas this did not occur in the third-party con-

dition. Moreover, if an effect of altruistic punishment was present, we would also expect an arousal activation in the third-party condition.

Finally, the observed pattern of vigor could reflect a combination of both self-loss and other-punishment: for example, vigor would be highest under circumstances of low self-loss and high other-punishment and lowest in the opposite case.

The present experiments based on the UG were not designed to decide among these possibilities. Unfortunately, the UG does not allow disentangling the two factors (self-loss and other-punishment) since they are mutually coupled: rejecting an offer of €x always results in a self-loss of €x and an other-punishment of €(10-x), where x is the value of the offer. Therefore, they vary hand in hand and in opposite directions by proposing scenarios defined by low self-loss and high other-punishment (e.g., rejection of €1 offers) to scenarios with high self-loss and low other-punishment (e.g., rejection of €3 offers), without admitting situations where both self-loss and other-punishment are simultaneously low or high. With this paradigm, we cannot determine whether the observed inverse relationship between vigor and offer level for rejected offers depends on either an increase in self-loss, a decrease in other-punishment, or a combination of both. We then need to find an alternative socio-economical game that allows us to better understand this relationship.

4.3.2 Does emotional arousal modulate vigor?

The emotions that humans experience are reflected in their movements (Noroozi et al., 2018), and it could be that the vigor level of a movement is a reflection of emotional arousal. Studies reported that eye movements can provide valuable insights into cognitive functions and affective states, showing that eye-related features (e.g., saccadic velocity, time to first fixation, fixation duration, etc.) were influenced by the emotional content of stimuli (Skaramagkas et al., 2021). Our findings show the highest levels of vigor when responders accepted €5 and rejected €1 offers, which are the offer levels for which responders reported feeling stronger positive/negative emotions (Civai et al., 2010). However, we did not assess people's affective state in this study, and future research could include questionnaires and measurements of skin conductance responses to further explore the relationship between emotional state and movement vigor.

4.3.3 Is vigor read out by others?

Humans are social beings endowed with a unique ability: we can read out information encoded in the movement of others. This skill allows us to predict in advance the future actions of other people and be able to respond accordingly (Becchio et al., 2018). For example, external observers can take advantage of subtle variations in movement kinematics and deduce others' intentions (Cavallo et al., 2016; Patri et al., 2020). Our findings demonstrate that social factors influence movement vigor, but is this information visible to an external observer? Can an observer read out movement vigor and infer the utility information that we assign to it? Further work is required to address these questions which could be pursued as proposed by Becchio et al. (2021), where the authors provide an operational guide to test this hypothesis.

4.4 Methods

4.4.1 Experimental model and subject details

The results discussed in this work were obtained by analyzing previously acquired data. In the following, we report a brief description of the task and procedures. For detailed information, see Turri et al. (2022).

Twenty-one right-handed participants (10 females; mean age 23; range 20-27) with normal or corrected-to-normal vision completed the task. None of the participants reported neurological or psychiatric disorders. Written informed consent was obtained from each participant. The research was approved by a local ethical committee (ASL 3 Genovese) and was carried out in accordance with the principles of the revised Helsinki Declaration (World Medical Association General Assembly, 2008). All participants received monetary compensation proportional to the amount of money gained during the experiment.

4.4.2 Method details

Task

Participants played a motor version of the Ultimatum Game (UG) as a one-shot game completing two sessions in the responder role. They were told that in each session, via a computer interface, they would play each UG trial with a different proposer selected from

a pool of 68 players at the Italian Institute of Technology. To avoid the occurrence of strategic considerations, they were informed that the proposers would be notified of their choices only at the end of the game. Participants were explained the UG rules: if they accepted the proposer's offer, the money would be divided as proposed; if they rejected it, none of the two players would receive anything. Unknown to the participants, the proposer was computer-simulated and all participants received the same set of offers (1, 2, 3, 4, or 5 euros out of 10), which mimicked the bidding pattern of a human proposer.

Apparatus

Participants sat in a height-adjustable chair, with their right hand and wrist resting on a table. Two vertical cylinders were placed in front of the hand position, one on his right and one on his left, at a comfortable distance to reach it. One cylinder was labeled as 'accept' and the other as 'reject'. The proposed offer was displayed together with the silhouette of the randomly chosen proposer on a screen placed in front of the participants (see Figure 4.1A for a schematic representation of the experimental setup).

Procedures

At the beginning of each trial, a green fixation cross was shown in the center of the screen for 1 s. This was followed by a screen showing a silhouette of the proposer with the message '[proposer's name] is thinking...' lasting 2, 3, 4, or 5 s. Then, the offer appeared ('[proposer's name] offer of €4') and remained visible for 3 seconds. Participants had to choose within this time window by reaching, grabbing, and moving one of the two cylinders to destination points placed on a platform. Following the decision, feedback on the money earned by the players was displayed for 2 s. For example, if the participant accepted: '[proposer's name] receives €6, you €4'; if the participant rejected: '[proposer's name] receives €0, you €0.' Finally, upon the appearance of a red fixation cross, participants were to return the cylinder to its initial position and prepare for a new UG trial. A schematic of the experimental design is shown in Figure 4.1B.

Participants underwent two sessions. Each session consisted of 80 trials: 68 UG trials and 12 control trials (6 movements to the right and 6 to the left). The offer set was the same for each participant and consisted of 12 €1 offers, 12 €2 offers, 12 €3 offers, 16 €4 offers, and 16 €5 offers. This set of offers mimics the bidding pattern of a human proposer (Sanfey et al., 2003). Participants were informed that monetary compensation would be

proportional to the money earned during the experiment. At the end of the experiment, we debriefed the participants. Post-experimental interviews confirmed that participants were unaware of the purpose of the study and believed the cover story.

The trial order was randomized among participants, and cylinder labels ('accept' and 'reject') were counterbalanced between sessions. The silhouette was female (male) in half of the trials. E-Prime software (v.2.0.10.242) was used for trial randomization and synchronization with the motion capture system.

Kinematic data acquisition

Movement kinematics were recorded using a motion capture system with eight near-infrared cameras (sampling frequency = 100 Hz; Vicon Motion Capture system). Participants were outfitted with 30 retroreflective markers. To track the reach-to-grasp movement, most of the markers (22) were placed on the right hand, wrist, arm, and elbow. The remaining markers were placed on the trunk and head to track the participants' posture. Also, the cylinders were outfitted with three markers each. For a more detailed description of the arrangement of the markers, see Turri et al. (2022).

Kinematic data preprocessing and computation of kinematic features. A visual inspection was performed on each kinematic trial to verify correct marker identification. The movement kinematics were filtered with a Butterworth low-pass filter (cutoff frequency of 6 Hz).

Based on previous research (Sackaloo et al., 2015; Summerside et al., 2018), as a set of features describing the vigor of movement, we chose to analyze the reaction time, movement time, peak, and time-to-peak velocity. In addition to this set of features, as a control, we decided to analyze also peak grip aperture, which we did not expect to be affected by the vigor of the movement.
These features, computed using custom software (Matlab; MathWorks, Natick, MA), were defined as:

- Reaction time (RT, in ms), i.e., the time elapsing between the stimulus onset (delivering of the offer) and the participant's reach onset (the first time at which the wrist velocity crossed a 20 mm/s threshold);
- Movement time (MT, in ms), i.e., the time elapsing between the participant's reach

onset and the reach offset (the time at which the wrist velocity dropped below a 20 mm/s threshold);

- Peak velocity (PV, in mm/s), i.e., the maximum of the module of the three-dimensional velocity vector of the *radio* marker;
- Time-to-peak velocity (TPV, in ms), i.e., the time from movement onset to the occurrence of PV;
- Peak grip aperture (PGA, in mm), i.e., the maximum Euclidean distance between the markers that were placed on the tips of the thumb and the index finger.

All features were computed considering the reach-to-grasp phase of the movement, from reach onset to reach offset.

4.4.3 Quantification and statistical analysis

Data preprocessing

Trials for which participants responded within the first 100 ms or after 3000 ms were excluded (<0.01% of the trials, 5 trials out of 2775). To normalize the positively skewed distributions of RT, MT, and TPV, we performed an inverse transformation defined as invX = -1000*(1/X) where X is the variable to be normalized, and we denoted the transformed variable as invRT, invMT, and invTPV. We multiplied by the factor -1000 to preserve the direction of effects, e.g., larger invRT meant a slower response, and to avoid too small values (Brysbaert & Stevens, 2018).

Outlier removal

For each kinematic feature, we excluded the points lying outside the range [Q1-1.5*IQR, Q3+1.5*IQR], where Q1 and Q3 are the first and third quartiles, respectively, and IQR is the interquartile range defined as Q3-Q1. For each analysis, 0.91 ± 0.73% (mean ± standard deviation) trials have been excluded.

Linear mixed-effects models to assess the effect of offer level and responders' choice on reach-to-grasp kinematics

We used linear mixed-effects models (LMEMs) to assess the effect of responders' choice, offer value, and their interaction, separately on each kinematic feature, with random ef-

fects at the subject level. Hence, we considered invRT, invMT, PV, invTPV, and PGA as dependent variables (DV), and the offer value (continuous variable), responders' choice (Accept, Reject), their interaction, session number (1, 2), and movements' direction (Left, Right) as fixed factors. DVs were z-scored before to LMEM fitting.

To determine the fixed and random effects to be included in the model, we first defined the most complex model as:

```
DV ~ Offer + Choice + Offer:Choice + Session + Direction
   + (Offer + Choice + Session + Direction | Subject)
```

We then followed a model selection procedure (Zuur et al., 2009) consisting of two phases:

1. Finding the optimal random effects structure by keeping the full fixed effects structure and selecting the nested model with the lowest Bayesian Information Criterion (BIC) (Schwarz, 1978) value, thus rewarding model fit and penalizing model complexity;

2. Finding the optimal fixed effects structure by keeping fixed the optimal random structure (found in phase 1) and conducting likelihood ratio tests (LRT) differing only by the presence or absence of one predictor.

For each model, the results of the model selection procedure, the estimate and confidence intervals (CI) of the model coefficients and statistical comparison for significant effects are reported in Appendix B.

The models were fitted using R and the function `lmer` from `lme4` package (Bates et al., 2015). To test significant interactions between categorical factors (e.g., responders' choice) and continuous variables (e.g., offer level), we assessed the statistical significance of linear trends (i.e., if a trend is significantly different from zero) and of contrasts between linear trends (i.e., if the trends are significantly different from each other) via `emtrends` and `contrast` functions from `emmeans` package (Searle et al., 1980). For any trend or contrast, we reported CIs and p-values (two-tailed) obtained from 10^4 bootstrap samples. The bootstrap distribution was obtained by fitting the models to data randomly sampled with replacement from the original dataset. The two-tailed empirical p-values are obtained from the bootstrap distribution and defined as $2 * \min\left(P\left[X \leq 0\right], P\left[X \geq 0\right]\right)$.

5. Conclusion and future directions

In this thesis, we discussed how movement kinematics plays a crucial role in elucidating hidden cognitive states, focusing in particular on social decision-making processes. Our findings, in accordance with the existing literature, corroborate the idea of an intimate connection between cognitive states and the sensorimotor system.

Specifically, with the first study (Chapter 3), we presented a motor version of the Ultimatum Game. This allowed us to track movement kinematics as participants played several game trials, yielding data with a very rich and detailed characterization of reach-to-grasp acts. Applying a well-known technique of unsupervised dimensionality reduction (i.e., t-SNE), we performed an initial inspection of the data, which reported that kinematic traces separate into clusters, each representing a single individual. This emphasizes how individuals are uniquely marked by their motor style. In light of this result, we applied a multivariate decoding model (i.e., logistic regression) at the single-subject, single-trial level to quantify whether and to what extent information of social decisions (i.e., choice and fairness) leaked into the motor outputs. After having verified that reach-to-grasp acts effectively encode a representation of participants' choice and offer' fairness, we looked into the weights characterizing each responder-specific model to understand how such representations are specified in the movement kinematics. In line with the result obtained using t-SNE, we observed that the embodiment of the social decision parameters is idiosyncratic, with only a few kinematic features consistently encoding this information across participants.

The second study (Chapter 4) focuses on a different aspect of movement kinematics and social decision-making. Building on recent research about movement vigor (Shadmehr & Ahmed, 2020), we examined whether social decisions influence the vigor of the reach-to-grasp acts. We directed our attention to specific kinematic variables related to movement

vigor: reaction time, movement time, wrist peak velocity, and time-to-peak velocity. Using linear mixed-effects modeling, we analyzed the effects of responders' choice and offer level on these kinematic variables at the group-level. As expected, we found a positive relationship between vigor and offer level when the offers were accepted. However, the fascinating novelty concerns rejections; we observed that responders' vigor increased as the unfairness of the offer increased.

These findings have raised intriguing new questions for future research. Below, I outline the most promising areas for future developments and provide some details on how these studies can be implemented to address these new questions.

1. With the first study, we speculate about individuality in motor solutions of social decisions, suggesting that each participant endows a unique kinematic signature. However, we cannot exclude the existence of motor phenotypes. To test this hypothesis, we would need a larger sample size and perform an unsupervised clustering analysis. Additionally, recent research demonstrated how neural substrates cluster as a function of the decision-making strategy adopted (van Baar et al., 2019). It would be worth exploring whether and how these networks covary with kinematics, and whether kinematics can be used as a marker for different decision-making strategies.

2. Studies from our lab demonstrated the innate ability of humans to read others' intentions from subtle variations in movement kinematics (Becchio et al., 2018; Cavallo et al., 2016; Patri et al., 2020). Given our results, the following question arises: do human observers detect changes in movement kinematics to infer social decision variables? Are they sensitive to both the responders' choice and the fairness of an offer, only one of the two aspects, or neither? One potential challenge is the high intra-trial and inter-responder variability that would make the observers' task very difficult, if not impossible. This could be mitigated by exposing the observers to additional sources of information (e.g., gaze and postural behavior).

3. It might be intriguing to extend our findings to different strategic decision-making settings. For example, as outlined in Chapter 3, we only showed that the kinematic patterns encoding choice generalize to mid-range offers. A possible solution to strengthen our findings on the consistency of kinematic patterns would be to have participants perform the Ultimatum Game, acting as responders, in both the *my-*

self (classical Ultimatum Game) and the *third-party* (on behalf of another player) condition, as in Civai et al. (2010). By doing so, we would obtain two separate datasets (one for the myself and one for the third-party condition) and we could test whether the individual kinematic pattern for choice/fairness obtained with the myself condition generalizes over the third-party data. The alternative hypothesis would be that the kinematics is also affected by the Ultimatum Game condition, showing different patterns when playing on behalf of another player.

4. The findings related to the second study left us with an open question: does rejection-related vigor reflect self-loss, other-punishment, or a combination of the two? In other words, does vigor decrease as the amount of money lost increases or as the punishment inflicted on defectors decreases? However, the experiment was not designed for discerning among these possibilities, and the Ultimatum Game paradigm is not an appropriate means to address this question. What we would need is a socio-economic game in which participants are given the opportunity to actively inflict different levels of other-punishment on defectors by incurring different levels of self-loss.

   A possible experimental design implementing the above features is the one devised by de Quervain et al. (2004) in which participants played a variant of the Trust Game. The first phase of the game adheres mainly to the classical Trust Game scheme and can be summarized as follows. Two players, the investor (player A) and the trustee (player B), are endowed with some monetary units (e.g., 10 MUs) and interact anonymously. Player A can decide whether to send (case 1) or not (case 2) his endowment to player B. If A does not trust B (case 2), both players remain with their endowment and the game ends. If A trusts B (case 1), the amount sent is quadrupled and B receives 40 MUs. Now, player B has a total of 50 MUs and player A has nothing. Player B has two options: (i) to act trustworthily, splitting the income equally (25 MUs each) and ending the game, or (ii) to keep all the MUs. The latter will begin the second phase of the game: the punishment phase. Player A is endowed with 5 extra MUs and can decide to keep the 5 MUs or to punish player B incurring a self-cost, according to a predetermined scheme (e.g., self-cost=2/4 and other-punishment=10/20/40).

   A motor version of this game would lead us to have kinematics associated with various pairs of self-loss/other-punishment, thus enabling us to understand whether

the kinematics reflect the self-loss, the other-punishment, or a combination of the two that could be represented by the ratio between other-punishment and self-loss (i.e., $\frac{other-punishment}{self-loss} = \frac{10}{2} = \frac{20}{4} = 5$ and $\frac{20}{2} = \frac{40}{4} = 10$).

In conclusion, we demonstrated that adapting traditional behavioral economic games to incorporate actions involving participants' movement is feasible and relatively straightforward. By combining this approach with advanced and rigorous machine learning analysis, we were able to quantitatively assess the information that flows from cognition to motor behavior. This ensemble of methodological aspects not only allowed us to study participants' behavior but also, more importantly, provided insight into the underlying decision-making processes.

References

Allais, M. (1953). Le comportement de l'homme rationnel devant le risque: Critique des postulats et axiomes de l'ecole americaine. *Econometrica*, *21*(4), 503-546. doi: 10.2307/1907921

Ansuini, C., Cavallo, A., Koul, A., Jacono, M., Yang, Y., & Becchio, C. (2015). Predicting object size from hand kinematics: A temporal perspective. *PLOS ONE*, *10*(3), 1-13. doi: 10.1371/journal.pone.0120432

Ansuini, C., Giosa, L., Turella, L., Altoè, G., & Castiello, U. (2008). An object for an action, the same object for other actions: Effects on hand shaping. *Experimental Brain Research*, *185*(1), 111-119. doi: 10.1007/s00221-007-1136-4

Barca, L., & Pezzulo, G. (2015). Tracking second thoughts: Continuous and discrete revision processes during visual lexical decision. *PLOS ONE*, *10*(2), 1-14. doi: 10.1371/journal.pone.0116193

Bates, D., Mächler, M., Bolker, B. M., & Walker, S. C. (2015). Fitting linear mixed-effects models using lme4. *Journal of Statistical Software*, *67*(1), 1-48. doi: 10.18637/jss.v067.i01

Baumgartner, T., Knoch, D., Hotz, P., Eisenegger, C., & Fehr, E. (2011). Dorsolateral and ventromedial prefrontal cortex orchestrate normative choice. *Nature Neuroscience*, *14*(11), 1468-1474. doi: 10.1038/nn.2933

Becchio, C., Koul, A., Ansuini, C., Bertone, C., & Cavallo, A. (2018). Seeing mental states: An experimental strategy for measuring the observability of other minds. *Physics of Life Reviews*, *24*, 67-80. doi: 10.1016/j.plrev.2017.10.002

Becchio, C., & Panzeri, S. (2019). Sensorimotor communication at the intersection between kinematic coding and readout: Comment on "The body talks: Sensorimotor communication and its brain and kinematic signatures" by Giovanni Pez-

zulo, Francesco Donnarumma, Haris Dindo, Alessandro D'Ausilio, Ivana Konvalinka, Cristiano Castelfranchi. *Physics of life reviews*, *28*, 39-42. doi: 10.1016/j.plrev.2019.01.019

Becchio, C., Pullar, K., & Panzeri, S. (2021). Costs and benefits of communicating vigor. *Behavioral and Brain Sciences*, *44*, e124. doi: 10.1017/s0140525x21000200

Bechara, A., & Damasio, A. R. (2005). The somatic marker hypothesis: A neural theory of economic decision. *Games and Economic Behavior*, *52*(2), 336-372. doi: 10.1016/j.geb.2004.06.010

Blount, S. (1995). When social outcomes aren't fair: The effect of causal attributions on preferences. *Organizational Behavior and Human Decision Processes*, *63*(2), 131-144. doi: 10.1006/obhd.1995.1068

Bogacz, R. (2007). Optimal decision-making theories: linking neurobiology with behaviour. *Trends in cognitive sciences*, *11*(3), 118-125. doi: 10.1016/j.tics.2006.12.006

Bolton, G. E., & Ockenfels, A. (2000). Erc: A theory of equity, reciprocity, and competition. *American Economic Review*, *90*(1), 166-193. doi: 10.1257/aer.90.1.166

Bolton, G. E., & Zwick, R. (1995). Anonymity versus punishment in ultimatum bargaining. *Games and Economic Behavior*, *10*(1), 95-121. doi: 10.1006/game.1995.1026

Botvinick, M., Nystrom, L. E., Fissell, K., Carter, C. S., & Cohen, J. D. (1999). Conflict monitoring versus selection-for-action in anterior cingulate cortex. *Nature*, *402*(6758), 179-181. doi: 10.1038/46035

Boyd, R., Gintis, H., Bowles, S., & Richerson, P. J. (2003). The evolution of altruistic punishment. *Proceedings of the National Academy of Sciences*, *100*(6), 3531-3535. doi: 10.1073/pnas.0630443100

Britten, K. H., Shadlen, M. N., Newsome, W. T., & Movshon, J. A. (1992). The analysis of visual motion: a comparison of neuronal and psychophysical performance. *Journal of Neuroscience*, *12*(12), 4745-4765. doi: 10.1523/jneurosci.12-12-04745.1992

Britten, K. H., Shadlen, M. N., Newsome, W. T., & Movshon, J. A. (1993). Responses of neurons in macaque mt to stochastic motion signals. *Visual Neuroscience*, *10*(6), 1157-1169. doi: 10.1017/s0952523800010269

Brysbaert, M., & Stevens, M. (2018). Power analysis and effect size in mixed effects models: A tutorial. *Journal of cognition*, *1*(1), 9. doi: 10.5334/joc.10

Byrd, R. H., Lu, P., Nocedal, J., & Zhu, C. (1995). A limited memory algorithm for bound constrained optimization. *SIAM Journal on Scientific Computing*, *16*(5), 1190-1208. doi: 10.1137/0916069

Calder, A. J., Lawrence, A. D., & Young, A. W. (2001). Neuropsychology of fear and loathing. *Nature Reviews Neuroscience*, *2*(5), 352-363. doi: 10.1038/35072584

Camerer, C. F. (2003). Strategizing in the brain. *Science*, *300*(5626), 1673-1675. doi: 10.1126/science.1086215

Camerer, C. F., & Thaler, R. H. (1995). Anomalies: Ultimatums, dictators and manners. *Journal of Economic Perspectives*, *9*(2), 209-219. doi: 10.1257/jep.9.2.209

Castiello, U. (2005). The neuroscience of grasping. *Nature Reviews Neuroscience*, *6*(9), 726-736. doi: 10.1038/nrn1744

Cavallo, A., Koul, A., Ansuini, C., Capozzi, F., & Becchio, C. (2016). Decoding intentions from movement kinematics. *Scientific Reports*, *6*(1), 1-8. doi: 10.1038/srep37036

Cavallo, A., Romeo, L., Ansuini, C., Podda, J., Battaglia, F., Veneselli, E., Pontil, M., & Becchio, C. (2018). Prospective motor control obeys to idiosyncratic strategies in autism. *Scientific Reports*, *8*(1), 1-9. doi: 10.1038/s41598-018-31479-2

Chapman, C. S., Gallivan, J. P., Wong, J. D., Wispinski, N. J., & Enns, J. T. (2015). The snooze of lose: Rapid reaching reveals that losses are processed more slowly than gains. *Journal of Experimental Psychology: General*, *144*(4), 844-863. doi: 10.1037/xge0000085

Cisek, P. (2007). Cortical mechanisms of action selection: the affordance competition hypothesis. *Philosophical Transactions of the Royal Society B: Biological Sciences*, *362*(1485), 1585-1599. doi: 10.1098/rstb.2007.2054

Cisek, P., & Pastor-Bernier, A. (2014). On the challenges and mechanisms of embodied decisions. *Philosophical Transactions of the Royal Society B: Biological Sciences*, *369*(1655), 20130479. doi: 10.1098/rstb.2013.0479

Civai, C., Corradi-Dell'Acqua, C., Gamer, M., & Rumiati, R. I. (2010). Are irrational reactions to unfairness truly emotionally-driven? dissociated behavioural and emo-

tional responses in the ultimatum game task. *Cognition*, *114*(1), 89-95. doi: 10.1016/j.cognition.2009.09.001

Civai, C., Crescentini, C., Rustichini, A., & Rumiati, R. I. (2012). Equality versus self-interest in the brain: Differential roles of anterior insula and medial prefrontal cortex. *NeuroImage*, *62*(1), 102-112. doi: 10.1016/j.neuroimage.2012.04.037

Cooper, D. J., & Dutcher, E. G. (2011). The dynamics of responder behavior in ultimatum games: A meta-study. *Experimental Economics*, *14*(4), 519-546. doi: 10.1007/s10683-011-9280-x

Corradi-Dell'Acqua, C., Civai, C., Rumiati, R. I., & Fink, G. R. (2013). Disentangling self- and fairness-related neural mechanisms involved in the ultimatum game: an fmri study. *Social Cognitive and Affective Neuroscience*, *8*(4), 424-431. doi: 10.1093/scan/nss014

de Quervain, D. J., Fischbacher, U., Treyer, V., Schellhammer, M., Schnyder, U., Buck, A., & Fehr, E. (2004). The neural basis of altruistic punishment. *Science*, *305*(5688), 1254-1258. doi: 10.1126/science.1100735

Donner, T. H., Siegel, M., Fries, P., & Engel, A. K. (2009). Buildup of choice-predictive activity in human motor cortex during perceptual decision making. *Current Biology*, *19*(18), 1581-1585. doi: 10.1016/j.cub.2009.07.066

Dotan, D., Meyniel, F., & Dehaene, S. (2018). On-line confidence monitoring during decision making. *Cognition*, *171*, 112-121. doi: 10.1016/j.cognition.2017.11.001

Dotan, D., Pinheiro-Chagas, P., Roumi, F. A., & Dehaene, S. (2019). Track it to crack it: Dissecting processing stages with finger tracking. *Trends in Cognitive Sciences*, *23*(12), 1058-1070. doi: 10.1016/j.tics.2019.10.002

Dufwenberg, M., & Kirchsteiger, G. (2004). A theory of sequential reciprocity. *Games and Economic Behavior*, *47*(2), 268-298. doi: 10.1016/j.geb.2003.06.003

Evgeniou, T., Micchelli, C. A., & Pontil, M. (2005). Learning multiple tasks with kernel methods. *Journal of machine learning research*, *6*(4), 615–637.

Falk, A., & Fischbacher, U. (2006). A theory of reciprocity. *Games and Economic Behavior*, *54*(2), 293-315. doi: 10.1016/j.geb.2005.03.001

Fehr, E., & Camerer, C. F. (2007). Social neuroeconomics: the neural circuitry of social preferences. *Trends in Cognitive Sciences*, *11*(10), 419-427. doi: 10.1016/j.tics.2007.09.002

Fehr, E., & Schmidt, K. M. (1999). A theory of fairness, competition, and cooperation. *The Quarterly Journal of Economics*, *114*(3), 817-868. doi: 10.1162/003355399556151

Fiedler, S., & Glöckner, A. (2012). The dynamics of decision making in risky choice: An eye-tracking analysis. *Frontiers in Psychology*, *3*, 1-18. doi: 10.3389/fpsyg.2012.00335

Fiedler, S., Glöckner, A., Nicklisch, A., & Dickert, S. (2013). Social value orientation and information search in social dilemmas: An eye-tracking analysis. *Organizational Behavior and Human Decision Processes*, *120*(2), 272-284. doi: 10.1016/j.obhdp.2012.07.002

Freeman, J. B., Dale, R., & Farmer, T. A. (2011). Hand in motion reveals mind in motion. *Frontiers in Psychology*, *2*, 59. doi: 10.3389/fpsyg.2011.00059

Freeman, J. B., Pauker, K., & Sanchez, D. T. (2016). A perceptual pathway to bias: Interracial exposure reduces abrupt shifts in real-time race perception that predict mixed-race bias. *Psychological Science*, *27*(4), 502-517. doi: 10.1177/0956797615627418

Friedman, J., Hastie, T., & Tibshirani, R. (2010). Regularization paths for generalized linear models via coordinate descent. *Journal of statistical software*, *33*(1), 1-22. doi: 10.18637/jss.v033.i01

Gabay, A. S., Radua, J., Kempton, M. J., & Mehta, M. A. (2014). The ultimatum game and the brain: A meta-analysis of neuroimaging studies. *Neuroscience & Biobehavioral Reviews*, *47*, 549-558.

Gallivan, J. P., Chapman, C. S., Wolpert, D. M., & Flanagan, J. R. (2018). Decision-making in sensorimotor control. *Nature Reviews Neuroscience*, *19*(9), 519-534. doi: 10.1038/s41583-018-0045-9

Ghaffari, M., & Fiedler, S. (2018). The power of attention: Using eye gaze to predict other-regarding and moral choices. *Psychological Science*, *29*(11), 1878-1889. doi: 10.1177/0956797618799301

Gigerenzer, G., & Gaissmaier, W. (2011). Heuristic decision making. *Annual Review of Psychology*, *62*(1), 451-482. doi: 10.1146/annurev-psych-120709-145346

Glimcher, P. W., & Rustichini, A. (2004). Neuroeconomics: The consilience of brain and decision. *Science*, *306*(5695), 447-452. doi: 10.1126/science.1102566

Gold, J. I., & Shadlen, M. N. (2007). The neural basis of decision making. *Annual review of neuroscience*, *30*, 535-574. doi: 10.1146/annurev.neuro.29.051605.113038

Gordon, J., Maselli, A., Lancia, G. L., Thiery, T., Cisek, P., & Pezzulo, G. (2021). The road towards understanding embodied decisions. *Neuroscience & Biobehavioral Reviews*, *131*, 722-736. doi: 10.1016/j.neubiorev.2021.09.034

Güth, W., Schmittberger, R., & Schwarze, B. (1982). An experimental analysis of ultimatum bargaining. *Journal of Economic Behavior & Organization*, *3*(4), 367-388. doi: 10.1016/0167-2681(82)90011-7

Henrich, J., Boyd, R., Bowles, S., Camerer, C., Fehr, E., Gintis, H., McElreath, R., Alvard, M., Barr, A., Ensminger, J., Henrich, N. S., Hill, K., Gil-White, F., Gurven, M., Marlowe, F. W., Patton, J. Q., & Tracer, D. (2005). "economic man" in cross-cultural perspective: Behavioral experiments in 15 small-scale societies. *Behavioral and Brain Sciences*, *28*(6), 795-815. doi: 10.1017/s0140525x05000142

Hoffman, E., McCabe, K. A., & Smith, V. L. (1996). On expectations and the monetary stakes in ultimatum games. *International Journal of Game Theory*, *25*(3), 289-301. doi: 10.1007/bf02425259

Ince, R. A., Mazzoni, A., Bartels, A., Logothetis, N. K., & Panzeri, S. (2012). A novel test to determine the significance of neural selectivity to single and multiple potentially correlated stimulus features. *Journal of Neuroscience Methods*, *210*(1), 49-65. doi: 10.1016/j.jneumeth.2011.11.013

Jeannerod, M. (1981). Intersegmental coodination during reaching at natural visual objects. *Attention and performance*, 153-169.

Kahneman, D. (2003). A perspective on judgment and choice: mapping bounded rationality. *The American psychologist*, *58*(9), 697-720. doi: 10.1037/0003-066x.58.9.697

Kahneman, D. (2011). *Thinking, fast and slow.* Farrar, Straus and Giroux.

Kahneman, D., & Tversky, A. (1979). Prospect theory: An analysis of decision under risk. *Econometrica*, *47*(2), 263-291. doi: 10.2307/1914185

Kawagoe, R., Takikawa, Y., & Hikosaka, O. (1998). Expectation of reward modulates cognitive signals in the basal ganglia. *Nature Neuroscience*, *1*(5), 411-416. doi: 10.1038/1625

Kieslich, P. J., & Hilbig, B. E. (2014). Cognitive conflict in social dilemmas: An analysis of response dynamics. *Judgment and Decision Making*, *9*(6), 510-522.

Kingma, D. P., & Ba, J. L. (2014). Adam: A method for stochastic optimization. *3rd International Conference on Learning Representations, ICLR 2015 - Conference Track Proceedings*. doi: 10.48550/arxiv.1412.6980

Knoch, D., Nitsche, M. A., Fischbacher, U., Eisenegger, C., Pascual-Leone, A., Fehr, E., Zu, U. H., & Helveticum, C. (2008). Studying the neurobiology of social interaction with transcranial direct current stimulation-the example of punishing unfairness. *Cerebral Cortex*, *18*, 1987-1990. doi: 10.1093/cercor/bhm237

Knoch, D., Pascual-Leone, A., Meyer, K., Treyer, V., & Fehr, E. (2006). Diminishing reciprocal fairness by disrupting the right prefrontal cortex. *Science*, *314*(5800), 829-832. doi: 10.1126/science.1129156

Korbisch, C. C., Apuan, D. R., Shadmehr, R., & Ahmed, A. A. (2022). Saccade vigor reflects the rise of decision variables during deliberation. *Current Biology*, *32*, 5374-5381. doi: 10.1016/j.cub.2022.10.053

Koul, A., Cavallo, A., Cauda, F., Costa, T., Diano, M., Pontil, M., & Becchio, C. (2018). Action observation areas represent intentions from subtle kinematic features. *Cerebral Cortex*, *28*(7), 2647-2654. doi: 10.1093/cercor/bhy098

Krajbich, I., Oud, B., Fehr, E., Healy, P. J., Coffman, L., Coffman, K., Woodford, M., Ratcliff, R., Caplin, A., & Rangel, A. (2014). Benefits of neuroeconomic modeling: New policy interventions and predictors of preference. *American Economic Review: Papers & Proceedings*, *104*(5), 501-506. doi: 10.1257/aer.104.5.501

Kreps, D. M., Milgrom, P., Roberts, J., & Wilson, R. (1982). Rational cooperation in the finitely repeated prisoners' dilemma. *Journal of Economic Theory*, *27*(2), 245-252. doi: 10.1016/0022-0531(82)90029-1

Larney, A., Rotella, A., & Barclay, P. (2019). Stake size effects in ultimatum game and dictator game offers: A meta-analysis. *Organizational Behavior and Human Decision Processes*, *151*, 61-72. doi: 10.1016/j.obhdp.2019.01.002

Lee, D. (2006). Neural basis of quasi-rational decision making. *Current Opinion in Neurobiology*, *16*(2), 191-198. doi: 10.1016/j.conb.2006.02.001

Lerner, J. S., Li, Y., Valdesolo, P., & Kassam, K. S. (2015). Emotion and decision making. *Annual review of psychology*, *66*, 799-823. doi: 10.1146/annurev-psych -010213-115043

Levinson, S. C. (1995). Interactional biases in human thinking. *Social Intelligence and Interaction*, 221-260. doi: 10.1017/cbO9780511621710.014

MacDonald, A. W., Cohen, J. D., Stenger, V. A., & Carter, C. S. (2000). Dissociating the role of the dorsolateral prefrontal and anterior cingulate cortex in cognitive control. *Science*, *288*(5472), 1835-1838. doi: 10.1126/science.288.5472.1835

Matthews, A. G. d. G., Van Der Wilk, M., Nickson, T., Fujii, K., Boukouvalas, A., León-Villagrá, P., Ghahramani, Z., & Hensman, J. (2017). Gpflow: A gaussian process library using tensorflow. *J. Mach. Learn. Res.*, *18*(40), 1-6.

McKinstry, C., Dale, R., & Spivey, M. J. (2008). Action dynamics reveal parallel competition in decision making. *Psychological Science*, *19*(1), 22-24. doi: 10.1111/j.1467-9280.2008.02041.x

Miller, E. K., & Cohen, J. D. (2001). An integrative theory of prefrontal cortex function. *Annual review of neuroscience*, *24*(1), 167-202.

Milstein, D. M., & Dorris, M. C. (2007). The influence of expected value on saccadic preparation. *Journal of Neuroscience*, *27*(18), 4810-4818. doi: 10.1523/jneurosci .0577-07.2007

Montobbio, N., Cavallo, A., Albergo, D., Ansuini, C., Battaglia, F., Podda, J., Nobili, L., Panzeri, S., & Becchio, C. (2022). Intersecting kinematic encoding and readout of intention in autism. *Proceedings of the National Academy of Sciences*, *119*(5), e2114648119. doi: 10.1073/pnas.2114648119

Murphy, K. P. (2012). *Machine learning: a probabilistic perspective*. MIT press.

Nash, J. F. (1950). Equilibrium points in n-person games. *Proceedings of the National Academy of Sciences*, *36*(1), 48-49. doi: 10.1073/pnas.36.1.48

Newell, B. R., & Shanks, D. R. (2014). Unconscious influences on decision making: A critical review. *The Behavioral and brain sciences*, *37*(1), 1-19. doi: 10.1017/ s0140525x12003214

Nocedal, J., & Wright, S. J. (1999). *Numerical optimization*. Springer.

Noroozi, F., Corneanu, C. A., Kamińska, D., Sapiński, T., Escalera, S., & Anbarjafari, G. (2018). Survey on emotional body gesture recognition. *IEEE transactions on affective computing*, *12*(2), 505–523. doi: 10.1109/TAFFC.2018.2874986

Padoa-Schioppa, C. (2011). Neurobiology of economic choice: A good-based model. *Annual Review of Neuroscience*, *34*(1), 333-359. doi: 10.1146/annurev-neuro-061010-113648

Panzeri, S., Harvey, C. D., Piasini, E., Latham, P. E., & Fellin, T. (2017). Cracking the neural code for sensory perception by combining statistics, intervention, and behavior. *Neuron*, *93*(3), 491-507. doi: 10.1016/j.neuron.2016.12.036

Paszke, A., Gross, S., Massa, F., Lerer, A., Google, J. B., Chanan, G., Killeen, T., Lin, Z., Gimelshein, N., Antiga, L., Desmaison, A., Xamla, A. K., Yang, E., Devito, Z., Nabla, M. R., Tejani, A., Chilamkurthy, S., Ai, Q., Steiner, B., ... Chintala, S. (2019). Pytorch: An imperative style, high-performance deep learning library. *Advances in Neural Information Processing Systems*, *32*, 8026–8037.

Patri, J. F., Cavallo, A., Pullar, K., Soriano, M., Valente, M., Koul, A., Avenanti, A., Panzeri, S., & Becchio, C. (2020). Transient disruption of the inferior parietal lobule impairs the ability to attribute intention to action. *Current Biology*, *30*(23), 4594-4605.e7. doi: 10.1016/j.cub.2020.08.104

Pedregosa, F., Varoquaux, G., Gramfort, A., Michel, V., Thirion, B., Grisel, O., Blondel, M., Prettenhofer, P., Weiss, R., & Dubourg, V. (2011). Scikit-learn: Machine learning in python. *the Journal of machine Learning research*, *12*, 2825-2830.

Pezzulo, G., & Cisek, P. (2016). Navigating the affordance landscape: Feedback control as a process model of behavior and cognition. *Trends in Cognitive Sciences*, *20*(6), 414-424. doi: 10.1016/j.tics.2016.03.013

Phelps, E. A., Lempert, K. M., & Sokol-Hessner, P. (2014). Emotion and decision making: multiple modulatory neural circuits. *Annual review of neuroscience*, *37*, 263-287. doi: 10.1146/annurev-neuro-071013-014119

Poncela-Casasnovas, J., Gutiérrez-Roig, M., Gracia-Lázaro, C., Vicens, J., Gómez-Gardeñes, J., Perelló, J., Moreno, Y., Duch, J., & Sánchez, A. (2016). Humans display a reduced set of consistent behavioral phenotypes in dyadic games. *Science advances*, *2*(8), e1600451. doi: 10.1126/sciadv.1600451

Rabin, M. (1993). Incorporating fairness into game theory and economics. *The American economic review*, 1281-1302.

Rabin, M. (2000). Risk aversion and expected-utility theory: A calibration theorem. *Econometrica*, *68*(5), 1281-1292.

Rapoport, A., & Chammah, A. (1965). *Prisoner's dilemma*. University of Michigan Press. doi: 10.3998/mpub.20269

Rasmussen, C. E., & Williams, C. K. I. (2005). *Gaussian Processes for Machine Learning*. The MIT Press. doi: 10.7551/mitpress/3206.001.0001

Ratcliff, R., & Rouder, J. N. (1998). Modeling response times for two-choice decisions. *Psychological Science*, *9*(5), 347-356. doi: 10.1111/1467-9280.00067

Resulaj, A., Kiani, R., Wolpert, D. M., & Shadlen, M. N. (2009). Changes of mind in decision-making. *Nature*, *461*(7261), 263-266. doi: 10.1038/nature08275

Rilling, J. K., & Sanfey, A. G. (2011). The neuroscience of social decision-making. *Annual review of psychology*, *62*(1), 23-48. doi: 10.1146/annurev.psych.121208.131647

Rosenbaum, D. A., Chapman, K. M., Weigelt, M., Weiss, D. J., & van der Wel, R. (2012). Cognition, action, and object manipulation. *Psychological Bulletin*, *138*(5), 924-946. doi: 10.1037/a0027839

Roth, A. E., & Erev, I. (1995). Learning in extensive-form games: Experimental data and simple dynamic models in the intermediate term. *Games and Economic Behavior*, *8*(1), 164-212. doi: 10.1016/s0899-8256(05)80020-x

Ruggeri, K., Alí, S., Berge, M. L., Bertoldo, G., Bjørndal, L. D., Cortijos-Bernabeu, A., Davison, C., Demić, E., Esteban-Serna, C., Friedemann, M., Gibson, S. P., Jarke, H., Karakasheva, R., Khorrami, P. R., Kveder, J., Andersen, T. L., Lofthus, I. S., McGill, L., Nieto, A. E., ... Folke, T. (2020). Replicating patterns of prospect theory for decision under risk. *Nature Human Behaviour*, *4*(6), 622-633. doi: 10.1038/s41562-020-0886-x

Runyan, C. A., Piasini, E., Panzeri, S., & Harvey, C. D. (2017). Distinct timescales of population coding across cortex. *Nature*, *548*(7665), 92-96. doi: 10.1038/nature23020

Sackaloo, K., Strouse, E., & Rice, M. S. (2015). Degree of preference and its influence on motor control when reaching for most preferred, neutrally preferred, and least

preferred candy. *OTJR Occupation, Participation and Health*, *35*(2), 81-88. doi: 10.1177/1539449214561763

Sally, D. (1995). Conversation and cooperation in social dilemmas: A meta-analysis of experiments from 1958 to 1992. *Rationality and Society*, *7*(1), 58-92. doi: 10.1177/1043463195007001004

Sanfey, A. G. (2007). Social decision-making: Insights from game theory and neuroscience. *Science*, *318*(5850), 598-602. doi: 10.1126/science.1142996

Sanfey, A. G., Loewenstein, G., McClure, S. M., & Cohen, J. D. (2006). Neuroeconomics: Cross-currents in research on decision-making. *Trends in Cognitive Sciences*, *10*(3), 108-116. doi: 10.1016/j.tics.2006.01.009

Sanfey, A. G., Rilling, J. K., Aronson, J. A., Nystrom, L. E., & Cohen, J. D. (2003). The neural basis of economic decision-making in the ultimatum game. *Science*, *300*(5626), 1755-1758. doi: 10.1126/science.1082976

Savage, L. J. (1954). *Foundations of statistics.* Wiley.

Schwarz, G. (1978). Estimating the dimension of a model. *The Annals of Statistics*, *6*(2), 461-464. doi: 10.2307/2958889

Searle, S. R., Speed, F. M., & Milliken, G. A. (1980). Population marginal means in the linear model: An alternative to least squares means. *American Statistician*, *34*(4), 216-221. doi: 10.1080/00031305.1980.10483031

Sebanz, N., & Shiffrar, M. (2009). Detecting deception in a bluffing body: The role of expertise. *Psychonomic Bulletin & Review*, *16*(1), 170-175. doi: 10.3758/pbr.16.1.170

Seideman, J. A., Stanford, T. R., & Salinas, E. (2018). Saccade metrics reflect decision-making dynamics during urgent choices. *Nature Communications*, *9*(1), 1-11. doi: 10.1038/s41467-018-05319-w

Shadlen, M. N., & Newsome, W. T. (2001). Neural basis of a perceptual decision in the parietal cortex (area lip) of the rhesus monkey. *Journal of Neurophysiology*, *86*(4), 1916-1936. doi: 10.1152/jn.2001.86.4.1916

Shadmehr, R., & Ahmed, A. A. (2020). *Vigor: Neuroeconomics of movement control.* MIT Press.

Shadmehr, R., & Ahmed, A. A. (2021). Précis of vigor: Neuroeconomics of movement control. *Behavioral and Brain Sciences*, *44*, e123. doi: 10.1017/s0140525x20000667

Shadmehr, R., Reppert, T. R., Summerside, E. M., Yoon, T., & Ahmed, A. A. (2019). Movement vigor as a reflection of subjective economic utility. *Trends in Neurosciences*, *42*(5), 323-336. doi: 10.1016/j.tins.2019.02.003

Simon, H. A. (1957). *Models of man; social and rational.* Wiley.

Skaramagkas, V., Giannakakis, G., Ktistakis, E., Manousos, D., Karatzanis, I., Tachos, N., Tripoliti, E. E., Marias, K., Fotiadis, D. I., & Tsiknakis, M. (2021). Review of eye tracking metrics involved in emotional and cognitive processes. *IEEE Reviews in Biomedical Engineering*. doi: 10.1109/rbme.2021.3066072

Slepian, M. L., Young, S. G., Rutchick, A. M., & Ambady, N. (2013). Quality of professional players' poker hands is perceived accurately from arm motions. *Psychological Science*, *24*(11), 2335–2338. doi: 10.1177/0956797613487384

Smith, P. L., & Vickers, D. (1988). The accumulator model of two-choice discrimination. *Journal of Mathematical Psychology*, *32*(2), 135-168. doi: 10.1016/0022-2496(88)90043-0

Song, J. H., & Nakayama, K. (2008). Numeric comparison in a visually-guided manual reaching task. *Cognition*, *106*(2), 994–1003. doi: 10.1016/j.cognition.2007.03.014

Song, J. H., & Nakayama, K. (2009). Hidden cognitive states revealed in choice reaching tasks. *Trends in Cognitive Sciences*, *13*(8), 360-366. doi: 10.1016/j.tics.2009.04.009

Spitzer, M., Fischbacher, U., Herrnberger, B., Grön, G., & Fehr, E. (2007). The neural signature of social norm compliance. *Neuron*, *56*(1), 185-196. doi: 10.1016/j.neuron.2007.09.011

Spivey, M. J., Grosjean, M., & Knoblich, G. (2005). Continuous attraction toward phonological competitors. *Proceedings of the National Academy of Sciences*, *102*(29), 10393-10398. doi: 10.1073/pnas.0503903102

Stanovich, K. E., & West, R. F. (2000). Individual differences in reasoning: Implications for the rationality debate? *Behavioral and Brain Sciences*, *23*(5), 645-665. doi: 10.1017/s0140525x00003435

Summerside, E. M., Shadmehr, R., & Ahmed, A. A. (2018). Vigor of reaching movements: Reward discounts the cost of effort. *Journal of Neurophysiology*, *119*(6), 2347-2357. doi: 10.1152/jn.00872.2017

Tabibnia, G., Satpute, A. B., & Lieberman, M. D. (2008). The sunny side of fairness: Preference for fairness activates reward circuitry (and disregarding unfairness activates self-control circuitry): Research article. *Psychological Science*, *19*(4), 339-347. doi: 10.1111/j.1467-9280.2008.02091.x

Ting, L. H., Chiel, H. J., Trumbower, R. D., Allen, J. L., McKay, J. L., Hackney, M. E., & Kesar, T. M. (2015). Neuromechanical principles underlying movement modularity and their implications for rehabilitation. *Neuron*, *86*(1), 38-54. doi: 10.1016/j.neuron.2015.02.042

Turri, G., Cavallo, A., Romeo, L., Pontil, M., Sanfey, A., Panzeri, S., & Becchio, C. (2022). Decoding social decisions from movement kinematics. *iScience*, *25*(12), 105550. doi: 10.1016/j.isci.2022.105550

Tversky, A., & Kahneman, D. (1974). Judgment under uncertainty: Heuristics and biases. *Science*, *185*(4157), 1124-1131. doi: 10.1126/science.185.4157.1124

Usher, M., & McClelland, J. L. (2001). The time course of perceptual choice: The leaky, competing accumulator model. *Psychological Review*, *108*(3), 550-592. doi: 10.1037/0033-295x.108.3.550

van Baar, J. M., Chang, L. J., & Sanfey, A. G. (2019). The computational and neural substrates of moral strategies in social decision-making. *Nature Communications*, *10*(1), 1-14. doi: 10.1038/s41467-019-09161-6

van der Maaten, L., & Hinton, G. (2008). Visualizing data using t-sne. *Journal of machine learning research*, *9*(11), 2579–2605.

von Neumann, J., & Morgenstern, O. (1944). *Theory of games and economic behavior*. Princeton University Press. doi: 10.1515/9781400829460

Wagner, A. D., Maril, A., Bjork, R. A., & Schacter, D. L. (2001). Prefrontal contributions to executive control: fmri evidence for functional distinctions within lateral prefrontal cortex. *NeuroImage*, *14*(6), 1337-1347. doi: 10.1006/nimg.2001.0936

Weg, E., & Zwick, R. (1994). Toward the settlement of the fairness issues in ultimatum games: A bargaining approach. *Journal of Economic Behavior & Organization*, *24*(1), 19-34. doi: 10.1016/0167-2681(94)90052-3

Wispinski, N. J., Gallivan, J. P., & Chapman, C. S. (2020). Models, movements, and minds: bridging the gap between decision making and action. *Annals of the New York Academy of Sciences*, *1464*(1), 30-51. doi: 10.1111/nyas.13973

Xu-Wilson, M., Zee, D. S., & Shadmehr, R. (2009). The intrinsic value of visual information affects saccade velocities. *Experimental Brain Research*, *196*(4), 475-481. doi: 10.1007/s00221-009-1879-1

Yamagishi, T., Horita, Y., Mifune, N., Hashimoto, H., Li, Y., Shinada, M., Miura, A., Inukai, K., Takagishi, H., & Simunovic, D. (2012). Rejection of unfair offers in the ultimatum game is no evidence of strong reciprocity. *Proceedings of the National Academy of Sciences of the United States of America*, *109*(50), 20364-20368. doi: 10.1073/pnas.1212126109

Yoon, T., Geary, R. B., Ahmed, A. A., & Shadmehr, R. (2018). Control of movement vigor and decision making during foraging. *Proceedings of the National Academy of Sciences of the United States of America*, *115*(44), E10476-E10485. doi: 10.1073/pnas.1812979115

Yoon, T., Jaleel, A., Ahmed, A. A., & Shadmehr, R. (2020). Saccade vigor and the subjective economic value of visual stimuli. *Journal of Neurophysiology*, *123*(6), 2161-2172. doi: 10.1152/jn.00700.2019

Zuur, A. F., Ieno, E. N., Walker, N., Saveliev, A. A., & Smith, G. M. (2009). *Mixed effects models and extensions in ecology with r*. Springer New York. doi: 10.1007/978-0-387-87458-6

A. Supplementary materials for Chapter 3: Study 1: Decoding social decisions from movement kinematics

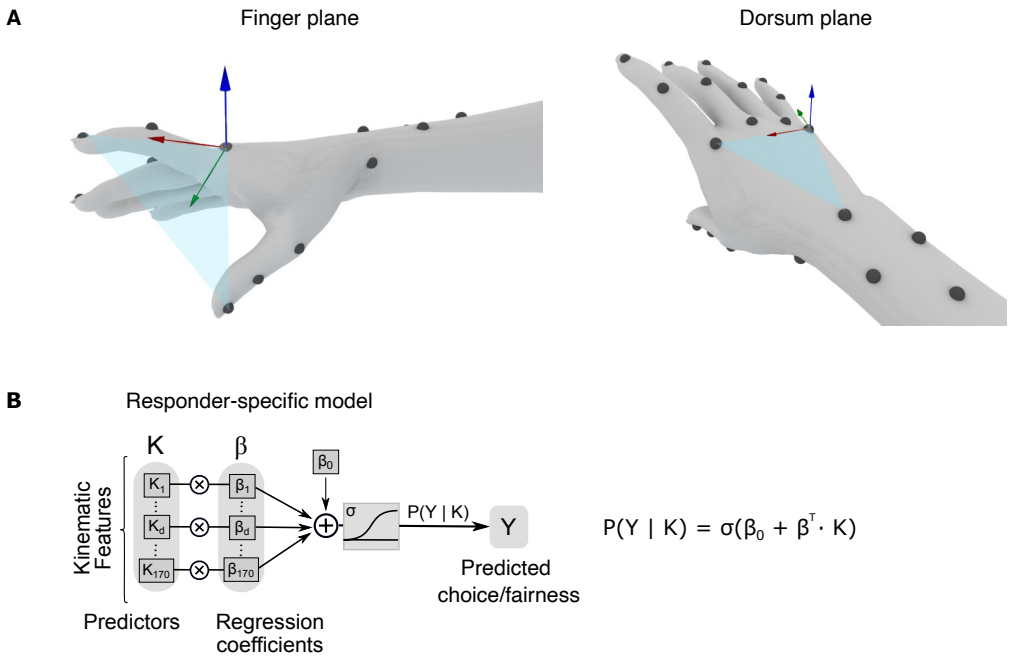

Figure A.1: Marker layout and block-diagram of the responder-specific logistic regression model. (**A**) Marker layout used to reconstruct hand/arm movements. Markers are represented as grey semi-spheres. Blu areas indicate the finger plane (left) and dorsum plane (right). The red, green, and blue arrows refer to the x-, y-, and z-coordinates of the finger/dorsum plane. (**B**) Block- diagram and equation of the responder-specific logistic regression model used to estimate choice and fairness information encoded in movement kinematics.

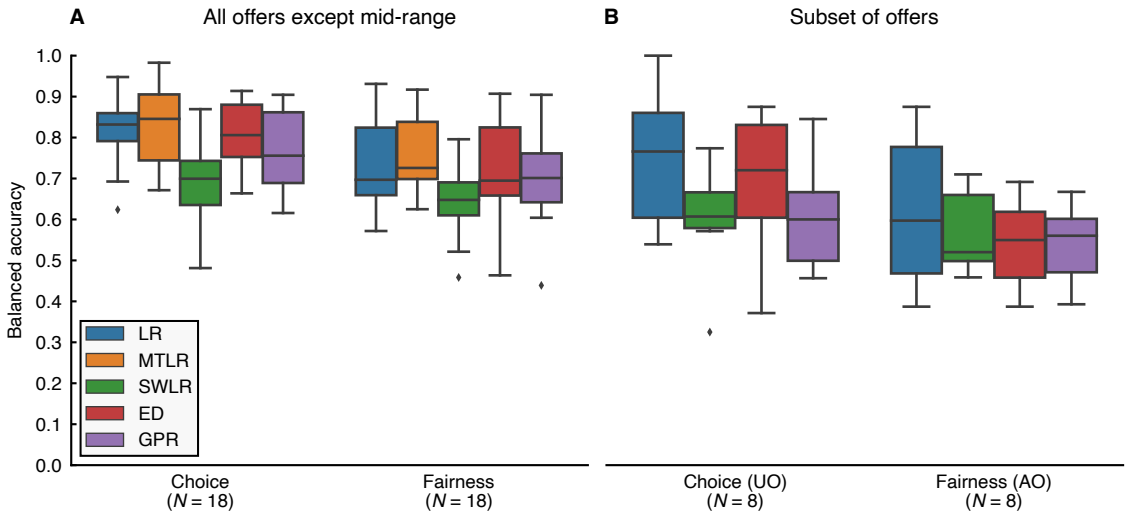

Figure A.2: Comparison of logistic regression with alternative classification approaches. (**A**) Boxplots of balanced prediction accuracies of choice and fairness obtained using Logistic Regression (LR), Multi-Task Logistic Regression (MTLR), Static Weights Logistic Regression (SWLR), Encoding-Decoding (ED), and Gaussian Process Regression (GPR). Classifiers were trained on rightward movements. (**B**) Boxplots of balanced prediction accuracies of choice on unfair trials only (UO), and fairness on accept trials only (AO) obtained using LR, SWLR, ED, and GPR. These analyses corroborate our choice of using the LR classifier for the main analyses of this article, because the LR performed at least as well as any other alternative classifier and was simple to interpret. N indicates the number of responders included in each analysis.

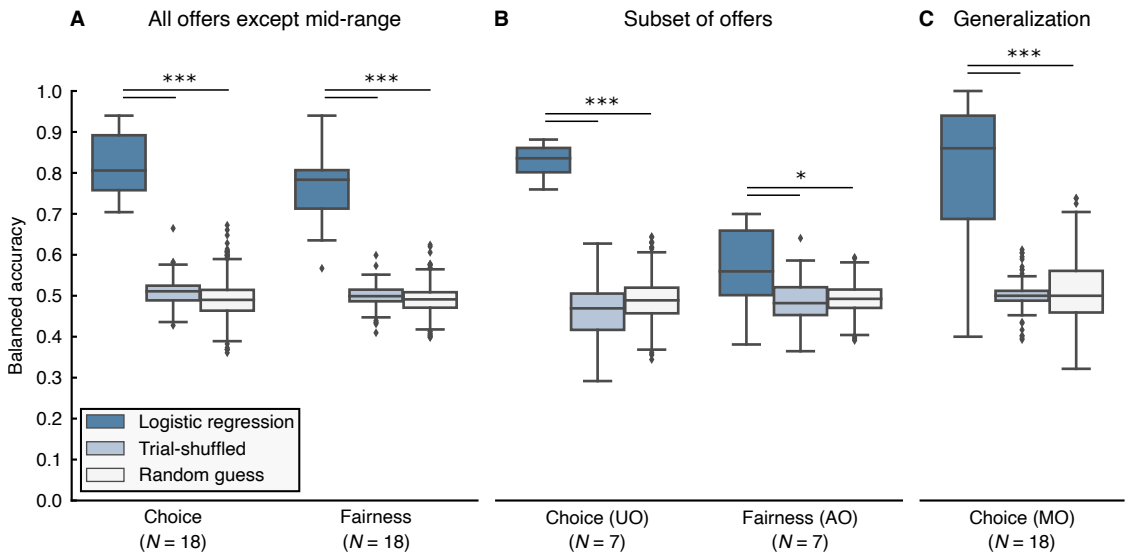

Figure A.3: Performance of logistic regression classifiers trained with leftward movements. (**A**) Boxplots of balanced prediction accuracies of responder-specific logistic regression classifiers trained on leftward movements to predict choice and fairness. Prediction accuracies were significantly higher for actual data than trial-shuffled data and random guesses. (**B**) Boxplots of balanced prediction accuracies of choice on unfair trials only (UO) and fairness on accept trials only (AO). (**C**) Boxplot of balanced prediction accuracies of choice on mid-range offers (MO). * indicates $p < 0.05$, ** indicates $p < 0.01$, and *** indicates $p < 0.001$. N indicates the number of responders included in each analysis.

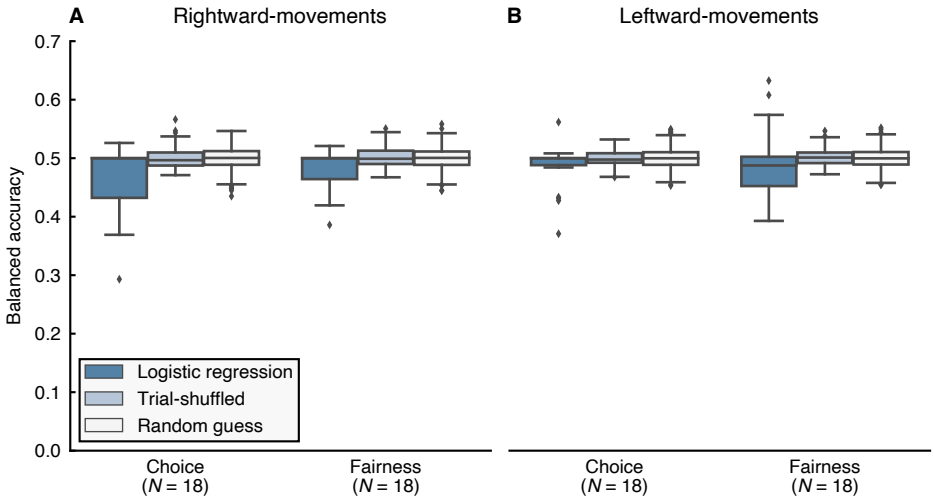

Figure A.4: Performance of logistic regression classifiers trained using a leave-one-subject-out testing approach. (**A**) Boxplots of balanced prediction accuracies of leave-one-subject-out (LOSO) logistic regression classifiers trained on rightward movements to predict choice and fairness. (**B**) Boxplots of balanced prediction accuracies of LOSO logistic regression classifiers trained on leftward movements to predict choice and fairness. For both rightward and leftward movements, prediction accuracies of LOSO classifiers trained with actual data were not significantly different from trial-shuffled data and random guesses. N indicates the number of responders included in each analysis.

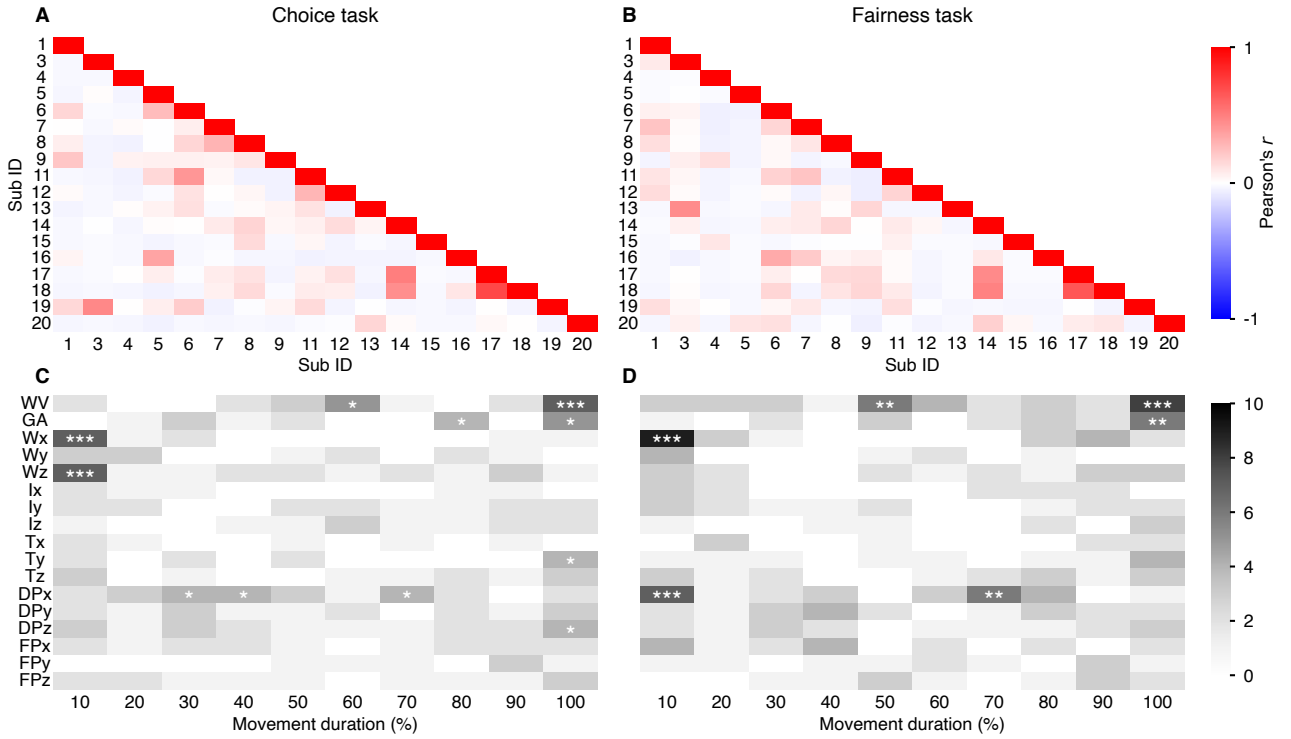

Figure A.5: Overlap of choice and fairness weights across responders of leftward movements. (**A** and **B**) Pearson correlation of the average logistic regression weights between each pair of responders for leftward movements for choice (**A**) and fairness (**B**) classification. (**C** and **D**) Number of responders, for each feature, for which the feature was statistically significant for choice (**C**) and fairness (**D**) classification. * indicates $p < 0.05$, ** indicates $p < 0.01$, and *** indicates $p < 0.001$.

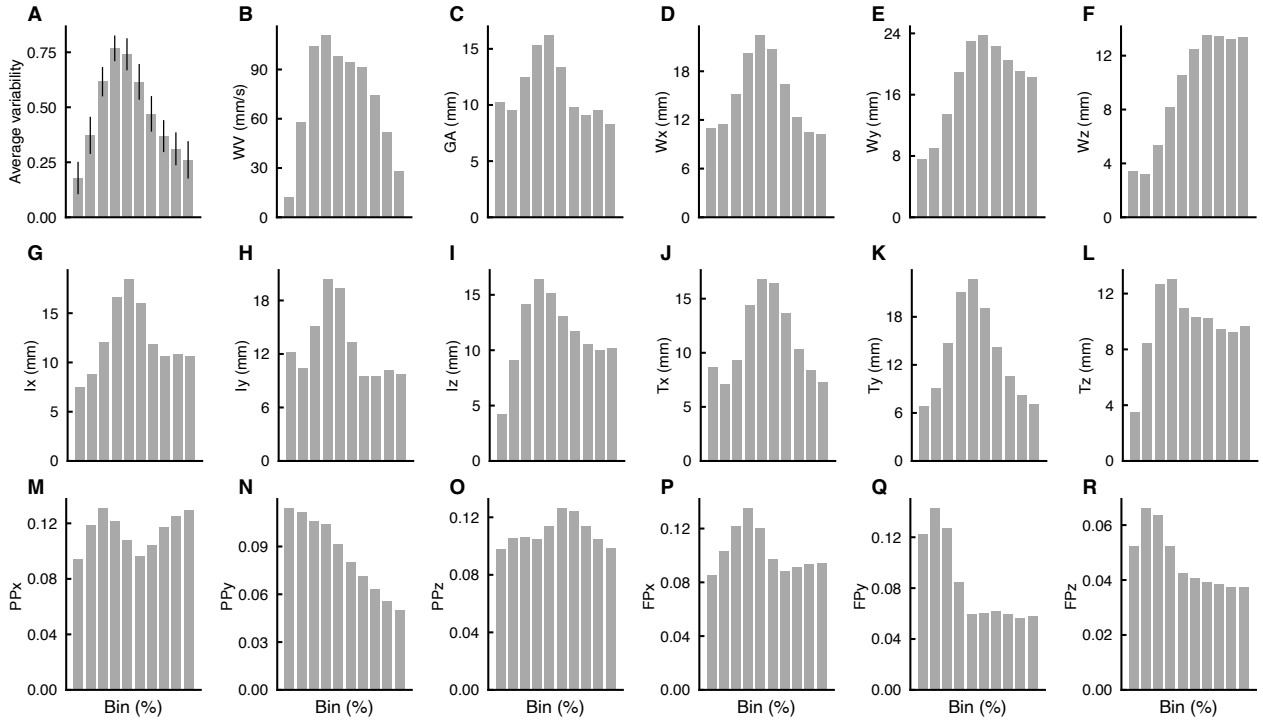

Figure A.6: Inter-individual variability of rightward movements. (**A**) Average (± SEM) of the normalized inter-individual variability across kinematic variables for the rightward movements. (**B-R**) Inter-individual variability for each kinematic variable for the rightward movements.

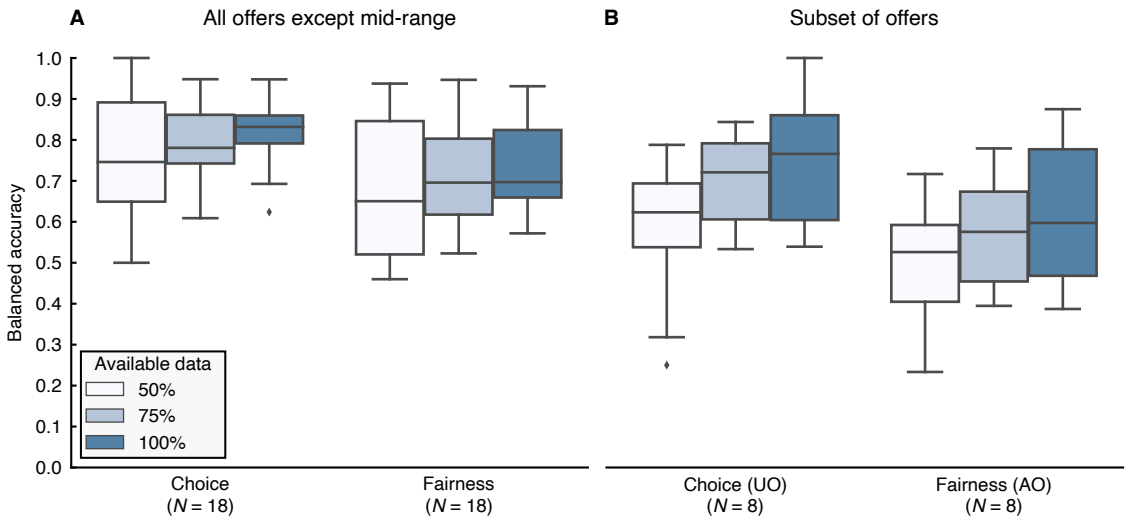

Figure A.7: Performance of logistic regression models as a function of the amount of responder-specific data. (**A**) Boxplots of balanced prediction accuracies of choice and fairness using 50%, 75% and 100% of rightward movements available for each responder. (**B**) Boxplots of balanced prediction accuracies of choice on unfair trials only (UO) and fairness on accept trials only (AO) using 50%, 75% and 100% of the rightward movements available for each responder. *N* indicates the number of responders included in each analysis.

Responder-specific logistic regression models

Rightward movements

				Trial-shuffled			Random guess	
	Median	**Q1**	**Q3**	**std**	**z**	***p***	**std**	**z**	***p***
Choice	.832	.791	.860	.027	11.600	<.001	.037	8.758	<.001
Fairness	.697	.659	.824	.028	7.986	<.001	.037	6.409	<.001
Choice (unfair only)	.766	.604	.860	.057	5.072	<.001	.032	8.182	<.001
Fairness (accepted only)	.597	.468	.777	.044	3.310	<.001	.026	4.734	<.001
Choice (mid-range)	.900	.800	.989	.047	7.200	<.001	.073	3.342	<.001

Leftward movements

				Trial-shuffled			Random guess	
	Median	**Q1**	**Q3**	**std**	**z**	***p***	**std**	**z**	***p***
Choice	.806	.758	.892	.034	9.070	<.001	.043	7.576	<.001
Fairness	.783	.713	.807	.029	9.284	<.001	.030	9.217	<.001
Choice (unfair only)	.836	.801	.861	.066	5.483	<.001	.048	7.114	<.001
Fairness (accepted only)	.559	.501	.659	.045	1.770	.070	.032	2.321	<.05
Choice (mid-range)	.860	.687	.940	.040	7.485	<.001	.074	3.890	<.001

Leave-one-subject-out logistic regression models

Rightward movements

				Trial-shuffled			Random guess	
	Median	**Q1**	**Q3**	**std**	**z**	***p***	**std**	**z**	***p***
Choice	.500	.433	.539	.015	-.427	.550	.020	-.385	.505
Fairness	.474	.422	.530	.015	-1.168	.960	.020	-.898	.903

Leftward movements

				Trial-shuffled			Random guess	
	Median	**Q1**	**Q3**	**std**	**z**	***p***	**std**	**z**	***p***
Choice	.498	.458	.551	.015	-.414	.510	.019	-.346	.519
Fairness	.488	.443	.529	.014	-.797	.820	.019	-.471	.719

Table A.1: Performance of single-subject and leave-one-subject-out logistic regression models against trial-shuffled data and random guesses. We report the median, Q1, and Q3. All p-values are computed by comparing the median value to the null-hypothesis distribution computed on trial-shuffled data and random guesses. For reference only, we also report (without using them to compute the p-value) the z-scores of the tested values with respect to the mean and standard deviation (std) of the null-hypothesis distributions.

Comparison of logistic regression with alternative classification approaches

Choice

	df	***t***	***p* (two-sided)**
LR vs MTLR	17	-0.28	.962
LR vs SWLR	17	8.04	<.001
LR vs ED	17	0.72	.962
LR vs GPR	17	3.30	<.05

Fairness

	df	***t***	***p* (two-sided)**
LR vs MTLR	17	-1.25	.680
LR vs SWLR	17	4.38	<.01
LR vs ED	17	0.22	.827
LR vs GPR	17	0.98	.682

Choice (unfair only)

	df	***t***	***p* (two-sided)**
LR vs SWLR	7	3.81	<.05
LR vs ED	7	1.75	.124
LR vs GPR	7	3.16	<.05

Fairness (accepted only)

	df	***t***	***p* (two-sided)**
LR vs SWLR	7	0.97	.613
LR vs ED	7	1.45	.573
LR vs GPR	7	1.10	.613

Table A.2: Comparison of logistic regression with alternative approaches. We report degrees of freedom, t statistics, and p-values of two-sided paired t-tests conducted to compare the performance of logistic regression (LR) with alternative models (MTLR, SWLR, ED, and GPR) for choice, fairness, choice (unfair only), and fairness (accepted only) classification of rightward movements. All p-values are Holm-Bonferroni corrected for the number of comparisons listed for each entry.

Overlap of choice and fairness weights across responders

Rightward movements

	Responders (*N*)	**Test probability**	***p* (one-sided)**
Choice	5 (18)	246/(170*18)	<.05
	6 (18)	246/(170*18)	<.01
	7 (18)	246/(170*18)	<.001
Fairness	5 (18)	290/(170*18)	<.05
	6 (18)	290/(170*18)	<.01
	7 (18)	290/(170*18)	<.001

Leftward movements

	Responders (*N*)	**Test probability**	***p* (one-sided)**
Choice	4 (18)	239/(170*18)	<.05
	6 (18)	239/(170*18)	<.01
	7 (18)	239/(170*18)	<.001
Fairness	5 (18)	272/(170*18)	<.05
	6 (18)	272/(170*18)	<.01
	7 (18)	272/(170*18)	<.001

Table A.3: Summary of binomial tests for overlap of choice and fairness weights across responders. We report the number of responders who had a significant weight for a given feature, and in brackets, the total number of responders, the test probability, computed as the number of significant weights over the total number of responders divided by the number of the possible significant weights (number of features * total number of responders), and the p-value of the one-sided binomial test

Number of trials for choice and fairness classification

Rightward movements

ID	Choice			Fairness			Choice (unfair only)			Fairness (accepted only)		
	R	**A**	**total**	**UF**	**F**	**total**	**R**	**A**	**total**	**UF**	**F**	**total**
1	12	38	50	19	31	50	12	7	19	7	31	38
2	0	55	55	24	31	55	0	24	24	24	31	55
3	12	38	50	19	31	50	12	7	19	7	31	38
4	25	32	57	25	32	57	25	0	25	0	32	32
5	19	30	49	19	30	49	19	0	19	0	30	30
6	7	35	42	13	29	42	7	6	13	6	29	35
7	12	42	54	24	30	54	12	12	24	12	30	42
8	27	32	59	27	32	59	25	2	27	2	30	32
9	16	29	45	16	29	45	16	0	16	0	29	29
10	1	51	52	21	31	52	1	20	21	20	31	51
11	21	32	53	21	32	53	21	0	21	0	32	32
12	22	32	54	24	30	54	21	3	24	3	29	32
13	29	29	58	27	31	58	23	4	27	4	25	29
14	23	29	52	23	29	52	23	0	23	0	29	29
15	22	31	53	22	31	53	22	0	22	0	31	31
16	18	41	59	26	33	59	17	9	26	9	32	41
17	21	39	60	27	33	60	20	7	27	7	32	39
18	24	32	56	24	32	56	24	0	24	0	32	32
19	26	33	59	25	34	59	24	1	25	1	32	33
20	27	32	59	27	32	59	23	4	27	4	28	32

Leftward movements

ID	Choice			Fairness			Choice (unfair only)			Fairness (accepted only)		
	R	**A**	**total**	**UF**	**F**	**total**	**R**	**A**	**total**	**UF**	**F**	**total**
1	17	43	60	28	32	60	16	12	28	12	31	43
2	0	56	56	24	32	56	0	24	24	24	32	56
3	16	45	61	29	32	61	16	13	29	13	32	45
4	24	30	54	24	30	54	24	0	24	0	30	30
5	23	38	61	28	33	61	22	6	28	6	32	38
6	16	50	66	34	32	66	16	18	34	18	32	50
7	12	45	57	25	32	57	12	13	25	13	32	45
8	21	30	51	20	31	51	20	0	20	0	30	30
9	24	40	64	32	32	64	23	9	32	9	31	40
10	2	55	57	25	32	57	2	23	25	23	32	55
11	24	31	55	25	30	55	24	1	25	1	30	31
12	23	30	53	22	31	53	21	1	22	1	29	30
13	27	28	55	22	33	55	20	2	22	2	26	28
14	25	33	58	25	33	58	24	1	25	1	32	33
15	23	32	55	23	32	55	22	1	23	1	31	32
16	15	37	52	22	30	52	15	7	22	7	30	37
17	18	31	49	19	30	49	18	1	19	1	30	31
18	24	32	56	24	32	56	24	0	24	0	32	32
19	23	30	53	23	30	53	23	0	23	0	30	30
20	22	28	50	21	29	50	20	1	21	1	27	28

Table A.4: Number of trials for individual responders. For each responder (ID), we report the number of trials available for choice and fairness classification and the distribution among classes (R=rejected, A=accepted, UF=unfair, F=fair).

Number of trials for choice classification of mid-range offers

	Rightward movements						*Leftward movements*					
ID	**Training set**			**Test set (3€)**			**Training set**			**Test set (3€)**		
	R	**A**	**total**	**R**	**A**	**total**	**R**	**A**	**total**	**R**	**A**	**total**
1	12	38	50	0	8	8	17	43	60	4	10	14
2	0	55	55	0	11	11	0	56	56	0	11	11
3	12	38	50	0	10	10	16	45	61	1	11	12
4	25	32	57	4	10	14	24	30	54	2	7	9
5	19	30	49	0	11	11	23	38	61	1	11	12
6	7	35	42	0	12	12	16	50	66	0	11	11
7	12	42	54	0	10	10	12	45	57	1	11	12
8	27	32	59	0	1	1	21	30	51	11	11	22
9	16	29	45	0	1	1	24	40	64	10	11	21
10	1	51	52	0	12	12	2	55	57	0	11	11
11	21	32	53	9	1	10	24	31	55	10	1	11
12	22	32	54	10	7	17	23	30	53	5	1	6
13	29	29	58	4	6	10	27	28	55	6	7	13
14	23	29	52	10	0	10	25	33	58	12	0	12
15	22	31	53	7	2	9	23	32	55	10	3	13
16	18	41	59	2	11	13	15	37	52	0	9	9
17	21	39	60	4	11	15	18	31	49	0	8	8
18	24	32	56	12	0	12	24	32	56	10	0	10
19	26	33	59	0	11	11	23	30	53	0	12	12
20	27	32	59	8	6	14	22	28	50	4	4	8

Table A.5: Number of trials for choice classification of mid-range offers for individual responders. For each responder (ID), we report the number of trials available for the training and test set (R=rejected, A=accepted).

Random effects structure selection (Fixed effects: Gender × Proposer Gender)				
Model	**Random effects**	**BIC**	**Deviance**	
m_0	Subject (intercept and Proposer Gender slope)	3364.4	3308.9	(singular fit)
m_1	**Subject (intercept)**	**3348.5**	**3308.9**	
m_2	null	3599.2	3567.5	

Fixed effects structure selection (Random effects: Subject intercept)				
Model	**Random effects**	**BIC**	**Deviance**	
m_1	Responder Gender × Proposer Gender	3348.5	3308.9	
m_2	Responder Gender + Proposer Gender	3341.5	3309.8	vs. m_1: $p>.05$
m_3	Responder Gender	3333.8	3310.0	vs. m_3: $p>.05$
m_4	Proposer Gender	3333.6	3309.9	vs. m_3: $p>.05$
m_5	**null**	**3325.9**	**3310.0**	**vs. m_4, m_5: $p>.05$**

Table A.6: Mixed Effects Model selection. We used Logistic Mixed Effects Models Effects to assess the effect of *Responder Gender* and *Proposer Gender* (*silhouette*). The notation *Gender* × *Proposer Gender* indicates both main effects of *Responder Gender* and *Proposer Gender*, and their interaction were included in the model. Retained models are highlighted in bold.

B. Supplementary materials for Chapter 4: Study 2: Social decision-making from a vigor perspective

Reaction time (invRT)

Random effects structure selection

Fixed effects: Offer + Choice + Offer:Choice + Direction + Session

Model	Random effects at subject-level	BIC	Deviance
m_0	Intercept, and Offer, Choice, Direction, Session slopes	5223.5	5049.2
m_1	Intercept, and Offer, Choice, Direction slopes	5278.4	5143.8
m_2	**Intercept, and Offer, Choice, Session slopes**	**5196.3**	**5061.6**
m_3	Intercept, and Offer, Direction, Session slopes	5240.5	5105.9
m_4	Intercept, and Choice, Direction, Session slopes	5225.9	5091.3
m_5	Intercept, and Offer, Choice slopes	5266.4	5163.5
m_6	Intercept, and Offer, Session slopes	5216.3	5113.3
m_7	Intercept, and Choice, Session slopes	5204.7	5101.7

Fixed effects structure selection

Random effects at subject-level: Intercept, and Offer, Choice, Session slopes

Model	Random effects	BIC	Deviance	LRT
m_2	Offer + Choice + Offer:Choice + Direction + Session	5170.5	5035.8	
m_8	Offer + Choice + Offer:Choice + Direction	5178.4	5051.6	vs. m_2: $p<.05$
m_9	Offer + Choice + Offer:Choice + Session	5165.9	5039.1	vs. m_2: $p>.05$
m_{10}	Offer + Choice + Offer:Choice	5174.6	5055.8	vs. m_8: $p>.05$ vs. m_9: $p<.05$
m_{11}	Offer + Choice + Session	5297.4	5178.6	vs. m_9: $p<.05$
m_{12}	Offer + Offer:Choice + Session	5168.1	5049.3	vs. m_9: $p<.05$
m_{13}	**Choice + Offer:Choice + Session**	**5165.9**	**5039.1**	**vs. m_9: *R***
m_{14}	Choice + Offer:Choice	5174.6	5055.8	vs. m_{13}: $p<.05$
m_{15}	Choice + Session	5301.9	5191.0	vs. m_{13}: $p<.05$
m_{16}	Offer:Choice + Session	5168.1	5049.3	vs. m_{13}: $p<.05$

Main effects and interaction of m_{13}

	χ^2	df	p
Main effect of Choice	10.18	1	<.01
Main effect of Session	16.19	1	<.001
Interaction of Offer and Choice	141.85	2	<.001

Table B.1: Mixed effects model selection for reaction time. We used linear mixed effects models to assess the effects of Offer, Choice, Offer:Choice, Direction, and Session on reaction time (invRT). Retained models are highlighted in bold. Reparameterized models are denoted by *R*; s.f. stands for 'singular fit'.

Movement time (invMT)

Random effects structure selection

Fixed effects: Offer + Choice + Offer:Choice + Direction + Session

Model	Random effects at subject-level	BIC	Deviance	
m_0	Intercept, and Offer, Choice, Direction, Session slopes	4285.3	4110.9	(s.f.)
m_1	Intercept, and Offer, Choice, Direction slopes	4475.4	4340.6	(s.f.)
m_2	Intercept, and Offer, Choice, Session slopes	4306.1	4171.3	
m_3	Intercept, and Offer, Direction, Session slopes	4264.5	4129.7	
m_4	Intercept, and Choice, Direction, Session slopes	4245.8	4111.0	
m_5	Intercept, and Offer, Choice slopes	4443.9	4340.9	
m_6	Intercept, and Offer, Session slopes	4275.5	4172.5	
m_7	**Intercept, and Choice, Session slopes**	**4239.9**	**4136.8**	
m_8	Intercept, and Choice slope	4448.3	4369.0	
m_9	Intercept, and Session slope	4270.1	4190.8	
m_{10}	Intercept	4512.6	4449.2	

Fixed effects structure selection

Random effects at subject-level: Intercept, and Offer, Choice, Session slopes

Model	Random effects	BIC	Deviance	LRT
m_7	Offer + Choice + Offer:Choice + Direction + Session	4211.5	4108.4	
m_{11}	Offer + Choice + Offer:Choice + Direction	4204.7	4109.6	vs. m_7: $p>.05$
m_{12}	Offer + Choice + Offer:Choice + Session	4226.3	4131.2	vs. m_7: $p<.05$
m_{13}	Offer + Choice + Offer:Choice	4220.3	4133.1	vs. m_{11}: $p<.05$ vs. m_{12}: $p>.05$
m_{14}	Offer + Choice + Direction	4205.7	4118.5	vs. m_{11}: $p<.05$
m_{15}	Offer + Offer:Choice + Direction	4204.0	4116.8	vs. m_{11}: $p<.05$
m_{16}	**Choice + Offer:Choice + Direction**	**4204.7**	**4109.6**	**vs. m_{11}: *R***
m_{17}	Choice + Offer:Choice	4220.3	4133.1	vs. m_{16}: $p<.05$
m_{18}	Choice + Direction	4202.0	4122.8	vs. m_{16}: $p<.05$
m_{19}	Offer:Choice + Direction	4204.0	4116.8	vs. m_{16}: $p<.05$

Main effects and interaction of m_{16}

	χ^2	df	p
Main effect of Choice	7.23	1	<.01
Main effect of Direction	23.55	1	<.001
Interaction of Offer and Choice	13.21	2	<.01

Table B.2: Mixed effects model selection for movement time. We used linear mixed effects models to assess the effects of Offer, Choice, Offer:Choice, Direction, and Session on movement time (invMT). Retained models are highlighted in bold. Reparameterized models are denoted by *R*; s.f. stands for 'singular fit'.

Peak velocity (PV)

Random effects structure selection

Fixed effects: Offer + Choice + Offer:Choice + Direction + Session

Model	Random effects at subject-level	BIC	Deviance	
m_0	Intercept, and Offer, Choice, Direction, Session slopes	4555.6	4381.4	(s.f.)
m_1	Intercept, and Offer, Choice, Direction slopes	4677.9	4543.3	
m_2	Intercept, and Offer, Choice, Session slopes	4671.3	4536.7	
m_3	Intercept, and Offer, Direction, Session slopes	4519.3	4384.6	
m_4	Intercept, and Choice, Direction, Session slopes	4516.2	4381.5	
m_5	Intercept, and Offer, Choice slopes	4651.9	4549.0	
m_6	Intercept, and Offer, Session slopes	4644.3	4541.3	
m_7	**Intercept, and Choice, Session slopes**	**4489.2**	**4386.2**	
m_8	Intercept, and Choice slope	4631.7	4552.5	
m_9	Intercept, and Session slope	4622.9	4543.7	
m_{10}	Intercept	4809.5	4746.1	

Fixed effects structure selection

Random effects at subject-level: Intercept, and Offer, Choice, Session slopes

Model	Random effects	BIC	Deviance	LRT
m_7	Offer + Choice + Offer:Choice + Direction + Session	4461.2	4358.3	
m_{11}	Offer + Choice + Offer:Choice + Direction	4454.3	4359.2	vs. m_7: $p>.05$
m_{12}	Offer + Choice + Offer:Choice + Session	4472.9	4377.9	vs. m_7: $p<.05$
m_{13}	Offer + Choice + Offer:Choice	4468.0	4380.9	vs. m_{11}: $p<.05$ vs. m_{12}: $p>.05$
m_{14}	Offer + Choice + Direction	4461.3	4374.2	vs. m_{11}: $p<.05$
m_{15}	Offer + Offer:Choice + Direction	4455.4	4368.2	vs. m_{11}: $p<.05$
m_{16}	**Choice + Offer:Choice + Direction**	**4454.3**	**4359.2**	**vs. m_{11}: *R***
m_{17}	Choice + Offer:Choice	4468.0	4380.9	vs. m_{16}: $p<.05$
m_{18}	Choice + Direction	4456.8	4377.6	vs. m_{16}: $p<.05$
m_{19}	Offer:Choice + Direction	4455.4	4368.2	vs. m_{16}: $p<.05$

Main effects and interaction of m_{16}

	χ^2	df	p
Main effect of Choice	9.03	1	<.01
Main effect of Direction	21.66	1	<.001
Interaction of Offer and Choice	18.37	2	<.001

Table B.3: Mixed effects model selection for peak velocity. We used linear mixed effects models to assess the effects of Offer, Choice, Offer:Choice, Direction, and Session on peak velocity (PV). Retained models are highlighted in bold. Reparameterized models are denoted by *R*; s.f. stands for 'singular fit'.

Time-to-peak velocity (invTPV)

Random effects structure selection

Fixed effects: Offer + Choice + Offer:Choice + Direction + Session

Model	Random effects at subject-level	BIC	Deviance	
m_0	Intercept, and Offer, Choice, Direction, Session slopes	4964.4	4790.3	(s.f.)
m_1	Intercept, and Offer, Choice, Direction slopes	5023.5	4889.0	(s.f.)
m_2	Intercept, and Offer, Choice, Session slopes	5003.2	4868.6	
m_3	Intercept, and Offer, Direction, Session slopes	4938.1	4803.6	
m_4	Intercept, and Choice, Direction, Session slopes	4930.2	4795.7	
m_5	Intercept, and Offer, Choice slopes	4997.6	4894.7	
m_6	Intercept, and Offer, Session slopes	4975.2	4872.3	
m_7	**Intercept, and Choice, Session slopes**	**4916.8**	**4813.9**	
m_8	Intercept, and Choice slope	4991.1	4912.0	
m_9	Intercept, and Session slope	4965.3	4886.1	
m_{10}	Intercept	5039.1	4975.8	

Fixed effects structure selection

Random effects at subject-level: Intercept, and Offer, Choice, Session slopes

Model	Random effects	BIC	Deviance	LRT
m_7	Offer + Choice + Offer:Choice + Direction + Session	4889.0	4786.1	
m_{11}	Offer + Choice + Offer:Choice + Direction	4882.0	4787.0	vs. m_7: $p>.05$
m_{12}	Offer + Choice + Offer:Choice + Session	4883.4	4788.5	vs. m_7: $p>.05$
m_{13}	Offer + Choice + Offer:Choice	4875.6	4788.6	vs. m_{11}: $p>.05$ vs. m_{12}: $p>.05$
m_{14}	Offer + Choice	4889.2	4810.1	vs. m_{13}: $p<.05$
m_{15}	Offer + Offer:Choice	4879.6	4800.4	vs. m_{13}: $p<.05$
m_{16}	**Choice + Offer:Choice**	**4875.6**	**4788.6**	**vs. m_{13}: *R***
m_{17}	Choice	4888.3	4817.1	vs. m_{16}: $p<.05$
m_{18}	Offer:Choice	4879.6	4800.4	vs. m_{16}: $p<.05$
m_{19}	null	4885.5	4822.2	vs. m_{17}: $p<.05$ vs. m_{18}: $p<.05$

Main effects and interaction of m_{13}

	χ^2	df	p
Main effect of Choice	11.83	1	<.001
Interaction of Offer and Choice	28.46	2	<.001

Table B.4: Mixed effects model selection for time-to-peak velocity. We used linear mixed effects models to assess the effects of Offer, Choice, Offer:Choice, Direction, and Session on time-to-peak velocity (invTPV). Retained models are highlighted in bold. Reparameterized models are denoted by *R*; s.f. stands for 'singular fit'.

Peak grip aperture (PGA)

Random effects structure selection

Fixed effects: Offer + Choice + Offer:Choice + Direction + Session

Model	Random effects at subject-level	BIC	Deviance
m_0	Intercept, and Offer, Choice, Direction, Session slopes	4722.6	4548.6
m_1	Intercept, and Offer, Choice, Direction slopes	4956.8	4822.3
m_2	Intercept, and Offer, Choice, Session slopes	4742.7	4608.3
m_3	Intercept, and Offer, Direction, Session slopes	4690.5	4556.0
m_4	Intercept, and Choice, Direction, Session slopes	4688.0	4553.5
m_5	Intercept, and Offer, Choice slopes	4936.1	4833.3
m_6	Intercept, and Offer, Session slopes	4713.8	4611.0
m_7	**Intercept, and Choice, Session slopes**	**4667.4**	**4564.6**
m_8	Intercept, and Choice slope	4923.4	4844.3
m_9	Intercept, and Session slope	4701.0	4622.0
m_{10}	Intercept	4955.8	4892.5

Fixed effects structure selection

Random effects at subject-level: Intercept, and Offer, Choice, Session slopes

Model	Random effects	BIC	Deviance	LRT
m_7	Offer + Choice + Offer:Choice + Direction + Session	4640.1	4537.3	
m_{11}	Offer + Choice + Offer:Choice + Direction	4632.2	4537.3	vs. m_7: $p>.05$
m_{12}	Offer + Choice + Offer:Choice + Session	4636.4	4541.5	vs. m_7: $p<.05$
m_{13}	Offer + Choice + Offer:Choice	4628.5	4541.5	vs. m_{11}: $p<.05$ vs. m_{12}: $p>.05$
m_{14}	Offer + Choice + Direction	4624.6	4537.6	vs. m_{11}: $p>.05$
m_{15}	Offer + Offer:Choice + Direction	4625.1	4538.1	vs. m_{11}: $p>.05$
m_{16}	Choice + Offer:Choice + Direction	4632.2	4537.3	vs. m_{11}: R
m_{17}	Offer + Choice	4620.8	4541.7	vs. m_{14}: $p<.05$
m_{18}	Offer + Direction	4617.2	4538.2	vs. m_{14}: $p>.05$
m_{19}	Choice + Direction	4624.6	4537.6	vs. m_{14}: $p>.05$
m_{20}	Offer	4613.5	4542.3	vs. m_{17}: $p>.05$ vs. m_{18}: $p<.05$
m_{21}	Choice	4614.3	4543.1	vs. m_{17}: $p>.05$ vs. m_{19}: $p<.05$
m_{22}	**Direction**	**4610.1**	**4538.9**	**vs. m_{18}: $p>.05$** **vs. m_{19}: $p>.05$**
m_{23}	null	4606.4	4543.1	vs. m_{21}: $p>.05$ vs. m_{22}: $p<.05$

Main effects and interaction of m_{22}

	χ^2	df	p
Main effect of Direction	4.17	1	$<.05$

Table B.5: Mixed effects model selection for peak grip aperture. We used linear mixed effects models to assess the effects of Offer, Choice, Offer:Choice, Direction, and Session on peak grip aperture (PGA). Retained models are highlighted in bold. Reparameterized models are denoted by R; s.f. stands for 'singular fit'.

Reaction time (invRT, retained model: m_{13})

Slope comparison				Coefficient values (effect size)			
	estimate	95% CI	*p*		estimate	95% CI	*p*
Accept - Reject	**-.346**	**[-.400, -.289]**	**<.001**	**Intercept**	**.344**	**[.094, .595]**	**<.01**
				Choice (accept)	**.308**	**[.152, .570]**	**<.01**
				Session (2)	**-.318**	**[-.443, -.190]**	**<.001**
				Offer:Choice (reject)	**.133**	**[.073, 0.192]**	**<.001**
				Offer:Choice (accept)	**-.212**	**[-.261, -.162]**	**<.001**

Movement time (invMT, retained model: m_{16})

Slope comparison				Coefficient values (effect size)			
	estimate	95% CI	*p*		estimate	95% CI	*p*
Accept - Reject	**-.060**	**[-.101, -.020]**	**<.01**	Intercept	.167	[-.212, .566]	.384
				Choice (accept)	**.111**	**[.031, .191]**	**<.01**
				Direction (left)	**-.334**	**[-.439, -.233]**	**<.001**
				Offer:Choice (reject)	.025	[-.009, 0.059]	.150
				Offer:Choice (accept)	**-.036**	**[-.057, -.014]**	**<.001**

Peak velocity (PV, retained model: m_{16})

Slope comparison				Coefficient values (effect size)			
	estimate	95% CI	*p*		estimate	95% CI	*p*
Accept - Reject	**.083**	**[.041, .126]**	**<.001**	Intercept	.300	[-.096, .698]	.129
				Choice (accept)	**-.131**	**[.218, .044]**	**<.01**
				Direction (left)	**-.441**	**[-.586, -.298]**	**<.001**
				Offer:Choice (reject)	**-.042**	**[-.078, .007]**	**<.05**
				Offer:Choice (accept)	**.041**	**[.019, .063]**	**<.001**

Time-to-peak velocity (invTPV, retained model: m_{16})

Slope comparison				Coefficient values (effect size)			
	estimate	95% CI	*p*		estimate	95% CI	*p*
Accept - Reject	**-.087**	**[-.150, -.025]**	**<.01**	Intercept	.116	[-.238, .471]	.519
				Choice (accept)	**.163**	**[.070, .254]**	**<.01**
				Offer:Choice (reject)	**.050**	**[.010, .089]**	**<.05**
				Offer:Choice (accept)	**-.058**	**[-.082, -.033]**	**<.001**

Peak grip aperture (PGA, retained model: m_{22})

Slope comparison				Coefficient values (effect size)			
n/a → Offer:Choice not significant					estimate	95% CI	*p*
				Intercept	-.052	[-.412, .328]	.794
				Direction (left)	**.114**	**[.003, .225]**	**<.05**

Table B.6: Significance of slopes comparison and coefficient values for retained models of reaction time, movement time, peak velocity, time-to-peak velocity, and peak grip aperture. We report the estimate, 95% bootstrap confidence interval (CI), and two-tailed bootstrap *p*-value for both slope comparison and coefficient values. Slope comparison was performed only for models with a significant interaction between offer and choice. Significant comparisons and effect sizes are highlighted in bold.